LIÈGE université
Gembloux
Agro-Bio Tech

Assessing irrigation water saving for crop production in Cambodia based on combined in situ and modelling approaches

Pinnara Ket

Promoteur: Prof. Aurore Degré,
Co-Promoteur: Dr Chantha Oeurng
2019

Assessing irrigation water saving for crop production in Cambodia based on combined in situ and modelling approaches

Pinnara Ket

Dissertation originale présentée en vue de l'obtention
du grade de docteur en sciences agronomiques et ingénierie biologique

Promoteur: Prof. Aurore Degré,
Co-Promoteur: Dr Chantha Oeurng
2019

Abstract

In recent decades, climate change has become the major constraint for agricultural production in Cambodia and leads to future concern of food security. Improving effective irrigation management, especially for non-rice crops that use less water is urgently needed.

The aim of this thesis is to contribute the development of vegetable production during the dry season in Cambodia. The specific objective of the research is to optimise irrigation water use at the on-farm level. We focused on developing a methodology for i) characterising soil hydraulic properties for crop models and ii) exploring the best irrigation scenarios for vegetable irrigation. Two growing season experiments with lettuce were conducted during 2016 and 2017 in five farm fields in the Chrey Bak catchment, Kampong Chhnnag Province, Cambodia.

Two approaches were tested to achieve irrigation water saving. Firstly, a method using a soil water model, HYDRUS-1D, was used to inversely estimate the van Genuchten soil hydraulic functions in the unsaturated zone. The five experimental fields had different soil textures, loamy sand, sand and loam, and the field data (i.e., irrigation amounts, weather, lettuce growth data, soil permeability, etc.) were collected and measured to feed the given model. To generate the soil parameters, the objective functions were generated using inverse data such as measured soil moisture dynamics and soil water retention curves, using a combination of a soil moisture sensor, 10HS, and soil potential sensor, MPS-2, for a 30 minute time step. Our analysis showed that the inverse modelling successfully estimated the soil water retention curve and soil water dynamic with reasonable accuracy when compared to the observed values. However, uncertainties of the simulation and data measurement were observed, especially for the SWRC in dry and wet conditions. For the second study approach, to explore irrigation water saving the AquaCrop model was used to simulate irrigation scheduling under water stressed conditions.

In the second study approach, to explore the irrigation water saving, the water driven model, AquaCrop was selected for simulating irrigation scheduling under water-stressed conditions. The crop growth parameters for lettuce were calibrated using field data from the 2017 experimental growing season from two fields that have sand and loam soil textures. In the calibration process the measured crop growth data were used, e.g. canopy cover and above ground biomass collected over a 3 day time step, taking into account the other factors of irrigation management such as drip irrigation and mulching. Then, the method for optimal irrigation scheduling was described. Two main categories of irrigation scheduling for deficit irrigation were developed. The first varied thresholds of readily available water content (RAW) for the stop irrigation point under different no water stress and stress conditions. The second decreased deficit irrigations below field capacity (FC). The results of the calibration for crop growth were quite satisfactory. A primer set of adjusted lettuce parameters was obtained. The results highlighted limitations of the model in defining heat stress and root depth of the vegetable. Primarily, analysis results of irrigation scheduling scenarios show the capabilities of the model to identify the optimum water saving alternatives under limited water conditions.

Overall, this PhD thesis opens perspectives for improving irrigation management for increased crop productivity in Cambodia.

Acknowledgements

It has been a great opportunity to pursue this PhD research that has opened my eyes to the scientific community. There have been many challenges in reaching the end of this research, which could not have happened without the support, guidance, advice and encouragement of the great people around me. First of all, I would like to specially thank and acknowledge my supervisor, Prof. Aurore Degré for her kind support, valuable advice, guidance, correction of my work, and valuable encouragement to overcome all the obstacles with positive thinking. Likewise, I would like to sincerely thank my co-supervisor Dr. Chantha Oeurng who has kindly given support, valuable advice, guidance, comments and suggestions during my research work.

I gratefully thank my co-authors and thesis committee, Prof. Sarah Garé, Dr. Lyda Hok, Prof. Jean-Thomas Cornélis and Dr. Seng Vang for their valuable and critical comments and suggestions for my publication and thesis work.

I would like to thank ARES-CCD for providing this PhD scholarship and supporting my research study, both at ULiege-Gembloux Agro Bio-Tech and the Institute of Technology of Cambodia. Particular thanks go to Prof. Charles Debouche, Prof. Michel Verleysen and the other ARES staff for continuing to support my research.

Sincere thanks to my colleagues in the BIOSE Department, Prof. Gilles Colinet, Stéphane Becquevort, Katia Berghmans, Francoise Toussaint, and to the colleagues from ITC, Mr. Norith Pol, Dr. Sarann Ly, Layheang Song, Sok Ty for their help and support during laboratory and research work and administrative challenges.

Thanks to my good friends Naghish, Lili, Sokny, Marie, Jullien, Maud for our discussions and sharing ideas during my time in Belgium.

Thanks to the students that provided intensive support during the field experiment in Cambodia.

Thanks to my family, my mum, sister and brothers for their unfailing support through it all.

Contents

List of figures

List of tables

1

Introduction

This chapter presents the general context for conducting this research, the thesis frame work, thesis objectives and the outline.

1.1 Thesis context

Currently, world agriculture consumes the largest proportion of freshwater resources, resulting in one of the greatest pressures on these resources (Saccon 2018). There is continuous growth in demand for irrigation water for crop cultivation to support the rapid world population growth, which is increasing at a rate of around 1.13 % or 80 million per year (Ringler et al. 2009; Tripathi et al. 2019). By 2050, the global population will be up to 9.6 billion, 34 % higher than today (Tripathi et al. 2019).

There are concerns that in the decades ahead, water use for irrigation cannot be increased in proportion to demand because of current limited natural water resources, this leads to the challenge to find sufficient water in the near future (Oki and Kanae 2006). Another hot topic issue is the effect of global climate change, which presents major constraints to agricultural production (Santamarta et al. 2014; Ali and Erenstein 2017; Saccon 2018; Tripathi et al. 2019).

Climate change is associated with extreme events such as water shortages, droughts and floods which are increasing in frequency and intensity (Capra and Consoli 2008; Luo et al. 2018). Over agricultural areas in many regions of the world, disasters arising from these extreme events have caused marked damage to agriculture, especially crop production, and threaten local to global food security (Lesk et al. 2016). In recent years, almost 25% of the damage and losses from climate-related disasters have been recorded in the agricultural sector of developing countries (Lesk et al. 2016).

In this context of population growth and climate change, enhancing future food security is the greatest challenge for farmers. This is especially true for poorer farmers from developing countries that are reliant on rain-fed agriculture (Poulton et al. 2016).

Cambodia is a developing country (Ngoc et al. 2018) that will face almost double population growth from its current 14.4 million (2014) to between 20.4 and 27.4 million by 2050 (Wokker et al. 2014).

Agriculture is among the mainstays of Cambodia's economy and it contributed 24.9% (current price) of the gross domestic product in 2017, after the industry and service sectors (Ecker and Diao 2011; Silva et al. 2013; Ngoc et al. 2018; MAFF 2018). Due to climate change effects, the agricultural sector's contribution to the economy has strongly decreased over the last five years (Figure 1.1-1).
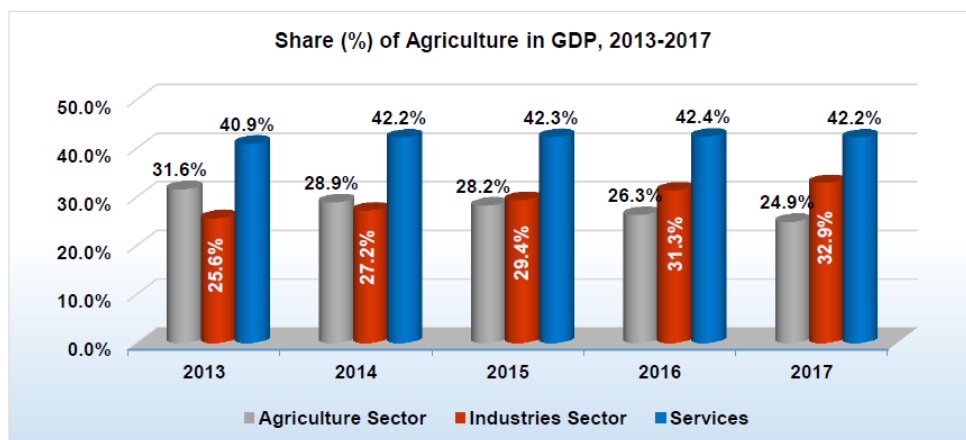
Source: Assessment by Ministry of Planning 2017

Figure 1.1-1 Contribution of different sectors to the national economy of Cambodia (MAFF 2018).

Cambodia is among the poorest countries in South-East Asia and the world (Damme et al. 2004; Goutard et al. 2015) and the agricultural productivity in Cambodia remains among the lowest in Asia and the Pacific (Silva et al. 2013). Eighty percent of Cambodia's population are poor, smallholder farmers who live in rural areas (Morton 2007; NIS 2015). The workforce in the agricultural sector was 54.2% (in 2010) and has decreased to 41.5% (2015), which is due to increasing migration from rural areas to urban areas and to other countries (MAFF 2018).

Rice is the key crop in the country with yields averaging ~3.0 ton ha^{-1} in 2013, which is a low level compared to China, Vietnam and Myanmar with 6.5, 5.3 and 4.1 ton ha^{-1}, while Australia and New Zealand have the highest yields of 10.4 ton ha^{-1} (Molle 2007; FAO 2013; Martin 2017; MAFF 2018). With cultivated agricultural land area totalling 3.7 million hectares in Cambodia, rice crops occupy 76% of cultivated land and the remaining 24% is covered by other significant crops such as cassava, maize, rubber, soybean, mungbean, sugar cane and vegetables (MWRM 2003; Tong et al. 2011; Martin 2017).

Cambodia has a tropical monsoon climate having two distinct seasons in the year, i.e., a rainy season (from May to mid-November) and a dry season with long periods of dry days without rain (Miyazawa et al. 2014). The average annual rainfall is 1400 mm in the central lowland regions (Chan 2015). With favourable precipitation during the rainy season, agriculture is heavily based on rain-fed production (Devendra and Thomas 2002; Molle 2007). Only 16% of the total cultivated land is irrigated during the dry season (Molle 2007).

The Cambodian agricultural sector faces some significant constraints including single crop production, lack of crop diversification, reliance on traditional technology and the effects of climate change. Predominantly, Cambodian agriculture is characterised by small scale farms with sizes that vary from 0.5 to 4.3 ha (Devendra and Thomas 2002), and low levels of technology and education due to the side effects

of the Khmer Rouge civil war and limited access to education facilities and poor institutional management in remote rural areas (Montgomery et al. 2017). The farmers share their traditional irrigation practices for rice cultivation from generation to generation without going to training schools. Because they are unable to assess surface or groundwater for irrigation during the dry season, farmers commonly can produce rice based only on unpredictable precipitation. Being rich in freshwater resources in Cambodia, about 2525 irrigation schemes have been developed across major provinces, which could potentially irrigate more than 1 million hectares (Silva et al. 2013; Sithirith 2017). However, most of these schemes are underperforming (Silva et al. 2013). Consequently, the vast proportion (96%) of wet rice land remains uncultivated during the dry season (Erban and Gorelick 2016).

During the dry season, in some areas where there is water available for irrigation, farm lands have the potential to diversify into high-value crops (e.g., off-season vegetables) that use less water. However, non-rice crop farming requires technical advice on suitable varieties, fertiliser and pesticide use, and water use efficiency (WUE) (Johnston et al. 2013b). Due to a lack of familiarity and limited knowledge of those crops, farmers consider that cultivating vegetables is highly risky (Tong et al. 2011; Silva et al. 2013). Notably, there is still significant importation of vegetables and fruits from neighbouring countries to Cambodian markets, especially to urban areas (Tickner 1996; NIS 2015). Furthermore, the consumption of vegetables by the rural population appears limited (Silva et al. 2013; NIS 2015).

Cambodia is one of the more disaster-prone countries in Southeast Asia, affected by climate change (WBG 2011). Certainly, climate change is a major concern for Cambodian agriculture. Severe and extreme events related to flood and drought have increasingly damaged the agricultural production of farmers (Kong et al. 2012). Over the period 1998-2002, as much as 70% of rice production loss was attributed to floods and 20% to droughts (WBG 2011). The worst flood was recorded in 2000 and severe droughts occurred in 2002, 2012, 2015 and 2016 (WBG 2011; Sithirith 2017). The growth in agriculture during the last 10 years, as presented by MAFF 2018 (Figure 1.1-2), indicates that growth has continually decreased over time. This growth decreased significantly from 2013 to 2015, i.e., from 4.3% in 2012 to 1.6% in 2013 and continued to decrease to 0.3% in 2014 and 0.2% in 2015. The decrease was caused by natural disasters, especially as a consequence of serious drought in 2014 and 2015 (MAFF 2018).
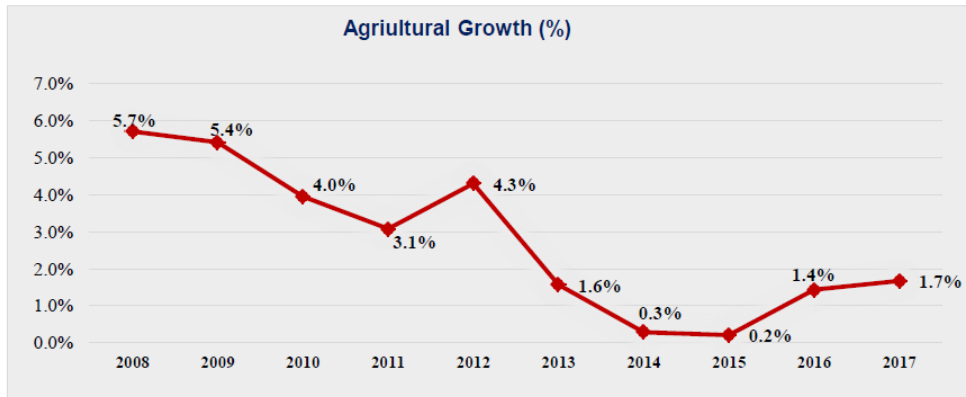
Source: Assessment by Ministry of Planning 2017

Figure 1.1-2 Agricultural growth of Cambodia within the last 10 years (MAFF 2018).

Moreover, due to projected climate changes in the lower Mekong River Basin to which Cambodia belongs, there is an expectation that pressures will be further exacerbated, e.g., the dry season will lengthen and intensify, and the rainy season will shorten and intensify with dramatic increases in rainfall in the wettest months (Mainuddin and Kirby 2009; Poláková et al. 2013). This will strongly increase the threat to food security in Cambodia.

Thus, agriculture in Cambodia faces both greatly increased demands for food and increased frequent extreme weather threats to production (Morton 2007; Mainuddin and Kirby 2009).

For these reasons, there is clearly an urgent need to improve agricultural water use efficiency. This can be an important pathway for poverty reduction and enhancement of food security (Zhang and Oweis 1999; Passioura 2006; Ortega et al. 2005; Mainuddin and Kirby 2009; Andarzian et al. 2011; Xinchun et al. 2017; Bigelow and Zhang 2018). Thus, improving the management of irrigation water is becoming an issue of paramount importance (Lorite et al. 2007). To date, the scientific research-based evidence on irrigation water use efficiency has not yet been established for Cambodia.

1.2 Conceptual framework and thesis objectives

The question of water use and improving water use efficiency (WUE = crop yield/evapotranspiration (ET)) is complex interaction between mainly soil and water management, and involves sustainable water use and water efficiency, nutrient management, farm measures, water quality, and preventing the loss of soil organic matter, etc. (Zhang and Oweis 1999; Rotter et al. 2011; Poláková et al. 2013; Poulton et al. 2016) (Figure 1.2-1).

In irrigated agriculture, to enhance WUE many aspects are considered, e.g., increasing the yield per unit of water (engineering and agronomic management

aspects), reducing losses of water to unusable sinks, reducing water degradation (environmental aspects), and reallocating water to higher priority uses (societal aspects) (Hewell 2001). It is believed that substantial changes in agricultural water use can be made to farm practices through the integration of scientific research by different irrigation stakeholders.

.
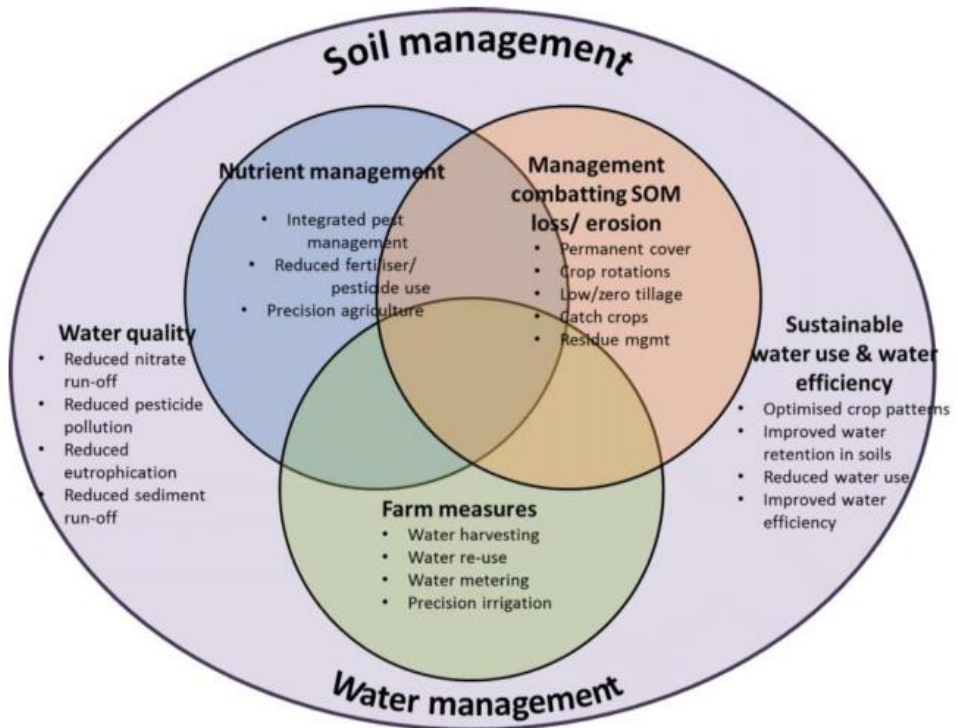
Figure 1.2-1 Potential sustainable soil and water outcomes through improved land and farm management (Poláková et al. 2013).

On the other hand, irrigation approaches are assessed based on different levels (field, watershed, basin, irrigation district, catchment, scheme, regional government) considering different outlooks, priorities and concerns (Figure 1.2-2) (Hewell 2001; Fabiani et al. 2016). For example, the regional managers and governments may focus more on investments that jeopardise the environment but create high economic impact (Fabiani et al. 2016).
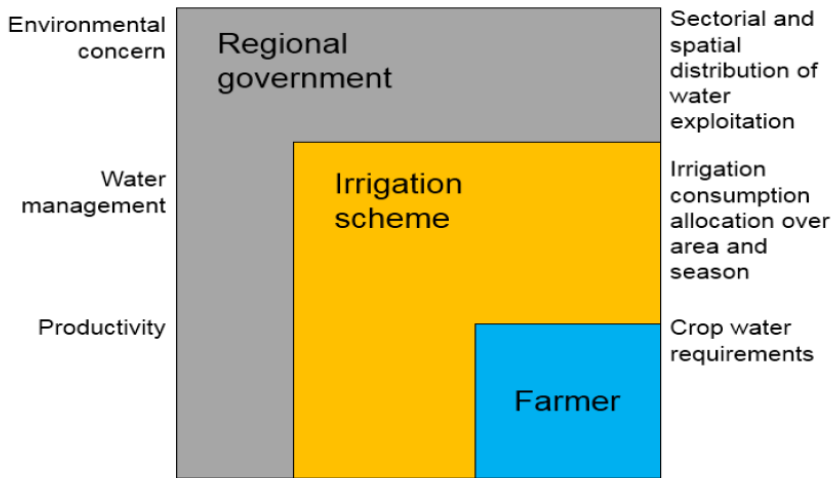
Figure 1.2-2 Irrigation management priorities (Fabiani et al. 2016).

For this present research we focused on the farm level, developing a methodology for improving irrigation water use efficiency that can contribute to meeting the challenges facing Cambodian farmers in cultivating vegetables during the dry season. There are options for improving irrigation WUE, e.g., regarding irrigation water management, agronomic or institutional improvement (Figure 1.2-3) (Poláková et al. 2013).
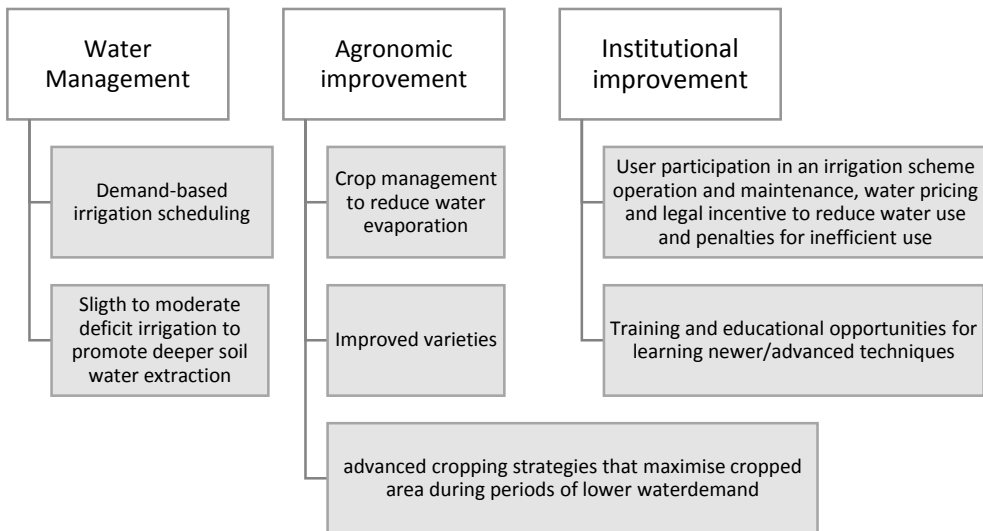
Figure 1.2-3 Option examples for improving irrigation efficiency at a field level (Hewell 2001).

Specifically, we will focus on water management improvement at the farm level.

Farmers generally lack the adequate means and incentives to know the crops' water use, actual irrigation applications, crop yield responses to different water management practices, and thus current on-farm water-efficiency levels (Levidow et al. 2014). The guidelines for irrigation applications should be developed for smallholder farmers, which could lead to sustainable use of the water resources allocated to agriculture (Geerts et al. 2010).

At first, we have to understand the concept of water use efficiency and the different processes which can affect WUE. The scheme in Figure 1.2-4 gives the processes influencing irrigation WUE off- and on-farm and its definition at different scales.

WUE can be defined by an output to input ratio between the water depth beneficially used by the sub-system under consideration and the total water supplied to that sub-system (Pereira et al. 2012).

In the case of on-farm application efficiency, the numerator is replaced by the amount of water added to the root zone storage and the denominator is the total water applied to that field (Pereira et al. 2012). Nowadays, there is a trend to promote increased water productivity (WP) as an important issue in irrigation, that may be generically defined as the ratio between the actual crop yield achieved (Ya) and the water use, expressed in kg/m^3 (Pereira et al. 2012).

Improving WP at a field level can be achieved through proper irrigation scheduling, reducing irrigation frequency and amounts (Zhang et al. 2004; Poláková et al. 2013). Appropriate irrigation scheduling is an effective way to achieve balanced water-saving and high crop yields (Wen et al. 2017). Elaborating irrigation schedules merely on the basis of field research is rather difficult and time consuming (Geerts et al. 2010). Irrigation scheduling simulation approaches, on the other hand, allow the assessment of crop irrigation requirements, support upgraded irrigation management practices, can assess the impacts of water stress on crop yields, as well as aiding the search for optimised water saving and environmentally friendly irrigation practices (Popova and Kercheva 2004; Geerts et al. 2010; Popova and Pereira 2011).

The overall objective of this research is to contribute to the development of vegetable production during the dry season in Cambodia using on-farm irrigation.

The specific objective is to optimise irrigation practices on-farm during dry seasons.

Through two case studies based on primary data in the Cambodian context, we will try to address the following two specific research questions:

(1) How to characterise soil hydraulic properties in order to use a soil water model?

(2) Which are the best scenarios to maximise water efficiency for vegetable irrigation during the dry season in Cambodia?

The framework of the study is presented in Figure 1.2-5.
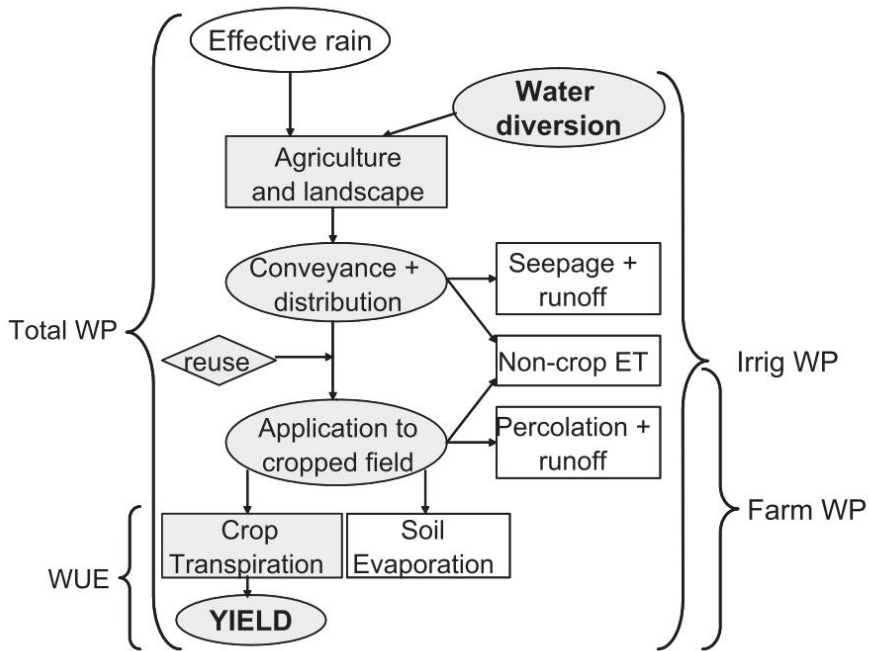
Figure 1.2-4 Different factors affecting irrigation efficiency off-and on-farm: grey boxes are the useful water for crop yield; white boxes are the water losses. water productivity at different scales also presented: (a) the plant, through the water use efficiency WUE; (b) the irrigated crop at farm scale (Farm WP); (c) the irrigated crop, at system level (Irrig WP); and the crop including rainfall and irrigation water (Total WP) (Pereira et al. 2012).
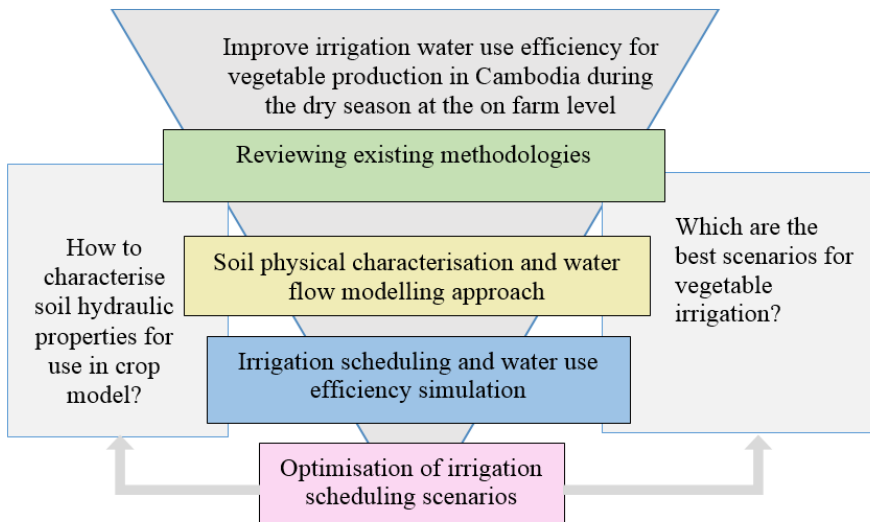
Figure 1.2-5 Framework of the study and research questions.

1.3 Thesis outline

This dissertation is structured into 7 chapters.

Chapter 1 describes the global context related to the water crisis, water issues in the Cambodian context, the problem statement and motivation for the thesis.

Chapter 2 reviews the up-to-date methodologies for defining the basic soil hydraulic properties, water flow models and crop models that have been used to address irrigation management.

Chapter 3 describes the environment of the study area addressed. The experiments are described.

Chapter 4 addresses research question 1 on how to characterise soil physical properties. There is a focus on the inversion method using water flow models to estimate soil water retention curves.

Chapter 5 addresses research question 2, what are the best scenarios for vegetable irrigation during the dry season in Cambodia.

Chapter 6 discusses the general outputs of the results. Limitations are discussed and followed by recommendations for subsequent work.

Chapter 7 gives a general conclusion and perspectives. It presents the key findings of the study approaches in this thesis and discusses some points for improving further research.

2

Literature Review

This chapter reviews the basics of water flows in soil, as well as different methods to determine the soil hydraulic properties. The chapter describes modelling approaches that are specific to water flow and irrigation scheduling.

2.1 Major soil hydraulic properties

2.1.1 Soil water retention curve

The soil water retention curve (SWRC) is a fundamental soil hydraulic property (SHP). SWRCs represent the relationship between soil water potential (h) and the soil water content (θ). The SWRC is needed to model water and solute movement in unsaturated soil (Liang et al. 2016; Hodnett and Tomasella 2002; May and Genuchten 2008). Therefore, it plays a major role for soil and water management within the frame of sustainable and improved agricultural productivity (Shwetha and Varija 2015; Patil et al. 2013).

SWRC is considered to be a difficult-to-measure soil hydraulic property (Botula et al. 2014). There are many direct and indirect methods to characterize the SWRC (Rashid et al. 2015). Direct measurement can be conducted in the laboratory with a small soil sample or in a small-scale in situ experiment using some devices (Le Bourgeois et al. 2016). Generally, SWRC is obtained directly by laboratory experiments using porous media-based methods such as the sand box, hanging water column, pressure cells, pressure plate extractors, and centrifuge (Smagin 2012). Tension disc infiltrometer experiments are commonly used for SWRC field experiments (Rashid et al. 2015; Ramos et al. 2006; Schwartz and Evett 2002; Ventrella et al. 2005; Lazarovitch et al. 2007; Verbist et al. 2009; Latorre et al. 2013). Soil moisture and soil water potential probes can also be used to obtain in situ SWRCs (Degré et al. 2017). Both laboratory and filed experiments have their own advantages and limitations. The field experiments can minimize the disturbance caused by soil sampling and unchanged soil boundary conditions, whereas laboratory experiments can measure SWRCs in a larger range, especially in the wettest and the driest events (Asgarzadeh et al. 2014). However, these direct measurement methods are time consuming and expensive (Hopmans and Simunek 1999a).

Because of the disadvantages of direct measurement, alternative indirect methods using computer modelling have been developed for fast and accurate prediction (Li et al. 2018b). A rapid approach is the use of pedotransfer functions (PTFs) based on easy-to-measure soil data such as soil texture, bulk density, and soil organicity (Wang et al. 2016, Van Den Berg et al. 1997).

PTFs have been classified into 3 types: i) Point/class/static estimation, ii) Parametric /continuous/dynamic estimation, iii) Physico-empirical model (Minasny et al. 1999) (Assouline and Or 2014). Point estimation involves an empirical function using multiple regression analysis that predicts θ(h) at a predefined pressure head values mostly at field capacity and wilting point (Minasny et al. 1999; Assouline and Or 2014).

Parametric PTFs use hydraulic models that describe the observed data across a range of pressure heads in a close-form equation with limited number of parameters to describe complete soil water retention curves (Minasny et al. 1999) (Vereecken et al. 2010). The well-known hydraulic models used include Brooks and Corey (1964), Campbell (1974) and van Genuchten (1980).

Generally a point/class PTF is easier to use, but its accuracy is limited (Reynolds et al. 2000). As demonstrated by Gupta and Larson (1979); Rawls et al. (1982) and

Wösten et al. (2001), the function used to develop the point PTFs have the general form:

$$\theta_h = a.\,\text{sand} + b.\,\text{silt} + d.\,\text{organic matter} + e.\,\text{dry bulk density} + \cdots$$
$$+ e.\,\text{variable X} \tag{2.1-1}$$

Where, θh is the soil water content at specific pressure head, h and a, b, c, d, e and x are regression coefficients. Variable X is any other basic easily-to measure soil properties (Wösten et al. 2001).

In spite of the advantages, the reliability of applying these relationships in other contexts is uncertain and requires cautious validation for different regions (Werisch et al. 2014). Another indirect method to estimate SWRCs is inverse modelling. This process aims to select optimal model parameters in order to match a set of measurements (Gutmann and Small 2007) and it is increasingly used to fit effective hydraulic properties (Wohling et al. 2008). This method provides an easy, reliable procedure and a more flexible experimental set up (Kumar et al. 2010). It requires less experimental effort and results in effective flow parameter estimation (Lambot 2002).

SWRC utilization

The SWRC have been used to determine the soil water thresholds indicating water availability for plant consumption (Datta and Stivers 2017). These thresholds indicated in Figure 2.1-1 are important for determining when and how much irrigation is needed.

Field capacity (FC) is un upper limit of soil water availability (de Jong van Lier 2017), an agronomic measure with prime application in irrigation management. It allows the determination of irrigation output without excessive leaching (de Jong van Lier 2017). Field Capacity (FC) has been defined as the vertical distribution of water content in the soil profile at 48h after sequential ponded infiltration and drainage with no evapotranspiration or rain (Ottoni Filho et al. 2014). Traditionally, field capacity (FC) is defined as the water content of a soil following saturation with water and after free drainage is negligible (Nemes et al. 2011; Meyer and Gee 1999). Field capacity can be frequently presented as the soil water content corresponding to measure soil matric potentials at different accepted values according to the countries (i.e., – 5 (the United Kingdom), -10 (the Netherlands), and – 33 kPa (the United States)) (Reynolds et al. 2000).

Permanent wilting point (PWP) is defined as the largest water content of a soil at which indicator plants, growing in that soil, wilt and fail to recover when placed in a humid chamber (Tolk 1998). This definition is based on results of numerous plant pot experiments in which the plants were well irrigated with ideal nutrient and at some growing stage the irrigation was ceased (Novák and Havrila 2006). The – 1500 kPa value is commonly used to estimate permanent wilting point. Exceptionally, many drought-tolerant crops such as wheat have the ability to survive and extract water at levels well below this value (Reynolds et al. 2000).

Available water storage capacity (AWC) is the water supply capacity of soils to crops in which the soil moisture is held between field capacity (FC) and permanent

wilting point (PWP) (Kirkham 2014; Berg et al. 1997; Van Den Berg et al. 1997; Kern 1995; Batjes 1996).

Readily available soil water content (RAW) refers to the fraction of total available water content that a crop can extract from the root zone without suffering water stress (Allen et al. 1998a).
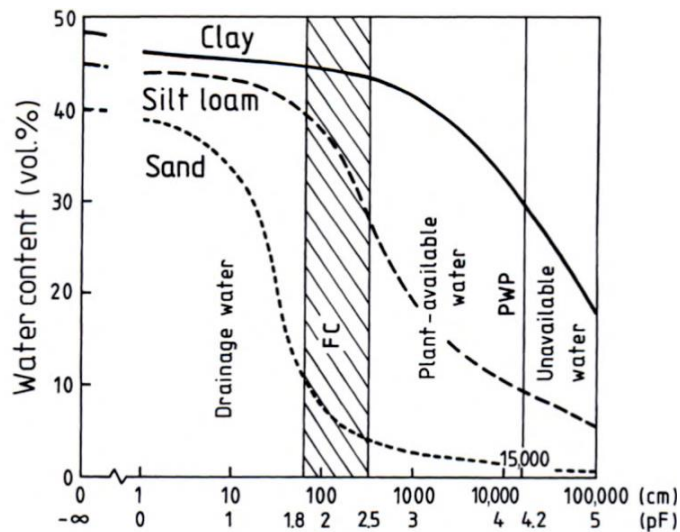
Figure 2.1-1 The relation between volumetric water content and water tension in different soils adjusted from Ehlers and Goss (2003).

2.1.2 *Soil hydraulic conductivity*

Soil hydraulic conductivity (K) plays a significant role in ecological, agricultural, and hydrological management (Tian et al. 2018). The hydraulic conductivity characterizes the ability of a soil to transmit water (van Genuchten and Pachepsky 2017). Many factors such as the pore-size distribution of the medium, and the tortuosity, shape, roughness, and degree of interconnectedness of the pores affect the K (van Genuchten and Pachepsky 2017). The hydraulic conductivity decreases considerably when the soil becomes unsaturated (van Genuchten and Pachepsky 2017). The unsaturated hydraulic conductivity function has a close relation to the water content, $K(\theta)$, or pressure head, $K(h)$. Accurate measurement and estimation of unsaturated hydraulic conductivity $K(h)$ is challenging and of great interest.

There are numerous methods of hydraulic conductivity measurement both under field conditions and in the laboratory (Zeng et al. 2013, Kucza and Ilek 2016). Some examples of laboratory and field measurements of K are the falling head, auger hole, Guelph permeameter, single-ring infiltrometer, double-ring infiltrometer and the inversed-auger-hole method, tension infiltrometers (Zeng et al. 2013). Of these options, tension infiltrometers have been increasingly used to measure K at various supply pressure heads in the field because they are water saving, repeatable and stable

in space and time (Zeng et al. 2013). Alternatively, indirect methods which use pedo-transfer functions to estimate saturated hydraulic conductivity (Ks) using readily available soil properties are often used (Xu et al. 2017; Becker et al. 2018). Some proposed PTFs frequently used in the literature to estimate Ks are presented in Ghanbarian et al. (2017). Rosetta is a PTF modelling tool that is used to estimate k (h) and Ks (Schaap et al. 2001; Elhakeem et al. 2018).

A large number of functions have been proposed over the years to describe the hydraulic conductivity function, K(h) (van Genuchten and Pachepsky 2017) that are often used in numerical models. A detailed review of the performance of many of these models is given by (Leij et al. 1997). Some known model equations are presented here.

The classical equations of Brooks and Corey (1964) for θ (h), K(h):

$$\theta(h) = \begin{cases} \theta_r + (\theta_s - \theta_r) \left| \dfrac{h_e}{h} \right|^\lambda & h < h_e \\ \theta_s & h \geq h_e \end{cases} \qquad (2.1\text{-}2)$$

$$K(h) = K_s S_e^{\frac{2}{\lambda+l+1}} \qquad (2.1\text{-}3)$$

where, as before, θ_r is the residual water content ($L^3 L^{-3}$), θ_s is the saturated water content ($L^3 L^{-3}$), h_e is often referred to as the air-entry value (L), l is a pore-size distribution index characterizing the width of the soil pore-size distribution, Ks is the saturated hydraulic conductivity (LT^{-1}), l a pore-connectivity parameter assumed to be 2.0 in the original study of Brooks and Corey (1964), and S_e(h) is effective saturation given by:

$$S_e(h) = \frac{\theta(h) - \theta_r}{\theta_s - \theta_r} \qquad (2.1\text{-}4)$$

As an alternative, (van Genuchten 1980) proposed a set of equations that improve a sigmoidal shape. The Mualem van Genuchten model, which is used to represent the functions K(h) and θ(h) in the flow models, is described as follows (van Genuchten 1980):

$$S_e(h) = \begin{cases} (1 + |\alpha h|^n)^m & h < 0 \\ 1 & h \geq 0 \end{cases} \qquad (2.1\text{-}5)$$

$$K(h) = K_s S_e^l \left[1 - \left(1 - S_e^{1/m} \right)^m \right]^2 \qquad (2.1\text{-}6)$$

where S_e(h) is the scaled water content at pressure head, h, α is related to the inverse of the air entry suction (L^{-1}) and n is the shape parameters, $m = 1 - 1/n$, (n>1) is a measure of the pore size distribution. Of these, θ_r, θ_s and K_s have a physical meaning, and α, n and l are empirical curve shape parameters (van Genuchten 1980;

Šimůnek et al. 2003). The parameter n affects the steepness of the curve. Large values of n result in a steeper curve (Radcliffe and Simunek 2010).Water flow models

Soil water models have been developed to interpret a specific scientific question or solve a prescribed practical problem or specific purpose (Ranatunga et al. 2008; Romano 2014). Categorisation of the models differs but often relies on the degree of complexity (physics-based, mechanistic and empirically-based models) (Ranatunga et al. 2008).

Empirical models are usually data-driven black-box models while inputs and outputs are empirical functions (Song-hao and Xiao-min 2011). Principally, they are based on field measurement at specified site and weather conditions. Practically, they have few parameters and require fewer inputs for those specific conditions.

Conceptual models are based on the mass water balance of infiltration, rainfall or irrigation, redistribution in the soil water zone, plant water uptake or actual evapotranspiration and percolation out (Panigrahi and Panda 2003). The models also include dynamics of crop root growth function. Similarly, they require fewer inputs and are commonly used at field scale and in agricultural water management (Panigrahi and Panda 2003).

Hydrodynamic models, or physically-based models, are more complex because they are based on the physical with continuous soil water flow including one or two-dimensional water flow using the principle of mass conservation and the Darcy's law (Song-hao and Xiao-min 2011; Ranatunga et al. 2008). The equation of Richards is well-known and the most widely used in soil moisture dynamic models (Romano 2014).

Some of the widely used numerical models for simulating variably saturated water flow and solute transport in soils are COUP DAISY, DAISY, HYDRUS, MACRO, RZWQM (Simunek 2005). Among these models, the HYDRUS numerical model is one of the most advanced and popular numerical computer models for the field of soil physics (Radcliffe and Simunek 2010). Therefore, in this research we selected HYDRUS for charactersing the soil hydraulic properties. The following, we introduce some concepts of Richard' equation and inverse modelling used in HYDRUS. The detail of the HYDRUD can be found in its manual, (version 4.16) (Šimůnek et al. 2005).

2.1.3 *Richards' equation*

Richards' equation (Richards 1931) is known as one of the governing equations of water flow and uses the principle of mass conservation and Darcy's law to describe the relationships between water potential, volumetric water content and hydraulic conductivity (Song-hao and Xiao-min 2011; Romano 2014).

$$\frac{\partial \theta}{\partial t} = \frac{\partial}{\partial z}\left[K(h)\frac{\partial h}{\partial z} - K(h)\right] - S \tag{2.1-7}$$

where θ is the volumetric water content, h is the pressure head (L), z is the distance from a reference surface (L), t is the time (T), K(h) is unsaturated hydraulic conductivity (LT^{-1}) as a function of h or θ, and S = sinks.

The Richards' flow equations can be solved using computer models based on relative simple analytical, semianalytical and more complex numerical solutions for a wide range of applications in the research and management of natural subsurface systems (Simunek 2005).

To solve practical problems, numerical solutions with increased computing power are generally used for dynamic field situations, e.g. under specified, realistic initial and boundary conditions, complex natural geologic and hydrologic conditions and control parameters in space and time (Romano 2014; Simunek 2005). The applications of numerical methods for solving variably saturated flow problems generally subdivide the time and spatial coordinates into smaller pieces using different methods such as classical finite differences (used in one-dimensional models), integrated finite differences, finite volumes and finite element methods (used in two- and three-dimensional models) in terms of a system of algebraic equations. The history of the development of various numerical techniques used in vadose zone flow models has been reviewed by Simunek (2005).

The initial and boundary conditions are needed to solve Richards' equation for numerical solutions. The initial condition is defined as the distribution of soil water contents or soil water pressure heads in the flow domain at the beginning of the simulation (Novák and Hlaváčiková 2018). Boundary conditions are prescribed at the boundaries of the modelled area, and they define the interaction between the flow domain and surrounding environment. The upper and lower boundary can be expressed in flux form or in "pressure-head" form.

2.1.4 Calibration of soil-water flow models

To simulate the water flow in soil, it is necessary to know all parameters in the governing equations that characterise the soil properties, such as the soil water retention and hydraulic conductivity functions (Novák and Hlaváčiková 2018). There are two methods to obtain these soil properties, e.g. the direct solution by estimations taken from field and laboratory measurements, and the inverse solution.

The parameter estimation or parameter optimisation involves the estimation of the unknown soil parameters needed in governing equations, by using relatively easily measured water contents, pressure heads and water fluxes (e.g. infiltration rates) present during soil-water movement. Aiming to produce minimal differences between measured and modelled data, the initial parameters are adjusted.

2.1.5 Inverse modelling

In advance of the calibration, "real" inverse modelling consists in running the model backwards using observed soil moisture in known conditions in order to deduce SWRC parameters and conductivity curve parameters (Hopmans et al. 2002, Vrugt et al. 2008, Ritter et al. 2003b).

Inverse modelling components

The inverse method integrates three interrelated functional components: i) transient flow measurement, ii) a numerical flow model simulating the measurement, iii) the optimisation algorithm (Figure 2.2-1) (Hopmans and Simunek 1999b). In the transient

flow experiment, the boundary and initial conditions are prescribed and various flow variables are measured, such as cumulative infiltration, irrigation, precipitation, evapotranspiration, etc. In the numerical flow model, initial parametric soil hydraulic functions are defined, which include saturated hydraulic conductivity and saturated soil water content using direct measurement or estimation with existing methods such as pedotransfer function methods. In the optimisation part, the algorithm estimates accurate parameters through the minimisation of an objective function of the difference between observed and simulated flow variables, using an iterative solution of the transient flow equation. The depth overviews and backgrounds of theory of inversion method can be found in (Vrugt et al. 2008; Hopmans et al. 2002; Hopmans and Simunek 1999).
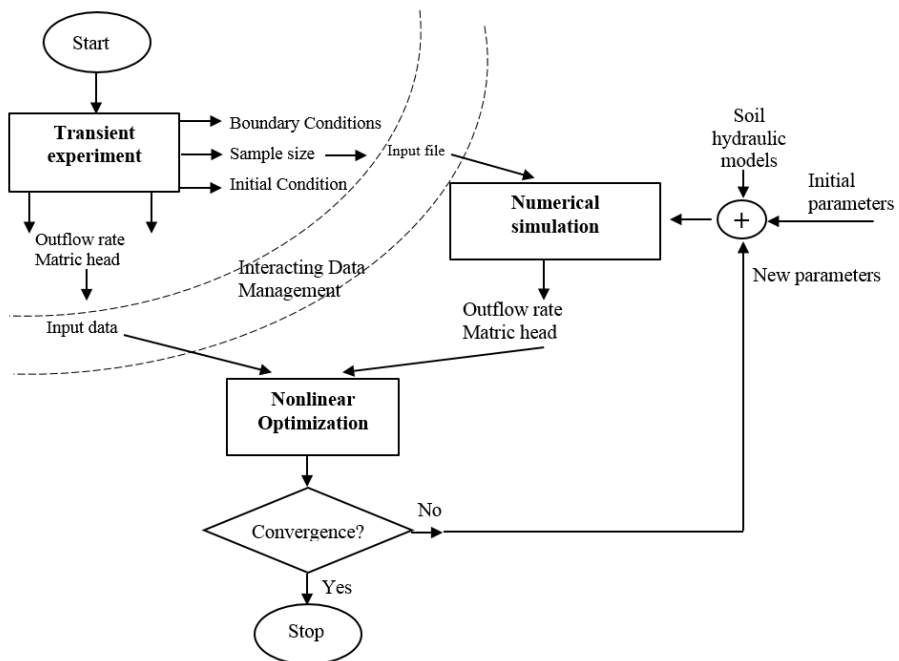
Figure 2.1-2 Process of inverse modeling approach (modified from Hopmans and Simunek 1999).

Parameter Optimization

The total of the difference between observed and simulated state variables to reach the desired hydraulic parameters is expressed by an objective function, ϕ, which may be defined as (Hopmans et al. 2002):

$$\phi(\beta, y) = \sum_{j=1}^{j=m_y} v_j \sum_{i=1}^{i=n_j} w_{i,j} \left[y_j^*(z, t_i) - y_j(z, t_j, \beta) \right]^2 \qquad (2.1\text{-}8)$$

where the right-hand side represents the residuals between the measured y_j^* and corresponding model-predicted (y_j) space-time variables using the soil hydraulic parameters of the optimized parameter vector β, β is the optimized parameter vector, t_j denotes time. m_y is types of all measurements, n_j is the number of measurements for a certain measurement type j, y_j^* may represent water flux density, cumulative water flow, soil water matric head, or soil water content values, v_j is weighting factor, $w_{i,j}$ is additional weighting factor to individual data, t is time (T), z is vertical coordinate (L).

The problem of the objective function often becomes ill-posed: unidentifiability (if more than one parameter set leads to the same model response, the parameters are unidentifiable), instability (small errors in the measured variable or in some fixed parameters may result in large changes of the optimized estimated parameters) and non-uniqueness (refers to the inverse relationship; if a given response leads to more than one set of parameters) (Carrera et al. 2005; Ritter et al. 2003b).

Inverse algorithm

An inverse method combines the numerical model with an algorithm for parameter estimation (Ritter et al. 2003b). Inverse numerical optimization that can be used with specific algorithms (Novák and Hlaváčiková 2018). Many algorithms have been developed to numerically solve and minimise the objective function following their own particular strategy, e.g. by a gradient-based search (Ritter et al. 2003).

The inverse algorithms may be classified into local and global search methodologies (Vrugt et al. 2008). The local method seeks a systematic improvement of the objective function using an iterative search starting from a single arbitrary initial point in the parameter space, while the global method uses multiple concurrent searches from different starting points that are conducted within the parameter space (Vrugt et al. 2008). The search for best parameters should consist of finding the global minimum of the objective function.

In soil hydrology, the simple local-search optimisation methods are the steepest descendent method, Newton's method, Gauss method, Levenberg–Marquardt method and the Simplex method. The Levenberg–Marquardt method for derivative-based search is commonly used, which evolves toward the true optimum in the search space in situations where the objective function exhibits a convex response surface over the entire parameter domain (Hopmans et al. 2002). The limitations of these methods are discontinuous first derivatives, curved multidimensional ridges, the inability of the observed experimental data to properly constrain all of the calibration parameters, which lowers the chance of finding a single unique solution (Vrugt et al. 2008).

More developed and robust global optimisation techniques that have been used for the estimation of the unsaturated soil hydraulic properties include the annealing–simplex method, genetic algorithms, multilevel grid sampling strategies, ant-colony optimisation, shuffled complex methods, Bayesian and multiobjective optimisation algorithms (NSGA-II, MOSCEM-UA, AMALGAM) (Vrugt et al. 2008).

2.2 Irrigation scheduling

Generally, irrigation is applied to avoid water deficits that reduce crop production. It plays an important role in building resiliency to climate variability and ensuring food security (Liang et al. 2016; Fereres and Rabanales 2007).

The irrigation water balance includes evaporation losses from the soil and the crop (evapotranspiration), and all the losses resulting from the distribution of water to the land (Fereres and Rabanales 2007). Effective irrigation water use needs a proper irrigation schedule. Irrigation scheduling involves determining when and how much to irrigate, using the proper amount of water to result in maximum crop yields and minimise leaching of water and nutrients to the groundwater. (Al-jamal et al. 2002; Jones 2004; García-vila and Fereres 2012; Sammis et al. 2012; Cambel and Cambel 2013).

Irrigation scheduling can be conventionally based on a water-balance accounting method, by monitoring the soil moisture deficit or by monitoring plant-water potential (stress) (Sammis et al. 2012; Jones 2004). The soil water measurement based method uses the soil moisture status, whether in terms of water content or water potential, as indicator of when to irrigate. The soil water balance calculation estimates the water balance in soil moisture over a period, given by the difference between the inputs (irrigation plus precipitation) and the losses (runoff plus drainage plus evapotranspiration). The plant stress sensing method is based on direct or indirect measurement of the plant water status or based on plant physiological responses to drought.

2.2.1 Irrigation scheduling models

In the context of increasing irrigation water scarcity, accurate scheduling using soundly based management methods and tools is becoming necessary for optimal water saving (Theiveyanathan et al. 2004). As a result, numerous irrigation scheduling models have been developed as research and/or management tools (Papajorgji and Shatar 2004; Pereira et al. 2003; Kanda et al. 2018). The irrigation scheduling simulation models are essentially of two types: water flux simulation models and soil water balance simulation models (Pereira et al. 2003).

Having complex processes of simulation and model parameterisation, the water flux models use the water fluxes entering and leaving the root zone to compute the water balance and require detailed information on the soil hydraulic properties, crop canopy characteristics and other parameters influencing water (and nutrient) extraction by the crop roots.

The soil water balance simulation models adapt the water content estimation using the input and output quantities of water to the soil reservoir with a predetermined time step. They require only essential soil water characterisation and basic crop data, and use simplified water-yield functions.

The soil water flux models include those using Richards' equation (Liu et al. 2006), e.g. the models SWACROP, WAVE (Vanclooster et al. 1994) and SWAP (Ahmad et al. 2002; Jorenush and Sepaskhah 2003).

Water-balance models are commonly used for irrigation scheduling as stand-alone applications or as components of crop growth models (Liu et al. 2006; Papajorgji and Shatar 2004).

Irrigation-scheduling models that are stand-alone applications include CROPWAT, WISE (Leib et al. 2001), ISM (George et al. 2000), SWB and ISAREG (Pereira et al. 2003). Some models (e.g. the Ritchie model) were integrated into crop simulation models such as CERES-Wheat and DSSAT.

The coupling of both types of model, i.e., water flux models and crop growth models, has been assessed (Kanda et al. 2018). Indeed, water flux models used in agriculture focus mainly on the soil physical processes and not the crop growth, with simplification of transpiration, while crop models focus on the crop development process by using the simplified water flow process (Kanda et al. 2018). The combination of both approaches therefore opens new perspectives (Li et al. 2011).

In recent decades, the FAO AquaCrop model has been widely used to predict crop productivity, water requirements and water use efficiency under water-limiting conditions (Raes et al. 2009b).

For the purpose of exploring various conditions of the irrigation strategies, we selected AquaCrop for estimating irrigation. We used soil parameters obtained from HYDRUS as complementary of the AquaCrop model. The following, we highlight the concepts of AquaCrop model used in this study approach. A detailed description is presented in Steduto et al. (2009a).

2.2.2 *AquaCrop Model*

The AquaCrop model is a crop water-driven productivity model developed by the FAO in 2009 Water is the key limiting factor for crop production in this model (Razzaghi et al. 2017). Inputs for the AquaCrop model consist of weather data, crop, and soil characteristics (soil profile and groundwater), and field management practice or irrigation management practices (Steduto et al. 2009a).

Canopy cover is a crucial feature of AquaCrop (Steduto et al. 2009a). Under unstressed condition, the exponential growth equation to simulate canopy development for the vegetative stage is:

$$CC = CC_o e^{CGC \times t} \qquad (2.2\text{-}1)$$

where CC is the canopy cover at time t and is expressed as fraction of ground covered, CC_o is initial canopy cover size (at t = 0) as a fraction (%), and CGC is the canopy growth coefficient in fraction per growing degree day (GDD), a constant for a crop under optimal conditions, but modulated by stresses.

In the condition of water stress, the CGC is multiplied by a water stress coefficient of expansive growth (Ks_{exp}):

$$CGC_{adj} = Ks_{exp}.CGC \qquad (2.2\text{-}2)$$

where Ks_{exp} ranges from 1 to 0, canopy growth begins to slow down below the maximum rate when soil water depletion reaches the upper threshold, and stops completely when the depletion reaches the lower threshold.

Crop transpiration is proportional to the canopy cover and given by:

$$Tr = Ks_{sto}Kc_{Tr}ET_o \qquad (2.2\text{-}3)$$

Ks_{sto} is the stress coefficient for stomatal closure. Kc_{Tr} is the crop transpiration coefficient (determined by canopy cover and $Kc_{Tr,x}$), $Kc_{Tr,x}$ is the coefficient for maximum crop transpiration, and ETo is reference evapotranspiration (mm).

Biomass production is computed from crop transpiration and crop water productivity normalised for ETo and CO_2 (Equation (2.3-4)). The extreme effect of low temperature on crop phenology, biomass accumulation, and harvest index, is considered with adjustment factors (Montoya et al. 2016; Raes et al. 2009b).

$$B = K_{s_b}.f_{WP}.WP^*.\frac{Tr}{ETo} \qquad (2.2\text{-}4)$$

where B is biomass, Tr is crop transpiration (mm day^{-1}), ETo is reference evapotranspiration (mm day^{-1}), and K_{s_b} is the stress coefficient for low-temperature effects on biomass production. f_{WP} is the adjustment factor to account for differences, if any exist, in the chemical composition of the vegetative biomass and harvestable organs. WP^* is normalised crop water productivity, defined as the ratio of biomass produced to water transpired, normalised for the evaporative demand and CO_2 concentration of the atmosphere.

The AquaCrop stress indicators include water storage (not enough water), waterlogging (too much water), air temperature (too high or too low), and soil salinity stress (too high).

2.3 Deficit irrigation

Under some circumstances, the maximum attainable income for an irrigated field may be achieved by deficit irrigation (English 1990). Deficit irrigation can aid in coping with situations where there is a restricted water supply or when full irrigation is not possible (Fereres and Rabanales 2007). The deficit irrigation (DI) concept was established in the 1970s (James and Lee 1971) and refers to irrigation below full crop evapotranspiration (ET) by considering the profit-maximising level of water use (Capra and Consoli 2008). By definition, DI is an optimisation strategy whereby net returns are maximised by reducing the amount of irrigation water applied to a crop to a level that results in some yield reductions caused by water stress (Lecler 1998).

DI has been applied in various aspects (Capra and Consoli 2008). Initially, some applications have stressed crops to under-irrigation during their entire biological cycle, while other authors have tried to find an irrigation strategy to maximise yield with a minimum rate of water application. A recent strategy is to use regulated deficit irrigation (RDI) or controlled deficit irrigation (CDI) which is based only on a

reduction of irrigation amounts during certain plant cycle phases (Capra and Consoli 2008).

DI scheduling strategies and approaches try to answer the questions "under-irrigate by how much?", "when should the deficit be imposed?" and "how should the deficit be imposed?" (Capra and Consoli 2008). It is recommended that an analytical economic return analysis is performed with all economic factors that influence the profitability of irrigation, and that the optimal depth of irrigation water is chosen (Capra and Consoli 2008; English 1990). For example, land or water can be the limiting factors in choosing the optimum water depth. Therefore, we need to choose the main strategic goal between the maximisation of food production and profit (Capra and Consoli 2008). The detailed concept of the economic analysis framework for DI is presented by English (1990). To quantify the level of DI it is first necessary to define the full crop ET requirements (Fereres and Rabanales 2007). Generally, small irrigation amounts increase crop ET linearly, and this ends with the curvilinear relationship because part of the water applied is not used in ET and is lost (Fereres and Rabanales 2007). When yield reaches its maximum value and additional amounts of irrigation do not increase it any further. However, irrigation is applied in excess to avoid the risk of a yield penalty and considered as full irrigation. In DI, the level of water application is less full irrigation and the losses are limited. This results in a higher water productivity of irrigation water under DI compared to full irrigation.

DI has been applied successfully for increased water productivity for various crops without causing severe yield reductions (Geerts and Raes 2009a). English and Raja (1996) presented three analyses of deficit irrigation in real world situations of wheat production in the northwestern USA, cotton production in California and maize production in Zimbabwe, taking into account the crop production functions and cost functions. Their analysis suggested that i) in land-limiting situations and abundant water, the estimated optimal deficit strategy would be 15% or 16%, which represents appreciable water savings, resulting in profit gains of 8% to 13%; ii) in situations where irrigable land is abundant and water is scarce, optimal deficits were much larger in the water-limiting cases, ranging from 28% to 59%, with associated gains in total farm income between 44% and 68%; iii) deficits averaging 64% were found to be economically equivalent to full irrigation in the water-limiting cases, and deficits averaging 30% were found to be equivalent to full irrigation in the land-limiting cases. Many studies have shown that deficit irrigation could decrease crop redundant growth, minimise water use and improve WUE with little or no yield decline (dos Santos et al. 2007; Wang et al. 2015; Yang et al. 2017).

Because examining the yield response to different water applications in field experiments is laborious and expensive, modelling is a tool often used for assessing and developing deficit irrigation strategies (Geerts and Raes 2009a). Models allow the combined assessment of different factors affecting yield in order to derive optimal irrigation quantities for different scenarios of DI, and evaluating the risk-efficiency of the strategies (Geerts and Raes 2009; Cortignani and Severini 2009; Peake et al. 2016).

For these reasons, in this present study we have developed a methodology for irrigation scheduling considering deficit irrigation for optimised irrigation in the context of limited water.

3

Materials and methods

This chapter describes the materials, methods and tools that were used during this research. It also presents details of the environment of the study area.

3.1 Experimental site environment

The experimental sites were situated in the Chrey Bak catchment, which has an area of approximately 700 km^2 (Chem et al. 2011), in the Tonle Sap region. This is located at latitude between 11°53 and 12°14 N, and longitude between 104°13 and 104°49 E, in Kampong Chhnang Province, 90 km from Phnom Penh, Cambodia (Figure 3.1-1).

Stung Chrey Bak catchment is one of the areas of focus for irrigation developments during the 1980s and 1990s, to address the severe food insecurity that affected the country after the Khmer Rouge civil war (1975-1978) and the externally imposed economic blockade (1979-1991) (Chann et al. 2011). The existing small scale irrigation projects from the Khmer Rouge era have been rebuilt and expanded (Chann et al. 2011). The cultivated area of wet and dry rice in the catchment totals around 10 367 ha (Phalla et al. 2011). Up to 55% of the irrigation system projects function during the early dry season from January to March. Accordingly, rice production fields have expanded during the dry season around the irrigation system areas. However, those irrigation systems do not provide enough water to deliver to all the cultivated land. Huge areas of fallow land remain during the dry season (Figure 3.1-2). Alternatively, the land could be cultivated with vegetables that use less water compared to rice. This region is abundant in groundwater, which can be managed by smallholder farmers to irrigate the crop through wells. Moreover, the production of vegetable crops on small and family farms is an agricultural sector that can benefit from this agronomic practice to increase the income of the farmers (Nascimento et al. 2018). However, most of these farmers have limited knowledge of planting as vegetable crops require different planting techniques to rice, especially for irrigation. Therefore, in this research we have the aim of introducing irrigation management to these farmers. Lettuce is among the more valuable and high demand vegetables in the region. Therefore, we selected lettuce for the irrigation experiment.

3.1.1 Climate

The catchment is influenced by the tropical monsoon which has two seasons: the dry season from December to May, and the rainy season from June to November. The climate data were collected from weather station W2 (104°40′21.767″ E; 12°10′45.965″ N), downstream of the catchment, which has been installed in the catchment since 2009 (Figure 3.1-1). From data recorded during 2012-2014, the mean annual temperature was 27°C. The mean annual minimum and maximum humidity ranges from 51 to 92 percent, respectively. Average solar radiation was from 16.8 to 18 mega joules per square metre per day. Mean annual precipitation ranged from 1600 mm to 1788 mm.
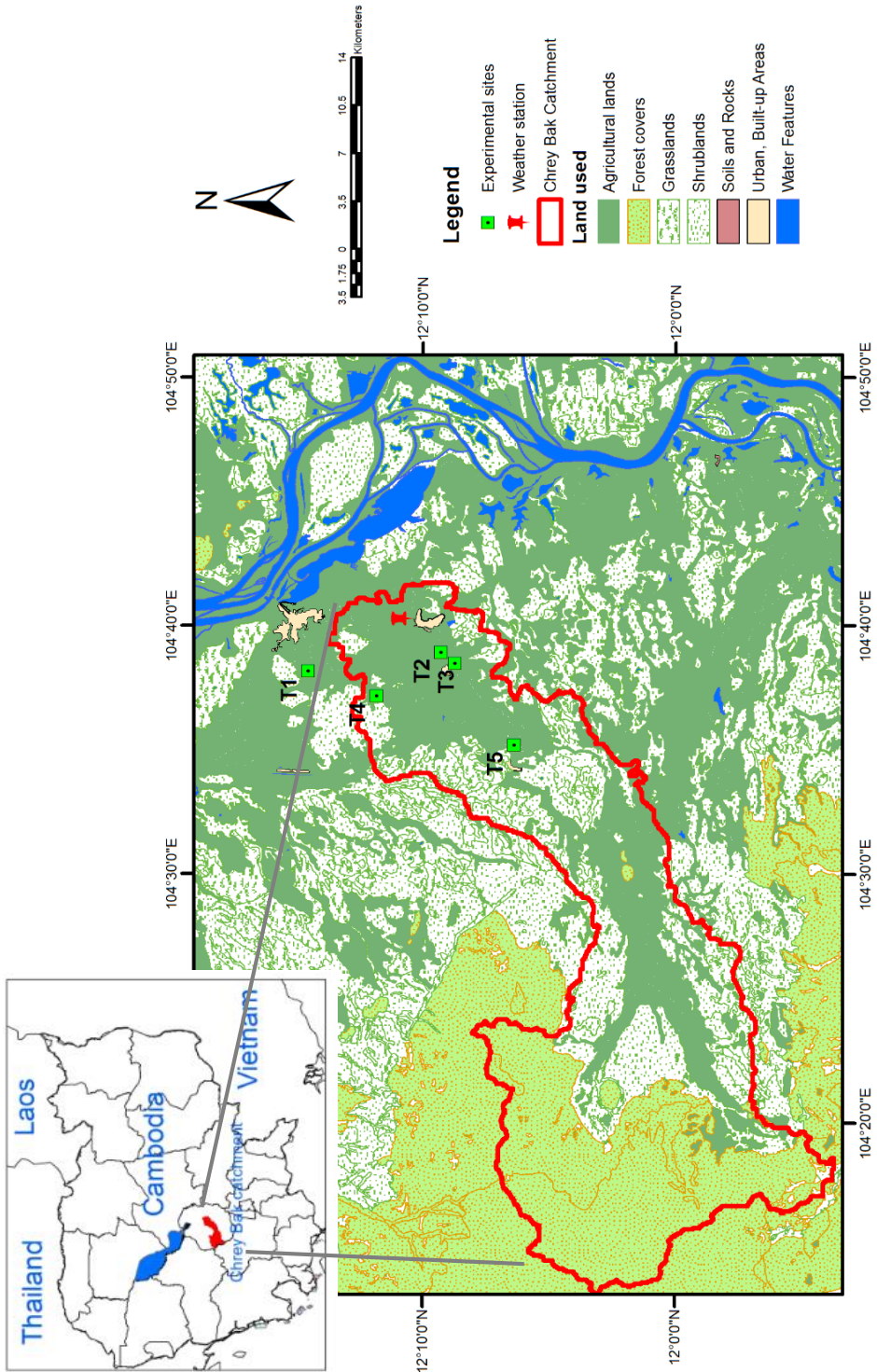
Figure 3.1-1 Map of the location of the experimental sites.

Figure 3.1-2 View of a paddy field during the dry season, downstream of Chrey Bak catchment, Kampong Chhnang Province.

3.1.2 *Groundwater in the Chrey Bak catchment*

It was observed that in this research catchment of Chrey Bak, groundwater was available in most of the area. There are abundant wells in the region. Most of the time, the people use this groundwater for domestic uses not irrigation. In this research, the irrigation experiments were conducted using groundwater. This PhD research is a part of a research project named "Improved surface-groundwater irrigation for crop diversification in Tonle Sap Lake Basin: Case study in Chrey Bak catchment". In another part of the project, the groundwater level was monitored in the Chrey Bak catchment during 2016 and 2017. The data from the research part is used to illustrate the groundwater variation in Figure 3.1-4. Observations of groundwater levels were taken in 15 bore wells throughout the catchment (Figure 3.1-3). The depth of wells varies from 2 to 15 m. Measurement with a water level meter was taken once a month from upstream (CB04, CB05, CB06, CB07, CB08, CB09 and CB10) to downstream areas (CB01, CB02, CB03, CB11, CB12, CB13, CB14 and CB15) from January 2015 to December 2016.

Figure 3.1-4 shows the monthly variation in groundwater levels and rainfall at the upstream and downstream parts of Chrey Bak catchment over the two years.

It is noted that upstream the groundwater varied from 2 to 5 m, while downstream it can vary from 1 to 9 m during the dry season. The largest drop in water level was recorded in the C13 well.
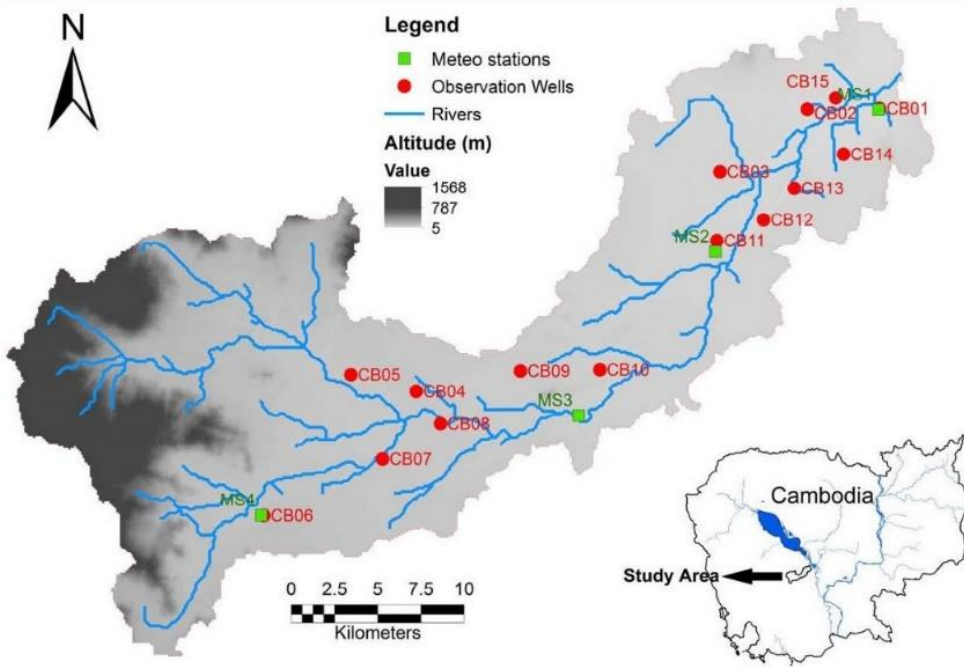
Figure 3.1-3 Location of monitoring wells (CB) in Chrey Bak catchment.
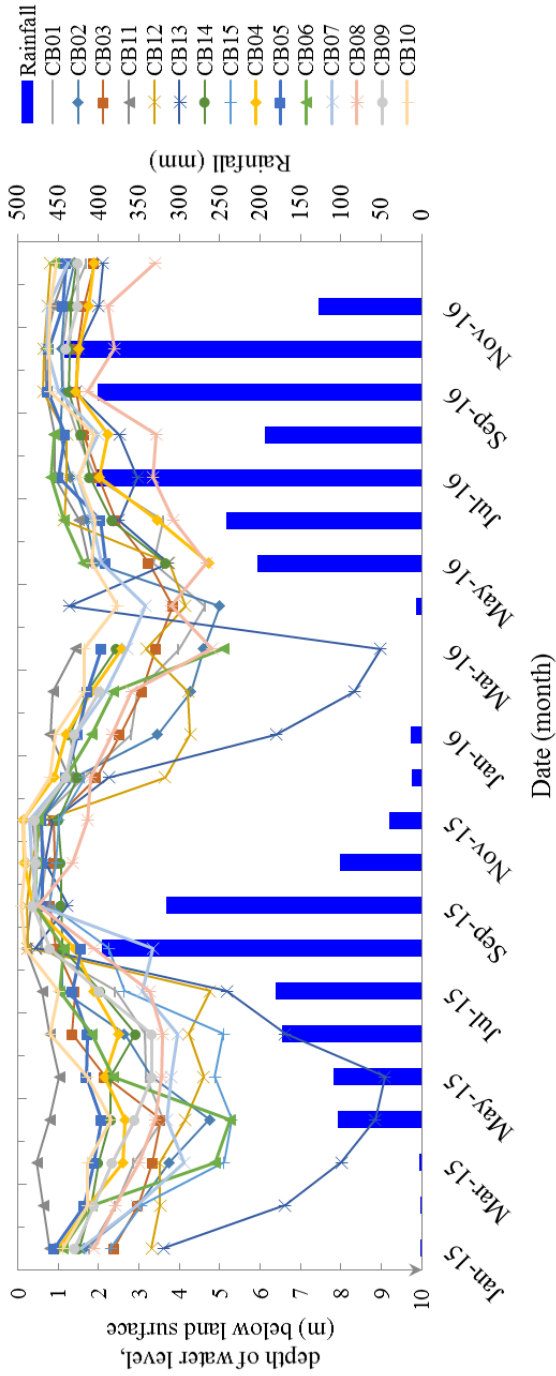
Figure 3.1-4 Seasonal variation in rainfall, groundwater level of Chrey Bak catchment

3.2 Experimentation

Five experimental sites indicated in Figure 3.1-1 are located in different villages in the lowland downstream of the catchment, named T1, T2, T3, T4 and T5, i.e., site T1 (104°38′13.539″ E 12°14′33.951″ N, at PreyMorn Village, site T2 (104°38′54.442″ E 12°9′15.482″ N, Chea Rov Village, site T3(104°38′35.317″ E 12°8′41.929″ N), Trapain Trach village, site T4 (104°37′16.24″ E 12°11′52.518″ N), Ou Roung Village, site T5 (104°35′15.321″ E 12°6′21.25″ N), Kouk Pouch Village. During the rainy season these sites are cultivated with rice and flooded.

The two seasonal growing experiments of planting lettuce using drip irrigation and groundwater were conducted over two years, 2016 and 2017. During the first growing season in 2016, the experiment was focused on the estimation of soil hydraulic properties in the five experimental sites, T1, T2, T3, T4 and T5. The data analysis of this experiment was performed in Chapter 4. The second experiment in 2017 was focused on crop growth characterisation in two experimental sites, i.e., T2 and T4.The experimental data in 2017 were analysed in Chapter 5. The total land area of each field was 400 m^2.

During the first growing season in 2016, lettuce was planted with a density of 16 plants m^{-2} in all five experimental sites (Figures 3.2-1 and 3.2-2). Lettuce seeds were sown in standard trays (123 holes). After 15 days, seedlings were transplanted into raised bed rows (0.30 m in height, with bed tops 0.50 cm wide and a top width of 1 m with no mulch cover). The organic compost was basally applied at the rate of 20 ton ha^{-1} before transplantation. Transplantation of the lettuce seedlings and harvesting took place on 30 January and 4 March, respectively. The soil was prepared by plowing before the construction of the beds. There was no rain during the experiment. Irrigation was applied using the drip irrigation system with groundwater pumping. The drip line has a 30 cm emitter space with manufacturer's maximum capacity of 3 L h^{-1}. The irrigation was performed by the farmers. We asked them to irrigate using their usual practices. Therefore, they irrigated twice daily, once in the morning and once in the evening. We estimated the irrigation amounts used by the farmers based on the fluctuation of measured soil moisture and the manufacturer's emitter irrigation rate.

For the second experiment for the second approach in chapter 5, the cultivation process was similar to that of the first growing season experiment. The second growing season for the lettuce experiment was conducted in August and September in 2017. Notably, this experiment took place during the rainy season due to time constraint during the research. Transplantation of the lettuce seedlings at sites T2 and T4 took place on 13 and 21 August, respectively. The harvesting of T2 and T4 took place on 27 and 24 September, respectively. This time, we used plastic covers to minimise soil moisture evaporation. We controlled the irrigation ourselves, dependent on the soil moisture depletion. As the lettuce cannot be grown well under heavy rain, UV plastic was used as a roof to cover bed rows to protect the crop. Due to the intense rain which flowed between the crop rows, water ponding at 20 cm below the top bed row level was observed between the lettuce rows at both sites during almost the entire growing period. This ponding kept the soil wet during the growing period. At site T4 irrigation was not applied after a week after planting, due to the benefit of water

ponding. At site T2, even though there was also water ponding in the field, the irrigation was applied every other day. The irrigation was determined by checking soil moisture (SM) using the feel and appearance method of Klocke and Fischbach (1984). The irrigation was performed when the SM was depleted below field capacity in the root zone at 5 cm, as lettuces were observed having a root depth of 5–10cm.

Figure 3.2-1 Views of the experimental sites during the growing season in 2016. a) site T1, b) Site T2, c) site T3, d) site T4.

Figure 3.2-2 Views of the experimental sites during the growing season in 2016 at site T5.

3.3 Measurement of soil properties

3.3.1 Soil profile description

Five pits of experimental sites with 1 metre depth (Figure 3.3-1) were dug at the beginning of the research in April 2015 to describe the soil profiles according to the United Nations' Food and Agriculture Organization (FAO) soil description guide (FAO 2006). Four of the sites presented as coarse soils, e.g. T1, T2, T3 and T5. The detailed soil description is presented in Table 3.3-1.

Figure 3.3-1 Soil pits at the experimental sites. a) site T1, b) Site T2, c) site T3, d) site T4.

Figure 3.3-2 Soil pits at the experimental site, T5.

Table 3.3-1 (Part I) Soil description of the study sites.

Sites	Soil FAO Description
T1	Horizon 1 (Ap): Depth: 0–20 cm, texture: loamy sand, structure: blocky subangular, soil colour: 10YR3/3, consistency of soil when dry: very friable, soil stickiness: slightly sticky, soil plasticity: slightly plastic, bulk density: 1.4–1.6 kg dm^{-3}.
	Horizon 2 (B1): Depth: 20–50 cm, texture: loamy sand, structure: blocky subangular, soil colour: 7.5YR7/6, consistency of soil when dry: very friable, soil stickiness: non-sticky, soil plasticity: non-plastic, bulk density: 1.4–1.6 kg dm^{-3}.
	Horizon 3 (B2): Depth: 50 cm+, texture: loamy sand, structure: single grain, soil colour: 7.5YR7/8, consistency of soil when dry: very friable, soil stickiness: non-sticky, soil plasticity: non-plastic, bulk density: 1.4–1.6 kg dm^{-3}.
T2	Horizon 1 (Ap1): Depth: 0–10 cm, texture: sand, structure: single grain, soil colour: 7.5YR5/3, consistency of soil when dry: loose, soil stickiness: slightly sticky, soil plasticity: slightly plastic, bulk density: 0.9–1.2 kg dm^{-3}.
	Horizon 2 (Ap2): Depth: 10–40 cm, texture: sand, structure: single grain and subangular, soil colour: 7.5YR7/3, consistency of soil when dry: loose, soil stickiness: slightly sticky, soil plasticity: slightly plastic, bulk density: 1.2–1.4 kg dm^{-3}.
	Horizon 3 (B): Depth: 40 cm+, texture: sand, structure: single grain and subangular, soil colour:7.5Y5/4, consistency of soil when dry: loose, soil stickiness: slightly sticky, soil plasticity: slightly plastic, bulk density: 1.2–1.4 kg dm^{-3}.
T3	Horizon 1 (Ap): Depth: 0–20 cm, texture: sand, structure: single grain to subangular, soil colour: 7.5YR5/6, consistency of soil when dry: loose, soil stickiness: slightly sticky, soil plasticity: slightly plastic, bulk density 1.2–1.4 kg dm^{-3}.
	Horizon 2 (B): Depth: 20–60 cm, texture: sand, structure: single grain to subangular, soil colour: 7.5YR5/6, consistency of soil when dry: loose, soil stickiness: slightly sticky, soil plasticity: slightly plastic, bulk density 1.2–1.4 kg dm^{-3}.
	Horizon 3 (C): Depth: 60 cm+: Bed rock.

Table 3.3-1 (Part II) Soil description of the study sites.

Sites	Soil FAO Description
T4	Horizon 1 (Ap1): Depth: 4–17 cm, texture: loam, structure: subangular, soil colour: 7.5YR5/3, consistency of soil when dry: hard, soil stickiness: sticky, soil plasticity: plastic, bulk density: 1.4–1.6 kg dm^{-3}.
	Horizon 2 (A2): Depth: 10–40 cm, texture: loam, structure: massive subangular, soil colour: 7.5YR6/3, consistency of soil when dry: very hard, soil stickiness: very sticky, soil plasticity: very plastic, bulk density: 1.0–1.2 kg dm^{-3}.
	Horizon 3 (B): Depth: 17 cm+, texture: silty clay, structure: massive subangular, soil colour: 7.5YR7/3, consistency of soil when dry: extremely hard, soil stickiness: very sticky, soil plasticity: very plastic, bulk density: 1.0–1.2 kg dm^{-3}.
T5	Horizon 1 (Ap): Depth: 0–30 cm, texture: loamy sand, structure: single grain to subangular, soil colour: 7.5YR5/4, consistency of soil when dry: soft, soil stickiness: slightly sticky, soil plasticity: slightly plastic, bulk density: 0.9–1.2 kg dm^{-3}.
	Horizon 2 (B): Depth: 30 cm+, texture: sandy loam, structure single grain to subangular, soil colour: 7.5YR7/3, consistency of soil when dry: hard, soil stickiness: sticky, soil plasticity: plastic, bulk density: 1.4–1.6 kg dm^{-3}.

3.3.2 Determination of the physicochemical properties

After pedological characterisation, soil samples were collected to measure soil chemical and physical parameters as indicated in (Table 3.3-2). The samples were air-dried and passed through a 2 mm mesh sieve for chemical analyses at the peodological laboratory, Gembloux Agro-Bio Tech. Some of the physical parameters, bulk density and pF curves were measured at the soil laboratory, Institute of Technology of Cambodia. The soils of each field were used to determine the soil texture, bulk density (BD) and SWRC with three replications at the laboratory. The soil textures were measured using a pipette method (Pansu and Gautheyrou 2007). The bulk densities were measured by the core method (Margesin and Schinner 2005). Porosity (∅) and void ratio (e) were calculated from bulk density (Bd) assuming an average mineral density of 2.65 g cm^{-3} (Andersland et al. 2004). pH of the water was measured by potentiometry (Liénard and Colinet 2018). Cation exchange capacity (CEC) was measured by exchangeable cations method described in Sparks et al. (1996). Electrical conductivity (EC) was measured by electrical conductivity meter (EC meter). We used colorimetric method described in Sparks et al. (1996) to measure extractable phosphors (P), extractable potassium (K). Soil organic carbon (C) was measured using Walkley-Black method. Kjeldahl Method was used to measured total nitrogen (N) concentrations.

3.3.2.1   Soil permeability

Soil permeability of the experimental sites was measured in-situ using a tension infiltrometer (Eijkelkamp Agrisearch Equipment, Giesbeek, Netherlands) (Figure 3.3-3). The supply pressure heads during the measurement were -5, -10, -15 cm. The Wooding (1968) method was used to analyse tension infiltrometer data to determine saturated hydraulic conductivities (Ks).
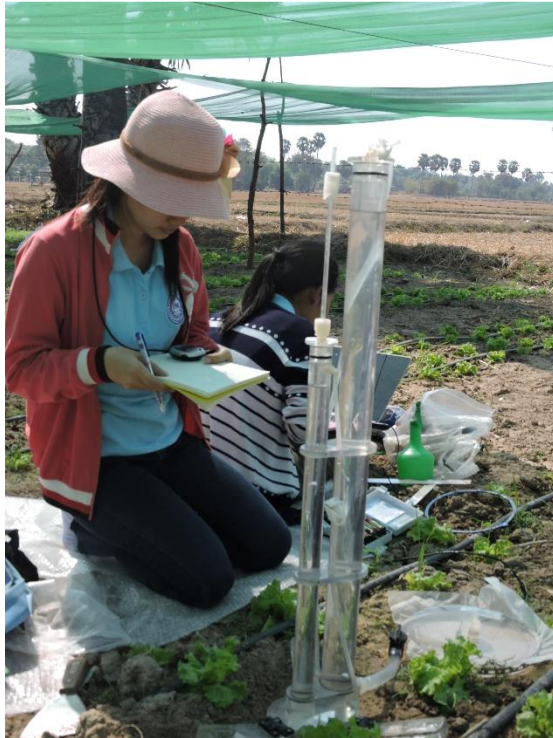
Figure 3.3-3 Hydraulic conductivity measurement with tension infiltrometer at the experimental fields.

3.3.2.2   Determining laboratory soil water retention curve (SWRC)

pF curves were measured using ceramic pressure plate plate (Eijkelkamp Agrisearch Equipment, Giesbeek, Netherlands) (Figure 3.3-4) with the head range of 6, 10, 30, 70, 100, 500 and 1500 kPa. The relative soil moisture was measured using oven dry during 24h at 75°C (Dane et al. 2002a).

Figure 3.3-4 pF cure measurement with ceramic pressure plate.

3.3.2.3 Determining in-situ soil water retention curve (SWRC)

In the first experiment in 2016, in situ SWRC data collection was conducted in the five experimental fields during the development stage of lettuce under drip irrigation during 2016 starting from 14 February (site T1), 18 February (sites T2 and T3), 23 February 2016 (sites T4 and T5). The SWRCs were measured using coupled inexpensive Decagon Devices sensors, e.g., soil moisture sensor 10HS (Decagon Devices, Pullman, WA, USA) and a soil water matric potential sensor MPS-2 (Decagon Devices, Pullman, WA, USA) connected to Em50 data logger (Decagon Devices, Pullman, WA, USA) (Fisher and Gould 2012). The sensors were installed horizontally near each other at depths of 10 cm and 20 cm below the soil surface between irrigated lettuces (see Figure 3.3-5) at sites T1, T2, and T3 and below the bare soil at sites T4 and T5. The sensor record was from 1 to 21 March 2016 at site T1, from 22 February to 21 March at site T2, from 14 February to 21 March at site T3, from 22 February to 21 March at sites T4 and from 7 to 21 March at site T5. Data from the sensors were recorded at 30 min intervals. The sensors of 10HS and MPS-2 for SWRCs measurement were available only at 20 cm depth at T1 and 10 cm depth at T5. The sensors are described below.

MPS-2 is the dielectric water matric potential sensor (Decagon Devices 2016). MPS-2 measures the water content of porous ceramic discs using a capacitive reading and converts the measured water content to water potential using the ceramic moisture

characteristic curve. The range of the measurement is from –10 to –500 kPa (pF 2.01 to pF 3.71). Sensor accuracy is ± 25% of the reading between –9 and –100 kPa. MPS-2 has been confirmed to have good reliability in its respective range (Degré et al. 2017). Accuracy can decrease up to approximately ± 35% and ± 50% at − 300 kPa and − 500 kPa, respectively (Decagon Devices 2011). The MPS-2 is pre-calibrated by the manufacturer and is not affected by soil type but requires correct installation with adequate hydraulic contact. The 10HS is a capacitance sensor related to dielectric permittivity (Decagon Devices 2010). 10HS has a measurement range of 0–0.57 cm^3 cm^{-3} and an accuracy of ± 0.03 $cm^3 cm^{-3}$. It operates at a frequency of 70 MHz and can be used at temperatures between 0 and +50°C with a permittivity measurement volume of 1 dm^3 (Visconti et al. 2014). Mittelbach et al. (2012) reported that the 10HS sensor fails to measure soil moisture (θ) above 0.4 cm^3 cm^{-3} and presents decreasing sensitivity in measuring θ with increasing θ, resulting in a poor ability to represent the variability in θ for moist conditions. The 10HS sensors in this study were calibrated following Decagon's step-by-step instructions (Cobos and Chamber 2005) using the calibrated equation in Table 3.3-2.

Table 3.3-2 Calibrated equations for 10HS at the different sites.

Site	Calibration Equation	R^2
T1	VWC = 0.0005 raw − 0.3715	0.98
T2	VWC = 0.0005 raw − 0.3712	0.95
T3	VWC = 0.0004 raw − 0.2591	0.98
T4	VWC = 7×10^{-7} raw^2 − 0.0008 raw + 0.2724	0.99
T5	VWC = 0.0005 raw − 0.3196	0.98

Figure 3.3-5 In-situ soil water retention curve measurement with a combination of 10HS and MPS-2 sensors. Installation of sensors (the picture was taken before inserting the sensors into the soil) at 10 and 20 cm depths.

3.3.2.4 Result of measurement of physicochemical soil properties

Table 3.3-3 presents the basic soil physical properties obtained from the measurement such as soil texture, soil bulk density, saturated hydraulic conductivity, and saturated soil moisture.

Some physicochemical soil properties are presented in Figures 3.3-6 to 3.3-11.

Among the sites, the percentage of sand, silt and clay ranged from 34 to 91%, 6 to 66% and 3 to 33%, respectively (Figure 3.3-6). Sand is the dominant particle in the area. Only T4 has fine soil, with similar sand and silt particles at 40 to 55%. Generally, all soils are acid having a pH below 7 (Figure 3.3-7). The pH ranged from 4.3 to 6.4. The highest pH values were observed in the fine soil at site T4, while the coarse soils tend to have low pH values, especially in deeper soil. Seng et al. (2005) characterised the chemical properties in Prey Khmer village, which has a sandy soil texture, and found a similar pH of 5.6. Soil organic carbon (C) ranges from 0.06 to 1.5% (Figure 3.3-8). The fine soil at T4 had the highest C and the coarse soils at the other sites were

relatively very low in C. Total nitrogen (N) concentrations, extractable phosphorous (P) and extractable potassium (K) in all sites ranged 1.2 to 15 mg/100 g, 0.01 to 2.8 mg/100 g and 0.3 to 49 mg/100 g, respectively (Figure 3.3.9). Unsurprisingly, K and N are dominant at T4 in the first surface layer and decreased significantly in the deeper layer. P has very low values in all sites. Overall, the coarse soils in other sites have very low N, P and K. Thus, the experimental sites are low in nutrients. It is noted that only the top soil of site T4 has very significant electrical conductivity (EC) of 141 μS, while the other soil layers and sites have low EC between 10-32 μS(Figure 3.3-10). The cation exchange capacity (CEC) ranged from 0.25-6.17 cmol+/kg(Figure 3.3-11). As expected, the coarse soils have very low CEC and the highest CEC was found for the finer soil at T4.

Table 3.3-3 Soil hydraulic properties.

Site	Depth	H	Clay (%)	Silt (%)	Sand (%)	Bd (g/cm³)	Ø	e	θ_{ini}	pH water	K_s	θ_s
T1	(0–10 cm)	Ap1	3.74	12.75	83.49	1.473 ± 0.01	0.44	0.80	0.13	4.66	1.41 ± 1.13	0.34 ± 0.01
	(10–20 cm)	Ap2	-	-	-	1.840 ± 0.10	0.31	0.44	0.13	-	-	-
T2	(0–10 cm)	Ap1	4.13	8.95	86.91	1.52 ± 0.06	0.43	0.74	0.27	5.17	0.46 ± 0.09	0.31 ± 0.015
	(10–20 cm)	Ap2	3.64	7.28	89.07	1.66 ± 0.02	0.37	0.60	0.27	4.89	-	-
T3	(0–10 cm)	Ap1	4.31	8.12	87.55	1.52 ± 0.02	0.43	0.74	0.13	4.46	1.45 ± 0.83	0.33 ± 0.007
	(10–20 cm)	Ap2	-	-	-	1.72 ± 0.06	0.35	0.54	0.13	-	-	-
T4	(0–10 cm)	Ap1	5.02	54.77	40.19	1.47 ± 0.08	0.45	0.80	0.19	6.25	0.26 ± 0.21	0.43 ± 0.023
	(10–20 cm)	Ap2	7.41	43.56	49.01	1.67 ± 0.01	0.37	0.59	0.19	4.87	-	-
T5	(0–10 cm)	Ap1	3.80	17.89	78.31	1.48 ± 0.05	0.44	0.79	0.12	5.35	0.31 ± 0.16	0.35 ± 0.005
	(10–20 cm)	A/Bp	23.87	18.83	57.28	1.77 ± 0.03	0.33	0.50		6.06	-	-

Note: H: horizon, Bd: Bulk density (g cm^{-3}), Ø: porosity (-), e: void ratio (-), θ_{ini}: initial water content (cm³ cm^{-3}), Ks: saturated hydraulic conductivity (mm s^{-1}), θ_s: saturated soil moisture (cm³ cm^{-3}).
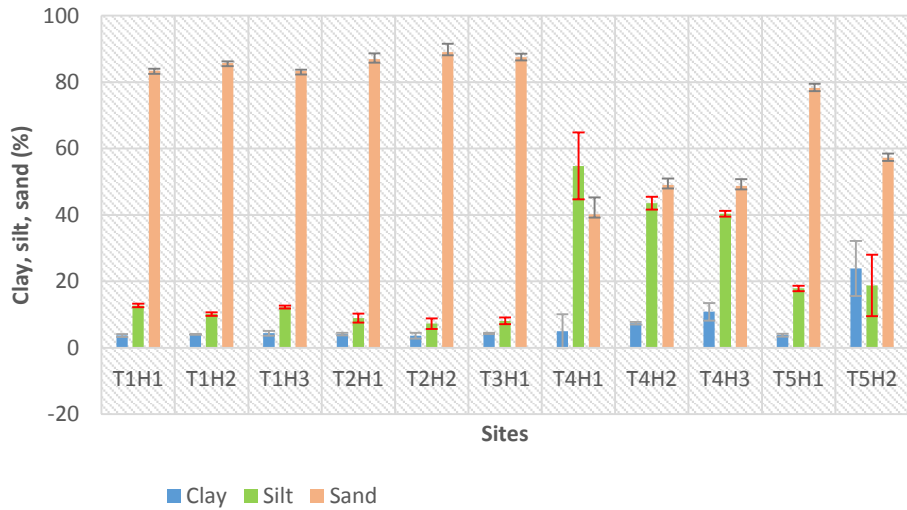
Figure 3.3-6 Soil particles for each site. Note: T1-T5 are site T1-T5, H1-H3 are soil horizon 1-3.
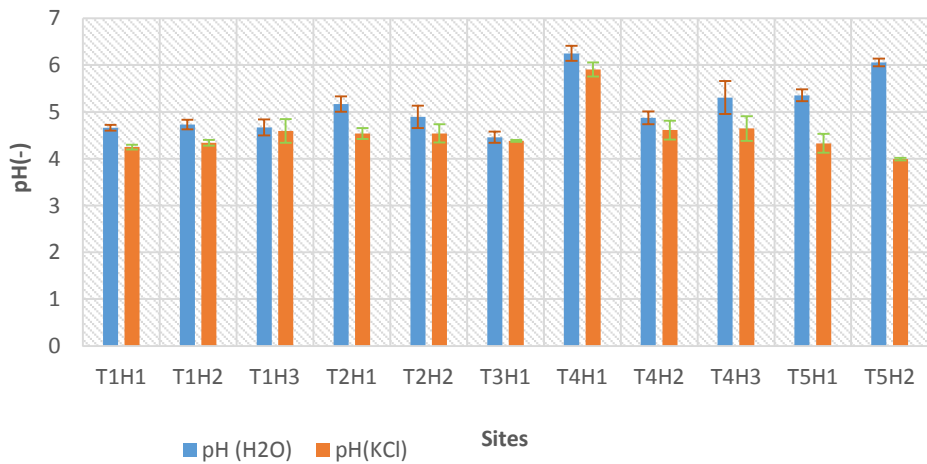
Figure 3.3-7 Soil pH for each site. Note: T1-T5 are site T1-T5, H1-H3 are soil horizon 1-3.
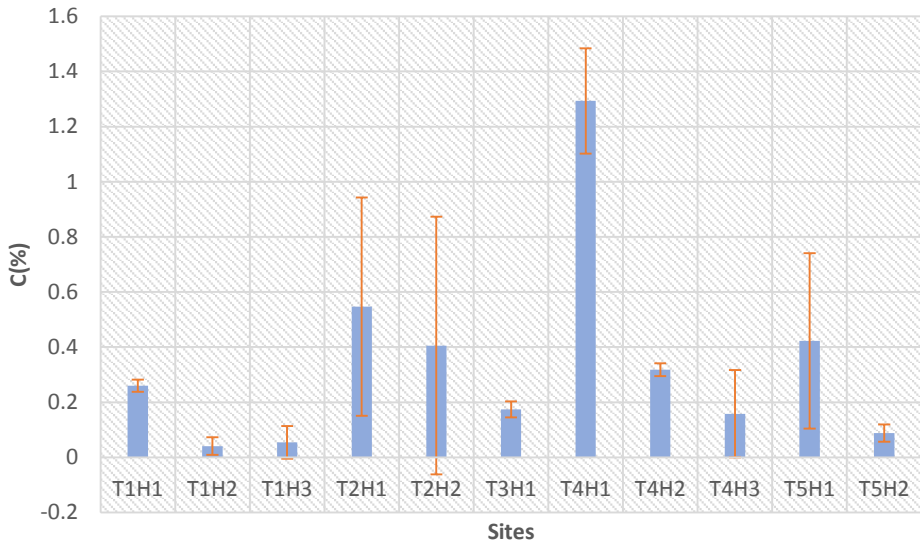
Figure 3.3-8 Soil organic carbon (C) for each site. Note: T1-T5 are site T1-T5, H1-H3 are soil horizon 1-3.
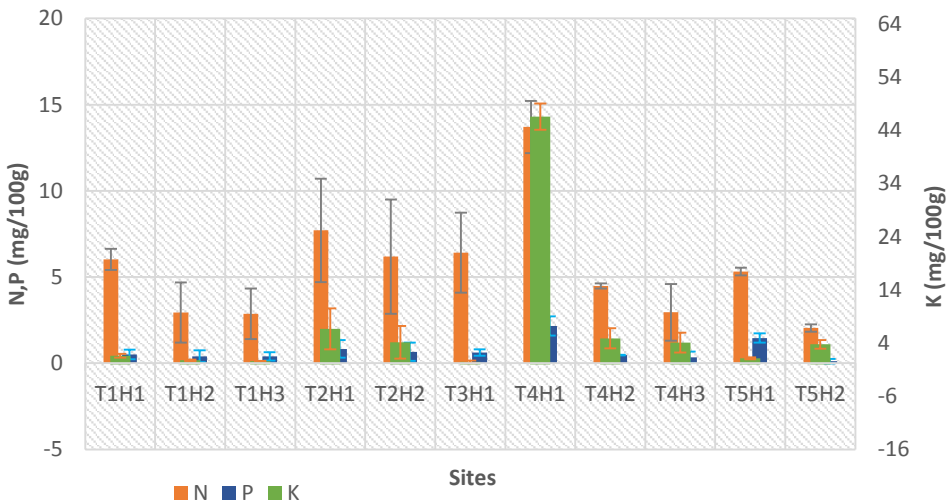
Figure 3.3-9 Total nitrogen (N) concentrations, extractable phosphors (P), extractable potassium (K) for each site. Note: T1-T5 are site T1-T5, H1-H3 are soil horizon 1-3.
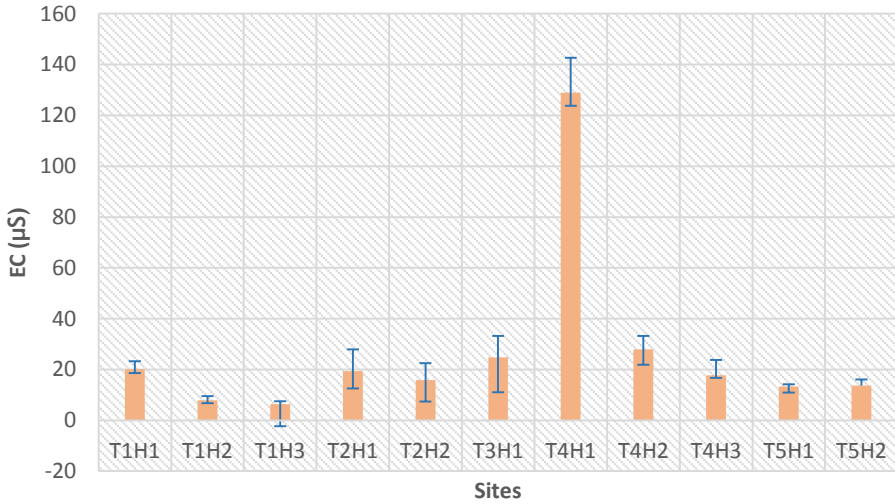
Figure 3.3-10 Electrical conductivity (EC) for each site. Note: T1-T5 are sites, H1-H3 are horizons.
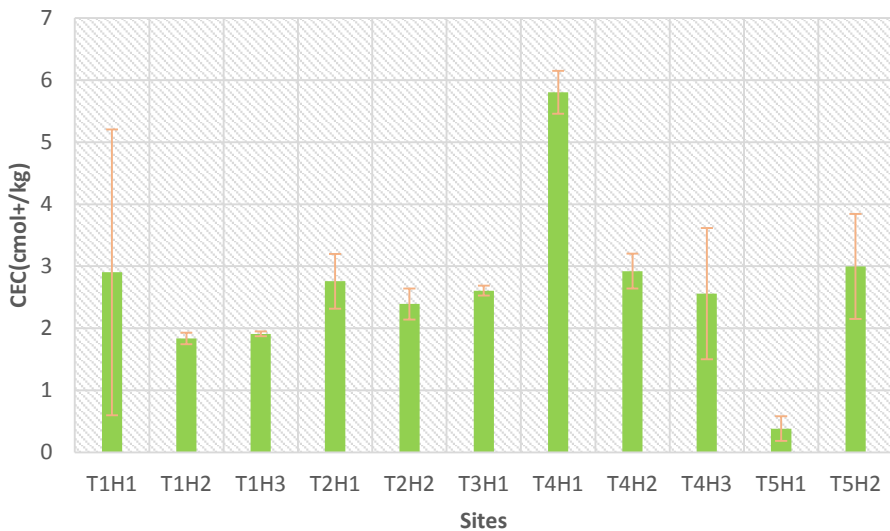
Figure 3.3-11 Cation exchange capacity (CEC) for each site. Note: T1-T5 are site T1-T5, H1-H3 are soil horizon 1-3.

3.4 Estimation of soil water retention curves (SWRC)

3.4.1 Comparison of different methods in estimating SWRC

We compared different methods: the Rosetta method, fitted field SWRC method, fitted laboratory SWRC method, and inverse solution modelling to evaluate their performance in estimating SWRC. The field data during the growing season in 2016 were used.

Rosetta method, Method 1 (M1)

The Rosetta pedotransfer function (Schaap, et al. 2002) was used to calculate the unknown van Genuchten parameters, θ_r, θ_s, α, n by considering the soil texture and bulk density.

Fitted field SWRC method, Method 2 (M2)

The field SWRCs were obtained from coupling the soil moisture sensor 10HS and potential sensor MPS-2 at depths of 10 cm and 20 cm in each field. The SWRC calculated using the van Genuchten (vG) equation (Equation (2.1-5)) was fitted to the field SWRC data by minimising the root mean square error (RMSE) (Equation (3.4-1)) between the model and the data using the SOLVER routine of Microsoft Excel software (Microsoft Company, Redmond, WA, USA). The initial values of vG parameters from the Rosetta method were used.

$$\text{RMSE} = \sqrt{\frac{\sum_{i=1}^{n}\left(\theta_{f,i} - \theta_{vG,i}\right)^2}{n}} \tag{3.4-1}$$

where $\theta_{f,i}$ denotes the experimental data, i.e., the measured 10HS soil water content at a given MPS-2 pressure head, $\theta_{vG,i}$ is the corresponding modelled soil water content, and n is the number of the (h, θ) data pairs.

Fitted laboratory SWRC data method, Method 3 (M3)

The same procedure as Method 2, the van Genuchten Equation were fitted with the the laboratory SWRC data by minimizing the objective equation (3.4-2), were used to obtain vG parameters from laboratory SWRC. The initial values of vG parameters from the Rosetta method were used.

$$\text{RMSE} = \sqrt{\frac{\sum_{i=1}^{n}\left(\theta_{lab,i} - \theta_{vG,i}\right)^2}{n}} \tag{3.4-2}$$

where $\theta_{lab,i}$ is the measured oven soil water content at a given pressure plate head, $\theta_{vG,i}$ is the corresponding modelled soil water content, and n is the number of the (h, θ) data pairs.

Inversion method, Method 4 (M4)

The inverse modeling using HYDRUS-1D was used to fit the in-situ SWRC.

Root water uptake S(h) of lettuce crop was simulated using the model of Feddes et al. (1978).

$$S(h) = \alpha(h) \times S_p \tag{3.4-3}$$

where α is the dimensionless function and varies between 0 and 1 depending on soil matrix potentials, Sp ($L^{-3}L^{-3}T^{-1}$) is the potential root water uptake and assumed to be equal to potential transpiration (T_p).

The upper condition for water flow was an atmospheric condition influenced by irrigation supply, and potential evapotranspiration, ETp (LT^{-1}) with a surface layer. The initial soil moisture profile at each layer site was set to the initial observed moisture data. The free drainage was considered as a boundary at the bottom of the soil domain. ETp was calculated from the reference evapotranspiration, ETo (LT^{-1}) by the equation below.

$$ET_p = K_c \times ET_o \tag{3.4-4}$$

where Kc is crop coefficient computed by Feddes et al. (1978). Default crop parameters of lettuce in Hydrus 1D were used. Daily ETo was simulated based on the FAO Penman-Monteith method (Allen et al. 1998b) in Hydrus-1D using daily meteorological data (e.g. precipitation, air temperature, solar radiation, relative humidity, and wind speed recorded in 5 min time steps) from weather station W2 (Figure 3.4-1).

Then, ETp was separated into potential evaporation, Ep (LT^{-1}) and potential transpiration, Tp (LT^{-1}) based on Beer's Law.

$$E_p = ET_p \times e^{-k.LAI} \tag{3.4-5}$$
$$T_p = ET_p - E_p \tag{3.4-6}$$

where k = extinction coefficient with default value of 0.463, LAI = leaf area index (L^2L^{-2}).

It is noted that at T4 and T5, the sensors were placed in the soil where the plants did not grow, therefore, no crop condition was considered for these sites. Also, there was only the retention curve data for 20 cm depth at T1.

The van Genuchten models for deriving the retention curve and the hydraulic conductivity function were adopted. Unknown parameters e.g. θ_r, θ_s, α, n, and l given were optimised to match the daily average observed soil water contents with the inversion algorithm implemented in the Hydrus-1D mode.

Observation nodes were set at 10 and 20 cm following the location of the 10HS and MPS-2 sensors. The Marquart-Levenberge nonlinear minimisation method (Gutmann and Small 2007; Levenberg 1944) used in Hydrus-1D is sensitive to the initial vG parameter values (Wang et al. 2016). The initial vG parameters predicted using Rosetta program of Method 1 were applied.
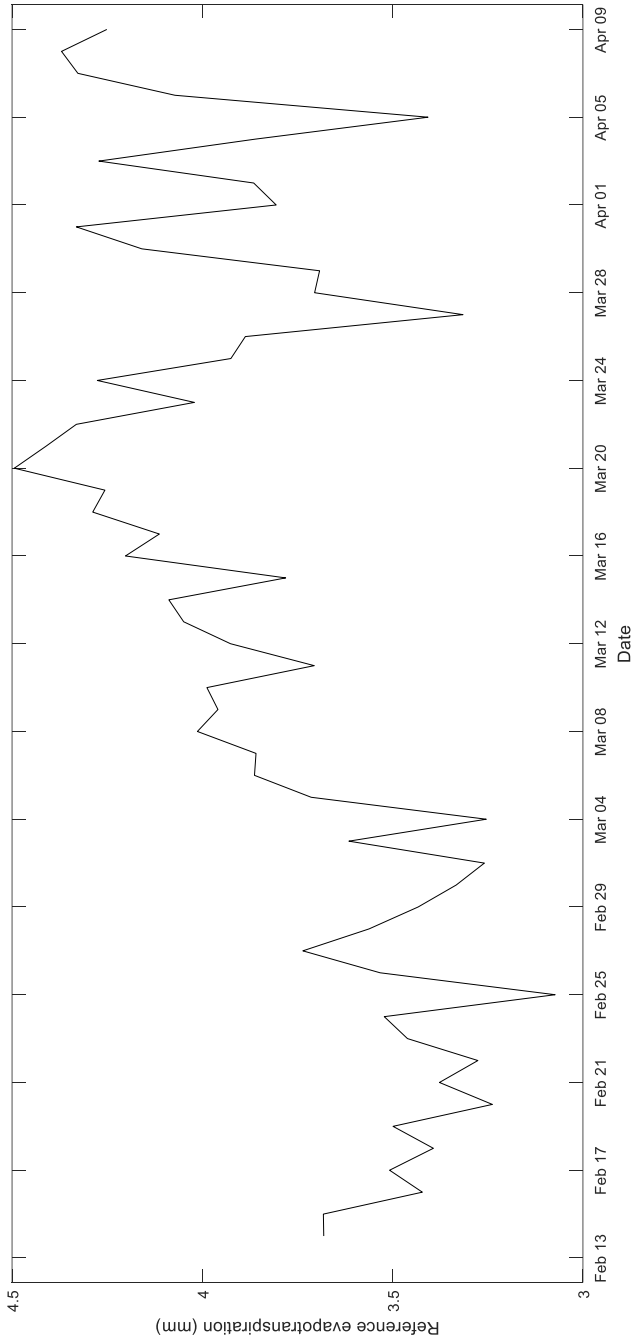
Figure 3.4-1 Daily reference evapotranspiration during the study period in 2016

Water flow simulation

To test the capability in hydrodynamic performance, all the parameters obtained from different methods were applied in a Hydrus-1D model to simulate the water flow and root water uptake. For the three methods (methods 1, 2, and 3), the saturated hydraulic conductivity obtained from tension infiltrometers was used in the hydraulic properties and the l parameter of vG model was fixed at l=0.5.

Model performance

Three widely used statistical parameters were applied to evaluate the performances of the different methods to simulate the water flow processes, e.g. root mean square error (RMSE), Nash-Sutcliffe coefficient (Nash), and correlation coefficient (R^2).

$$RMSE = \sqrt{\frac{\sum_{i=1}^{n}(O_i - S_i)^2}{n}} \tag{3.4-7}$$

$$Nash = 1 - \frac{\sum_{i=1}^{n}(O_i - S_i)^2}{\sum_{i=1}^{n}(O_i - \overline{O})^2} \tag{3.4-8}$$

$$R^2 = \left(\frac{\sum_{i=1}^{n}(O_i - \overline{O})(O_i - \overline{S})}{\sqrt{\sum_{i=1}^{n}(O_i - \overline{O})^2 \sum_{i=1}^{n}(O_i - \overline{S})^2}}\right)^2 \tag{3.4-9}$$

where O and S = observed and simulated values at time/place i respectively; n= total amount of the data. When Nash and R^2 are close to 1, it is considered to be satisfied (Krause and Boyle 2005). RMSE should be close to zero for a good performance. The unit of RMSE is in $cm^3\,cm^{-3}$.

The result of this comparison of the different methods are presented in Appendix.

4

Estimating Soil Water Retention Curve by Inverse Modelling from Combination of In Situ Dynamic Soil Water Content and Soil Potential Data

This chapter focused on estimating the soil hydraulic properties using inverse modelling. This work has been published in Soil System Journal.

4.1 Introduction

In agriculture, soil water in unsaturated porous soil media is crucial for crop development (Zijlstra and Dane 1996). Adequate characterization of soil water movement can improve agricultural water management fundamentally and economically (Schwen et al. 2011; Huang et al. 2018; Lai and Ren 2016). The soil water retention curve (SWRC) is considered to be a paramount and a priori property of the hydraulic behavior of soils (Schwen et al. 2011; Le Bourgeois et al. 2016; Vereecken et al. 2016; Peters and Durner 2008; Moret-Fernández and Latorre 2017; Hopmans and Simunek 1999). SWRCs are essentially required to estimate the soil water availability for plant use, and to simulate water and solute flow in vadose zones (Gupta and Larson 1979). The definition and measurement of the SWRC are described in the section 2.1.1 (Chapter 2).

In recent decades, an inverse solution has appeared as an attractive procedure to obtain SWRCs (Abbaspour et al. 2001; Wohling et al. 2008). Inversion estimation can be an easy and reliable procedure (Kumar et al. 2010). Several existing simulation model software tools include inverse estimation as embedded functions within the program (Osorio-Murillo et al. 2015). This approach involves estimating a set of limited unknown model parameters by using easily measurable variables (model output) such as water flow to compare to observation through the process of objective function optimization (Hopmans and Simunek 1999; Abbaspour et al. 2001). The soil hydraulic functions for inversion are described principally by analytical functions (van Dam et al. 1992) such as Gardner Gardner (1958), Durner (1994), Campbell (1974), and van Genuchten (1980). van Genuchten has gained wide recognition in generating a reasonable SWRC from various laboratory and field experiments (Lambot 2002). However, this model may not properly describe the hydrodynamic functioning of clay soils (Fuentes et al. 1992). Obtaining accurately the important parameters of the function is still a great challenge (Shi et al. 2015). The limitations of inverse modelling are mostly related to the solution uniqueness, and insufficient data due to limited measurement range of instruments used (Hopmans and Simunek 1999; Li et al. 2018). Minimization of the these problems can be obtained with the following precautions: (i) it should have inverse input data for objective function with a wide range of water content, soil pressure head and additional retention curve data from simultaneously measuring pressure head and water content data in the soil profile (Kool et al. 1985, Toorman et al. 1992, Eching and Hopmans 1993, Simůnek and van Genuchten 1997); (ii) initial soil parameter values should be reasonably close to their true values (Kool et al. 1985). Some studies proved that including water content or infiltration rate alone will not provide uniqueness of the optimized parameters in the inverse solution (Eching and Hopmans 1993; Simůnek and van Genuchten 1997). Schelle et al. (2013) recommended that instrumentation of a lysimeter equipped with pressure head sensors can significantly improve parameter identifiability of the inverse solution.

The inverse solution has been successfully applied to laboratory experiments with quick and precise results (Le Bourgeois et al. 2016; Simůnek and van Genuchten 1997; Schelle et al. 2013; Kechavarzi et al. 2009). A recent laboratory method for SWRC determination using transient water release and imbitions (TWRI) method

was developed by Wayllace and Lu (2011). This transient method involves using physical tests using electrical balance, and numerical tests using inverse modelling with HYDRUS and the van Genuchten model (Wang and Xiang 2014). The procedure presents a fast, accurate, and simple testing tool for obtaining SWRC and hydraulic conductivity functions of various types of soils under drying and wetting conditions. To date, this approach has been applied in geotechnical engineering with few experimental results establishing its validity and generality (Wang and Xiang 2014; Lu 2014; Mun et al. 2016; Lu et al. 2013; Lu and Godt 2013).

In the field conditions, numerous studies of the inverse estimation technique have been applied (Wang et al. 2016; Simůnek and van Genuchten 1997; Ritter et al. 2003). Notably, the HYDRUS model has increasingly and successfully been used for inverse estimation particularly in in situ conditions (Le Bourgeois et al. 2016; Verbist et al. 2009; Wohling et al. 2008; Köhne et al. 2009; Filipović et al. 2018). Lai and Ren (2016) determined soil hydraulic parameters at field scale by inverse modelling using combined HYDRUS-1D and PEST models. The authors confirmed that there are no unique effective average properties for a heterogeneous field to simulate field water content. Their results showed that the inverse modelling approach simulated soil water dynamics well, but still needs to be improved for layered soils, especially with fine-textured soil layer. Inverse modelling with the HYDRUS model was successfully performed by Filipović et al. (2018) who used infiltration experiments with tension disc infiltration data to estimate soil hydraulic properties. Similarly, Rashid et al. (2015) conclude that the HYDRUS inverse solution approach applied to infiltration data measured with a tension disc infiltrometer is a useful method to characterize soil hydraulic properties. Le Bourgeois et al. (2016) investigated an inverse modelling method using HYDRUS-1D and the NSGA-II algorithm to estimate soil hydraulic properties from in situ water content measurement. Their calibrated Mualem–van Genuchten parameters had very low uncertainty and could still result in a good simulation of water flow.

Previous studies on earlier inverse modelling studies mostly using HYDRUS focused on identifying soil hydraulic properties using infiltration experiments based on using tension disc infiltrometer data as discussed above. Thus, it is more interesting to inverse the soil hydraulic properties using field retention curve data with a fine timestep of dynamic soil moisture content and pressure head measured simultaneously.

The objectives of this study are twofold: (i) to estimate soil properties for retention curve using inverse modelling with HYDRUS-1D with input field data of dynamic water content and SWRCs; and (ii) to evaluate its ability to simulate the water flow process in a case study of Cambodian soils.

4.2 Materials and Methods

The experiment of lettuce irrigation was conducted in five experimental sites (T1, T2, T3, T4 and T5) in 2016. The experiment and data collection were described in Chapter 3.

4.2.1 5-Min Timestep Reference Evapotranspiration Computation

The reference evapotranspiration (ETo) was calculated based on standardized American Society of Civil Engineers (ASCE) Penman-Monteith equation (ASCE-PM) (Irmak et al. 2005; Allen et al. 2005) using meteorological data collected in 5-min timesteps (e.g., precipitation, air temperature, solar radiation, relative humidity, and wind speed) from the weather station (Figure 3.1-1). The standardized ASCE-PM equation is:

$$\text{ET}_o = \frac{0.408\Delta(\text{R}_n - \text{G}) + \gamma\dfrac{\text{C}_n}{\text{T} + 273}\text{U}_2(\text{e}_s - \text{e}_a)}{[\Delta + \gamma(1 + \text{C}_d\text{U}_2]} \qquad (4.2\text{-}1)$$

where ET_o is the standardized grass-reference evapotranspiration(ET) (mm 5-min^{-1}), Δ is the slope of saturation vapour pressure versus air temperature curve (kPa °C^{-1}), Rn is the calculated net radiation at the crop surface (Mega Joule (MJ) m^{-2} 5-min^{-1}), G is the heat flux density at the soil surface (MJ m^{-2} 5-min^{-1}), T is the air temperature at 1.5 to 2.5 m height (°C), U_2 is the wind speed at 2-m height, e_s is the saturation vapour pressure (kPa), e_a is the actual vapour pressure (kPa), γ is the psychrometric constant (kPa °C^{-1}). C_n is the numerator constant that changes with reference surface and calculation timestep (900 °C mm s^3 Mg^{-1} day^{-1} for 24 h timesteps, and 37 °C mm s^3 Mg^{-1} h^{-1} for hourly timesteps for the grass-reference surface, so 3.083 °C mm s^3 Mg^{-1} h^{-1} for 5-min timestep). Cd is the denominator constant that changes with reference surface and calculation timestep (0.34 s m^{-1} for 24 h timesteps, 0.24 s m^{-1} for hourly timesteps during daytime, and 0.96 s m^{-1} for hourly night time for hourly or shorter time steps for the grass-reference surface) (Allen et al. 2006). The values for Cn and Cd are associated with bulk surface resistance (r_s) and aerodynamic roughness of the surface (r_a) (Irmak et al. 2005, Tolk et al. 2015). The values $\text{r}_{s-daytime} = 50$ s m^{-1} and $\text{r}_{s-nighttime} = 200$ s m^{-1} were adapted in this study. The 5-min step G was a function of R_n ($\text{G}_{5min-day\,time} = 0.1$ R_n and $\text{G}_{5min-night\,time} = 0.5$ R_n).

4.2.2 Partitioning Crop Evapotranspiration

When the soil has full canopy cover, crop evapotranspiration (ET_c) is often assumed to be similar to transpiration (Kool et al. 2014). The soil not shadowed by crops is exposed to radiation, which is considered to be soil evaporation (Paredes et al. 2014). Therefore, crop transpiration is closely related to canopy cover. Partitioning of crop evapotranspiration (ET_c, mm min^{-1}) into soil evaporation (E, mm min^{-1}) and crop transpiration (T, mm min^{-1}) was based on the method proposed and described by Gallardo et al. (1996). Crop transpiration (T) was estimated according to reference evapotranspiration (ET_o) and ground canopy cover (G) using the following equation.

$$\text{T} = \text{ET}_o\text{K}_{c\,max}(0.63 + 1.373\text{G} - 0.0039\text{G}^2)/100 \qquad (4.2\text{-}2)$$

where T is the crop transpiration (mm min^{-1}), ET_o is the reference evapotranspiration (mm min^{-1}). $\text{K}_{c\,max}$ is the maximum crop coefficient (K_c) value. When ground cover is less than 10%, a K_c of lettuce is about 1.05 if it is well irrigated

(Doorenbos and Pruitt 1977). When a canopy cover reaching about 75%, lettuce has a $K_c > 1.05$ and $K_{c\ max} = 1.10$ was adapted for lettuce during the mid-season. G is the ground cover percentage, $G = Gx/[1 + e(a+bN)]$. Gx is maximum ground canopy cover (%). The coefficients a = 6.58 and b = −10.02 were adapted in this study. N is normalized accumulative reference evapotranspiration.

Soil evaporation (E) was partitioned with below equation.

$$E = ET_o K_{c\ max} - T \tag{4.2-3}$$

At site T4 and T5, sensors were placed in the soil profile where plants did not grow. Therefore, there was no partitioning ET_c at these sites. The crop input data for partitioning are shown in Table 4. The maximum crop canopy covers were measured using a smartphone camera at 1 m height at harvest time and converted into canopy cover percentage using the Canopeo smartphone app.

Table 4.2-1. Crop data for partitioning crop evapotranspiration.

Sites	Growing Stage	K_c	G_x (%)
T1	Mid-season	1.1	35
T2	Mid-season	1.1	57
T3	Development stage	0.78 to 1.1	44

4.2.3 Model Set-Up

We used the HYDRUS-1D software (version 4.16) (Šimůnek et al. 2005) for parameter estimation by inverse method. HYDRUS-1D simulates nonequilibrium procedures based on the governing modified Richards' equation (Equation (2.2-1)) to simulate water flow (May and Genuchten 2008; Richards 1931).

The van Genuchten (vG) model (van Genuchten 1980) was selected to describe the soil water retention functions (Equation (2.1-5)). The soil hydraulic conductivity, $K(\theta)$ was based on the Mualem (1976) model (Equation (2.1-6)). l of the equation Mualem was set to be 0.5 recommended by Mualem (1976).

The period of simulation was 21, 28, 36, 29 and 12 days at sites T1, T2, T3, T4 and T5 respectively during February and March 2016 according to the available data from the soil sensors, 10HS and MPS-2.

Air-Entry Value

The air-entry value (AEV) is a critical and commonly used variable obtained from the SWRC for estimating other unsaturated soil properties, i.e., permeability (Soltani et al. 2017; Zhai and Rahardjo 2013). AEV is defined as the suction at which drainage of the soil pores begins (Radcliffe and Simunek 2010; Barbour 1998). AEV occurs usually between –h = 1 to 10 kPa (Radcliffe and Simunek 2010). The AEV reflects the maximum soil pore size and the soil texture (Assouline and Tessier 1998). A decrease in soil grain size leads to an increase in AEV and flattening of the SWRC slope (Barbour 1998). A coarse-grained soil has a lower air-entry value, and lower residual suction than a fine-grained soil (Gallage and Uchimura 2010). Besides soil texture, other effects listed by Wang et al. (2000) are soil structure, initial water

content, contact angle, organic matter, clay content, and bulk density. Gallage and Uchimura (2010) found that soils with low density have lower AEV and residual suction than soils with a high density. Numerically, AEV is related to the α and n parameters of the vG model (Assouline and Tessier 1998). Lower values of α indicate that the air-entry region is broad (Radcliffe and Simunek 2010). Soltani et al. (2017) has proposed simplified methods to determine AEV as below.

$$h_{AEV} = \frac{10^{\frac{m+1}{2.3nm}\left[1-\left(\frac{m+1}{m}\right)^m\right]}}{\alpha m^{\frac{1}{n}}} \tag{4.2-4}$$

4.2.4 Time-Variable Boundary and Initial Conditions

HYDRUS-1D input data components in this study include input data for the variable boundary condition (i.e., evapotranspiration, transpiration, and irrigation), soil hydraulic properties and inverse input data (soil moisture in time and retention curve data). The variable boundary condition of this study is illustrated in Figure 4.2-1.

The upper boundary condition was set to an atmospheric condition influenced by irrigation supply, and crop evapotranspiration with a surface layer as indicated in the following equation:

$$-K\left(\frac{\partial h}{\partial z} + 1\right) = q_o(t) \quad z \geq 0; \, t = 0 \tag{4.2-5}$$

where $q_o(t)$ is the difference between irrigation, transpiration, and evaporation rate.

The free/zero-gradient drainage boundary condition is suitable for water flow simulation of unsaturated soil in which the soil domain of interest is not affected by groundwater (Seki et al. 2015; Yates 2000). The process allows water to leave a flow domain by gravity, assuming a unit vertical hydraulic gradient without external forced drainage conditions (Yates 2000). Based on these conditions and the assumptions of no influence of the groundwater to the studied soil profile, the free drainage was considered at the bottom of the soil domain. The free drainage condition is represented as follows:

$$-K\left(\frac{\partial h}{\partial z} + 1\right) = 0 \quad z = L_{sp}; \, t > 0 \tag{4.2-6}$$

Where L_{sp} is the soil profile assumed at 40 cm depth.

HYDRUS-1D can give water flow at any specific soil depth (Mazzacavallo and Kulmatiski 2015). The observation nodes were set at 10 and 20 cm following the location of the 10HS and MPS-2 sensors. The soil moisture at the beginning of the simulation in the soil profile domain was set to the initial observation from these 10HS sensors.
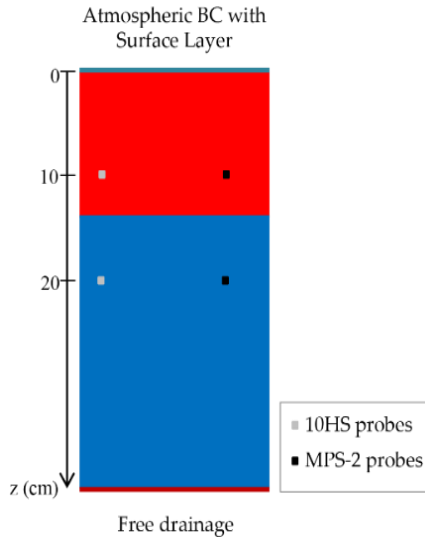
Figure 4.2-1 Scheme of boundary condition of HYDRUS in present study.

The initial soil hydraulic parameters (e.g., θ_r, θ_s, α, n and l) were determined by the Rosetta method of Schaap et al. (2001) based on soil texture, and initial K_s parameters were obtained from tension infiltrometer measurement.

Table 4.2-2 Initial input van Genucten (vG) parameters for inverse modelling.

Sites	Soil Depth	vG Parameters					
		θ_r (cm³ cm⁻³)	θ_s (cm³ cm⁻³)	α (cm⁻¹)	n (-)	K_s (mm min⁻¹)	l (-)
T1	10 cm	0.057	0.41	0.0124	2.28	1.41	0.5
(Loamy sand)	20 cm	0.057	0.41	0.0124	2.28	1.41	0.5
T2	10 cm	0.045	0.43	0.0145	2.68	0.46	0.5
(Sand)	20 cm	0.045	0.43	0.0145	2.68	0.46	0.5
T3	10 cm	0.045	0.43	0.0145	2.68	1.45	0.5
(Sand)	20 cm	0.045	0.43	0.0145	2.68	4.95	0.5
T4	10 cm	0.078	0.43	0.0036	1.56	0.26	0.5
(Loam)	20 cm	0.078	0.43	0.0036	1.56	0.26	0.5
T5 (loamy sand)	10 cm	0.057	0.41	0.0124	2.28	0.31	0.5

4.2.5 *Inverse Solution*

In HYDRUS-1D, the Marquart-Levenberge method is used to optimize the soil hydraulic parameters (Wang et al. 2016, Gutmann and Small 2007; Levenberg 1944;

Vrugt et al. 2001). The optimization process to generate vG parameters by the model in this study is to minimize the difference between simulated and observed values of water content, $\theta(t)$, and soil water retention data, $h(\theta)$ through an objective function, $\Phi(\theta(t), h(\theta))$ as described below (Šimůnek et al. 1998).

$$\Phi(b, p) = \sum_{j=1}^{m} \sum_{i=1}^{n_j} \left[p_{ij}^* - p_{ij}(b) \right]^2 \tag{4.2-7}$$

where m is the two types of dataset, i.e., soil water content $\theta(t)$, and retention curve $h(\theta)$, n_j is the number of measurements of the jth dataset, p_{ij}^* and $p_{ij}(b)$ are the observations and predictions for the jth measurement set, b (e.g., θ_r, θ_s, α, n, and K_s) is the vector of optimsed parameters. The first set of measurements is water content in time, $\theta(t)$ using 10HS measurement, and the second is the retention curve $h(\theta)$ from simultaneous measurement of 10HS soil water content and MPS-2 soil water potential. The hydraulic parameters for two soil depths at 10 and 20 cm were optimized simultaneously in the inversion process.

To evaluate the model performance, we used three fitted statistical indicators, e.g., the root mean square error (RMSE), the Nash and Sutcliffe model efficiency (NSE), and the coefficient of determination (R^2) with the following expressions.

$$RMSE = \sqrt{\frac{\sum_{i=1}^{n_j} \left(p_{ij}^* - p_{ij}(b) \right)^2}{n_j}} \tag{4.2-8}$$

$$NSE = 1 - \frac{\sum_{i=1}^{n_j} \left(p_{ij}^* - p_{ij}(b) \right)^2}{\sum_{i=1}^{n_j} \left(p_{ij}^* - \overline{p_{ij}^*} \right)^2} \tag{4.2-9}$$

$$R^2 = \left(\frac{\sum_{i=1}^{n_j} \left(p_{ij}^* - \overline{p_{ij}^*} \right) \left(p_{ij}^* - \overline{p_{ij}(b)} \right)}{\sqrt{\sum_{i=1}^{n_j} \left(p_{ij}^* - \overline{p_{ij}^*} \right)^2 \sum_{i=1}^{n_j} \left(p_{ij}^* - \overline{p_{ij}(b)} \right)^2}} \right)^2 \tag{4.2-10}$$

where p_{ij}^* and $p_{ij}(b)$ are the observation and simulation as described above, n_j is total amount of the data. R2 ranges between 0 and 1. Value 1 indicates that the simulation dispersion is equal to the observation, whereas R2 equals to 0, there is no any correlation between them (Krause and Boyle 2005). The lower RMSE value is, the better model performs (Moriasi et al. 2007). NSE values are between $-\infty$ and 1.0 (1 perfect fit) (Moriasi et al. 2007). If $0 < NSE < 1.0$, it is considered to be an acceptable performance, otherwise a negative NSE indicates unacceptable performance (Moriasi et al. 2007; Autovino et al. 2018; Jiang et al. 2016).

4.3 Results

4.3.1 *Evapotranspiration Computation*

4.3.1.1 5-Min Timestep ET$_o$

Figure 4.3-1 illustrates the result of reference evapotranspiration (ET$_o$) computed based on the Penman-Monteith equation (Equation (4.2-1)) by using meteorological data collected at 5 min resolution over the growing season from February to March 2016. 5-min ET$_o$ between February and March ranged from 0.000143 to 0.075 mm 5-min^{-1}, with a mean value of 0.017 mm 5-min^{-1}. The accumulative 5-min ET$_o$ in daily estimates ranged from 4 to 6 mm day^{-1}, which are reasonable values for this study area climate. Nobuhiro et al. (2010) found that the average daily evapotranspiration levels during the late rainy season and the middle of the dry season in central Cambodia were 4.3 and 4.6 mm day^{-1}, respectively, and the maximum daily ET$_o$ levels were 5.2 and 5.7 mm day^{-1} respectively.
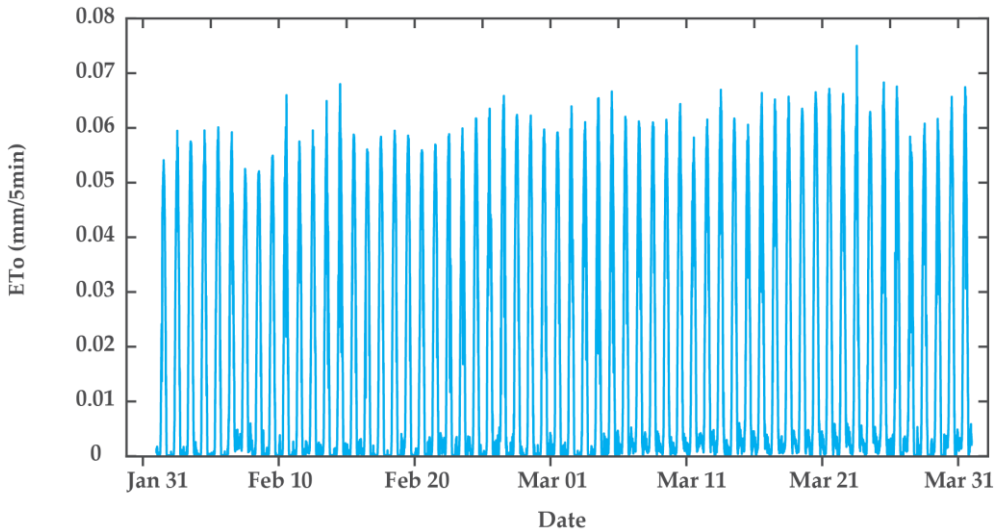
Figure 4.3-1 5-min timestep reference evapotranspiration during growing season in 2016, estimated based on standardized ASCE Penman-Monteith approach.

4.3.1.2 Partition of Crop Evapotranspiration

Results of estimation of transpiration and evaporation from partitioning crop evapotranspiration (ET$_c$) based on the method proposed by Gallardo et al. (1996) at sites T1, T2 and T3 are presented in Figure 4.3-2. The transpiration estimation at site T1 and T2 was done during mid-season with full canopy cover of 35% and 57% respectively and during development stage at T3 reaching the full canopy cover of 44%. The results show that soil evaporation was the main part of ET$_c$ during the growing season. The soil evaporation ranged from 47% to 67% at the maximum canopy cover stage in the three sites.
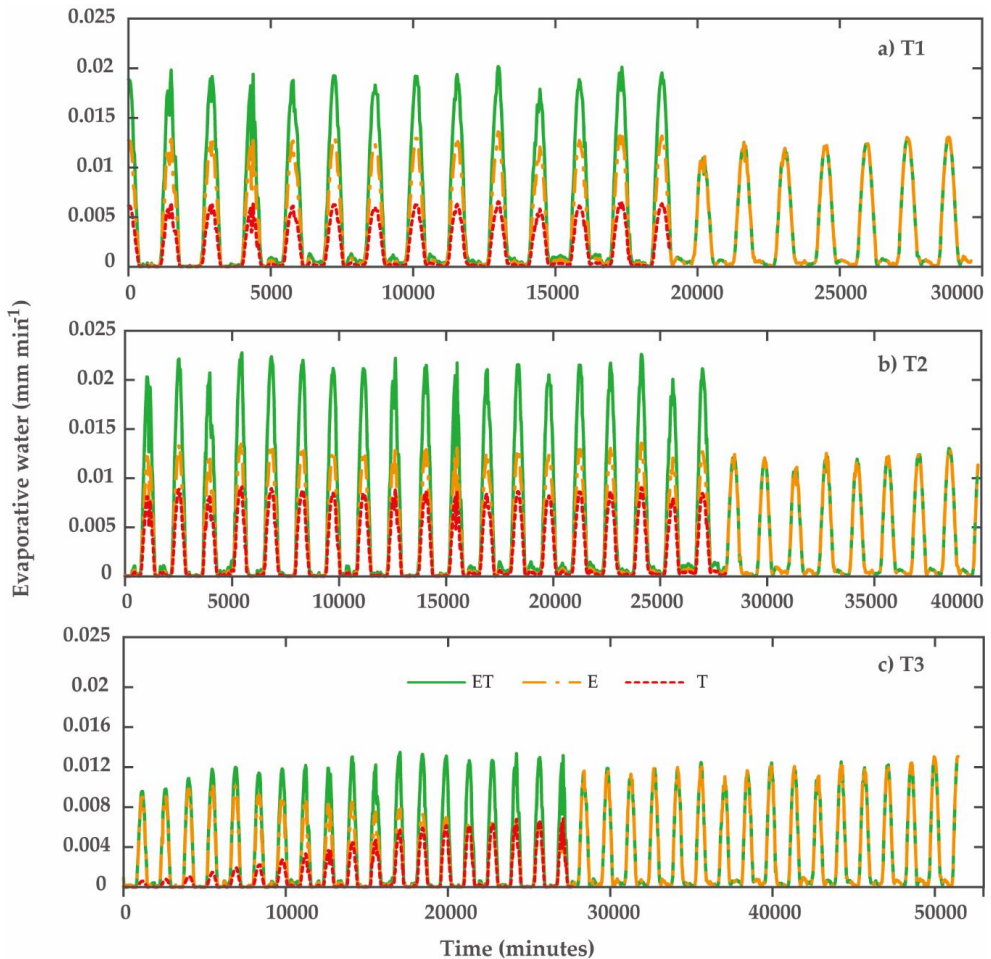
Figure 4.3-2 Partitioning crop evapotranspiration. ET is crop evapotranspiration, E is evaporation, T is crop transpiration, (a) at site T1; (b) at site T2; (c) at site T3.

4.3.2 Inversion Estimation

4.3.2.1 Estimated Parameters and Model Evaluation

The inverse estimation technique using HYDRUS-1D has been successfully used to determine the soil hydraulic function of van Genuchten (vG) parameters in the two soil depths of 10 cm and 20 cm in the five experimental sites. Table 4.3-1 shows the results of optimised vG parameter sets in all experimental sites. The estimated θ_s ranged from 0.35 to 0.43 cm^3 cm^{-3} for loamy soils (T1 and T5), 0.30 to 0.35 cm^3 cm^{-3} for sand soils (T2 and T3) and 0.32 to 0.37 cm^3 cm^{-3} for loam soil (T4). It was noted that these estimations are similar to the measured values. At site T4, the estimated θ_s (ranging from 0.32–0.37 cm^3 cm^{-3}) is much lower than the measured value (0.43 cm^3 cm^{-3}). Commonly, the laboratory-measured θ_s can be smaller than in situ values because of incomplete saturation and air entrapment of the soil (Verbist et al. 2009,

Schwartz and Evett 2003), while it is possibly over/underestimated in the laboratory-measured θ_s (Abbasi et al. 2003).

For the computation of saturated hydraulic conductivity parameters, it was noted that inputting low initial measured saturated conductivity in sand soil during the optimization process with $K_s = 0.43$ mm min^{-1} at site T2 and $K_s = 1.45$ mm min^{-1} at site T3 resulted in a divergence of the model. In that case, initial K_s were estimated using Rosetta method of Schaap et al. (2001) based on soil texture. Therefore, $K_s = 4.95$ mm min^{-1} from Rosetta method at sites T2 and T3 was selected as the initial value and resulted in convergence. It highlights the need for reasonable input values before an inversion process.

The fitted K_s in Table 4.3-1 were quite higher than the measured values from the tension infiltrometer (TI) in sites T1, T2, T3. The difference between in situ measured and simulated values of K_s is most probably due to the different time and space at the measurement from the scale at which the processes are modelled (Verbist et al. 2009). It is commonly known that agricultural soils frequently exhibit extensive spatial and temporal changes in pore characteristics that cause variation change in soil hydraulic conductivity, K(h). On the other hand, it was noted that K_s were measured by TI at the soil surface. Thus, it caused the limitation both on K(h) extrapolation towards saturation and on its application to extended depth (10 and 20 cm) (Yoon et al. 2007). Another potential reason can be due to the limitations of TI method in measurement in the coarse soil texture. The result study of March (2000) suggested that TI method underestimated K_s under high permeability conditions. Similarly, Yoon et al. (2007) observed that there was greater fluctuation in measuring hydraulic conductivity near the saturated condition especially for sandy soil affected by the presence of irregular distribution of macropore possibly with entrapped air. The other limitations were described by Roulier et al. (2000) mainly associated with the simplifying assumptions of the analysis methods and instrumental restriction (Yoon et al. 2007). Indeed, K_s obtained from TI was estimated indirectly and assuming only matrix flow, that might lead to inaccurate K_s (Rezaei et al. 2016).

Therefore, the inverse model estimation suggested a reasonable value of K_s using the observed soil water dynamic. There were low estimated K_s of coarse soils at this soil depth at site T3 at 20 cm and T5 at 10 cm. The soil compaction at 20 cm soil depth could be the reason of the low estimated permeability at site T3. It was noted that at site T5 the second soil layer below 15 cm depth was highly compacted and that could lead to the low K_s estimation for this loamy sand at 10 cm depth. In contrast, the measured K_s in T4 and T5 are similar to the optimized values. This suggests that a tension infiltrometer might be useful in determining K_s for inverse estimation for fine soil type.

These results also suggest that for further work, a sensitivity analysis of the vG parameters could be interesting, to investigate the constraints of its impact on the simulation.

Table 4.3-1 Soil hydraulic vG parameter sets derived from inversion estimation.

Sites	Depth	θ_r	θ_s	α	n	K_s	l	h_{AEV}
T1	10 cm	0.041	0.35	0.0009	2.46	4.95	0.5	5.75
(Loamy sand)	20 cm	0.044	0.43	0.002	1.85	4.95	0.5	2.28
T2	10 cm	0.038	0.30	0.0033	1.52	2.43	0.5	1.32
(Sand)	20 cm	0.003	0.35	0.0053	1.26	2.43	0.5	0.86
T3	10 cm	0.015	0.33	0.0005	2.33	4.95	0.5	100.9
(Sand)	20 cm	0.026	0.35	0.0004	2.34	0.26	0.5	12.64
T4	10 cm	0.08	0.32	0.0013	1.61	0.38	0.5	3.37
(Loam)	20 cm	0.08	0.37	0.0009	1.93	0.15	0.5	5.16
T5 (loamy sand)	10 cm	7.9871×10^{-6}	0.35	0.0005	2.09	0.29	0.5	9.60

Note θ_r and θ_s in cm^3 cm^{-3}, α in mm^{-1}, K_s in mm min^{-1}, h_{AEV} in kPa.

Tables 4.3-2 and 4.3-3 show the evaluation model performances of the inverse estimation to generate SWRCs and water flow, respectively. After inversion, the results showed the improvement of model performance in SWRC simulation with lower RMSE (ranging from 0.01 to 0.04 cm^3 cm^{-3}) and higher coefficients of NSE (ranged from 0.53 to 0.99) and determination (R^2) (ranging from 0.78 to 0.99) (Table 4.3-2). Similarly, water flow simulation resulted in satisfied performance with RMSE ranged from 0.02 to 0.03 cm^3 cm^{-3}, NSE from 0.64 to 0.83 and R^2 from 0.85 to 0.99 (Table 4.3-3). Overall, these results confirm that the inverse modelling with HYDRUS-1D can predict soil water retention curve and dynamic water content in the soil profile with a reasonable degree of accuracy.

Table 4.3-2 Evaluation of model performance in simulation of soil water retention curve (SWRC) before and after inversion.

Sites	Depth	Simulation with Initial Input Parameters			After Inversion		
		RMSE (cm³ cm⁻³)	NSE	R²	RMSE (cm³ cm⁻³)	NSE	R²
T1	20 cm	0.044	−3.78	0.20	0.010	0.73	0.99
T2	10 cm	0.08	−5.06	0.16	0.016	0.75	0.91
	20 cm	0.04	0.36	0.92	0.002	0.99	0.99
T3	10 cm	0.05	−0.14	0.85	0.048	0.00	0.78
	20 cm	0.06	0.31	0.90	0.024	0.83	0.97
T4	10 cm	0.019	0.32	0.76	0.015	0.53	0.94
	20 cm	0.028	0.75	0.98	0.026	0.78	0.98
T5	10 cm	0.038	−0.13	0.86	0.012	0.89	0.99

Table 4.3-3 Evaluation of model performance in simulation of water flow before and after inversion.

Sites	Depth	Simulation with Initial Input Parameters			After Inversion		
		RMSE (cm³ cm⁻³)	NSE	R²	RMSE (cm³ cm⁻³)	NSE	R²
T1	10 cm	0.05	0.41	0.99	0.02	0.84	0.99
	20 cm	0.03	0.45	0.99	0.02	0.72	0.99
T2	10 cm	0.11	−5.66	0.14	0.02	0.64	0.85
	20 cm	0.13	−12.40	0.07	0.02	0.75	0.99
T3	10 cm	0.05	0.42	0.99	0.03	0.83	0.99
	20 cm	0.06	0.31	0.90	0.02	0.83	0.97
T4	10 cm	0.08	−1.64	0.31	0.03	0.65	0.98
	20 cm	0.07	−0.20	0.53	0.03	0.82	0.99
T5	10 cm	0.05	−1.09	0.41	0.02	0.67	0.96

4.3.2.2 Soil Water Retention Curves

Figure 4.3-3 and 4.3-4 show the soil water retention curves before and after inversion. Simulated SWRCs are close to the observation in all sites and depths. The excellent fits were at site T1 at 20 cm depth (loamy sand soil) (RMSE = 0.01 cm^3 cm^{-3}) and at site T2 at 20 cm depth (RMSE = 0.002 cm^3 cm^{-3}). Otherwise, the other SWRCs in the other sites and depths fitted fairly well with RMSE, ranging from 0.016 to 0.048 cm^3 cm^{-3}.

The data of field SWRC at near-saturated and driest points in all experimental sites were not presented because of data inaccuracy and limitation from the sensors (10HS and MPS-2) at these wet and dry ranges. MPS-2 is unable to provide accurate pressures at the wet end of the SWRC because of the air-entry limit (Degré et al. 2017). The acceptable measured ranges of the sensors were selected for inverse input data. Despite its limitations, MPS-2 can be useful in a drier range and to pilot irrigation (Degré et al. 2017). Similarly, the errors from the 10HS sensor can be due to its accuracy limitations in measuring the water content in moist conditions (Mittelbach et al. 2012). On the other hand, the effect of temperature on the 10HS sensor response could have caused significant data errors in the fine soil and for high water content, especially at upper soil layers where there is higher temperature fluctuation (Kargas and Soulis 2011).
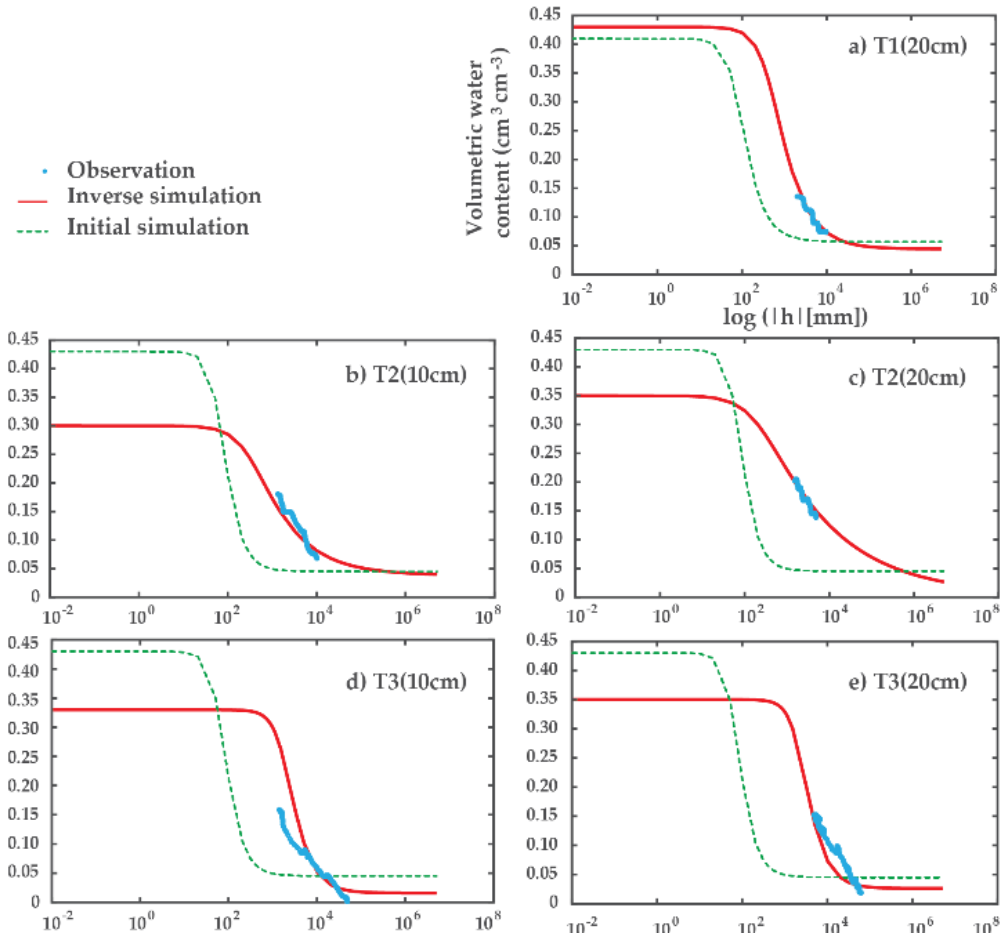
Figure 4.3-3 SWRC in before and after inversion solution. (a) SWRC at 20 cm depth at site T1; (b) SWRC at 10 cm depth at site T2; (c) SWRC at 20 cm depth at site T2; (d) SWRC at 10 cm depth at site T3, (e) SWRC at 20 cm depth at site T3. The measured soil water potential (h) ranged from −20 to −95 kPa at site T1, from −13 to −99 kPa and −15 to −48 kPa at soil depth of 10 and 20 cm respectively at site T2, from −14 to −476 kPa and −48 to −608 kPa at 10 and 20 cm respectively at site T3.
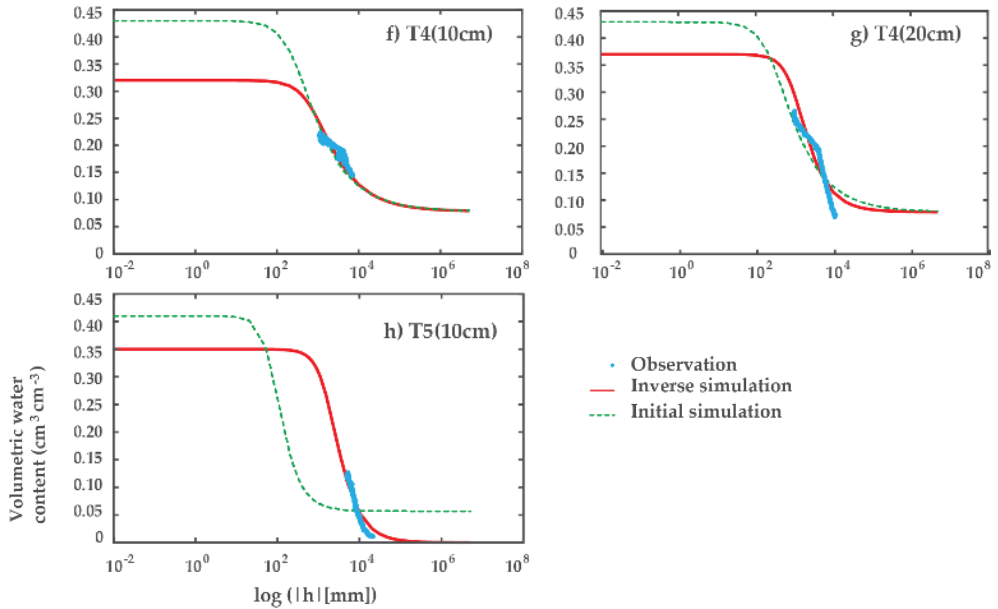
Figure 4.3-4 SWRC in before and after inversion solution. (f) SWRC at 10 cm depth at site T4; (g) SWRC at 20 cm depth at site T4; (h) SWRC at 10 cm depth at site T5. The measured soil water potential (h) ranged from from −11 to −69 and −10 to −111 kPa at 10 and 20 cm respectively at T4, from −48 to −212 kPa at 10 cm at site T5.

The estimated AEV of the tested soils are shown in Table 4.3-1. AEV ranged from 0.86 to 12.64 kPa. AEV of loamy sand were from 2.28 to 9.60 kPa, sand were from 0.86 to 12.64 kPa, and loam were 3.37 to 5.16 kPa. Reference (Hao et al. 2015) showed that the soil with higher sand content has smaller AEV using laboratory pressure plate extractor test. They also found the effect of initial water content on the AEV. The sand soil with higher initial water content has larger AEV (i.e., the soil with sand content of 20% to 60% resulted in AEV of 6.04 to 1.94 kPa respectively). Similarly, Konyai et al.(2009), using pressure plates for defining SWRCs, found the AEV of loamy sand ranged from 1.30 to 2.00 kPa and loam soil of 0.90 kPa. However, those results were from the laboratory. It is seen that the generated SWRC at site T3 with high sand content proposed a higher AEV of 10.09 and 12.64 kPa. The physical environmental effects to the SWRC of sand soil are complex in their observations at near real AEV. The limitation of sensors to catch the accuracy of the low range of suction can be the main reason for the high estimated AEV of the sand soil at T3. In Figures 4.3-4 and 4.3-5, the generated initial SWRC from the Rosetta method are often obtained from laboratory SWRC. The inverse estimated SWRC reflected the effect of the dynamic physical environmental. Therefore, it is interesting to investigate the field SWRC with the influence of the in situ environment.

4.3.2.3   Dynamic Soil Water Content

Observed and simulated soil water content distributions in the soil profile at 10 and 20 cm at the 5 experimental sites are shown in Figures 4.3-5 and 4.3-6, respectively. The fluctuation of soil water content was coming from only irrigation applied at sites T1, T2, T3 and T4. The water flow simulation in all sites gave good and excellent correlations between observed and simulated water contents in the soil profile (i.e., R^2 values ranged from 0.85 to 0.99). It is noted that the water flow simulation was similar to the soil moisture observation in the wet range but widely over/underestimated in the end dry events after the inversion (i.e., RMSE ranged from 0.02 to 0.03 cm^3 cm^{-3} and NSE ranged from 0.67 to 0.84). The important factor influencing the simulation model performance is the assumption of homogeneous soil properties through the entire simulation. This assumption is not flexible to real phenomena e.g., the dynamic change of soil hydraulic properties during the growing season, the macropore flow, and lateral flux of soil moisture. Schwen et al. (2011) revealed that the accuracy of the soil water flow simulation, especially of that near the surface, can be improved by using time-variable hydraulic parameters. Despite several simplifying assumptions of HYDRUS-1D model, the results of the inversion yet provided reasonable estimates of water dynamics and a better improvement from the initial simulation.
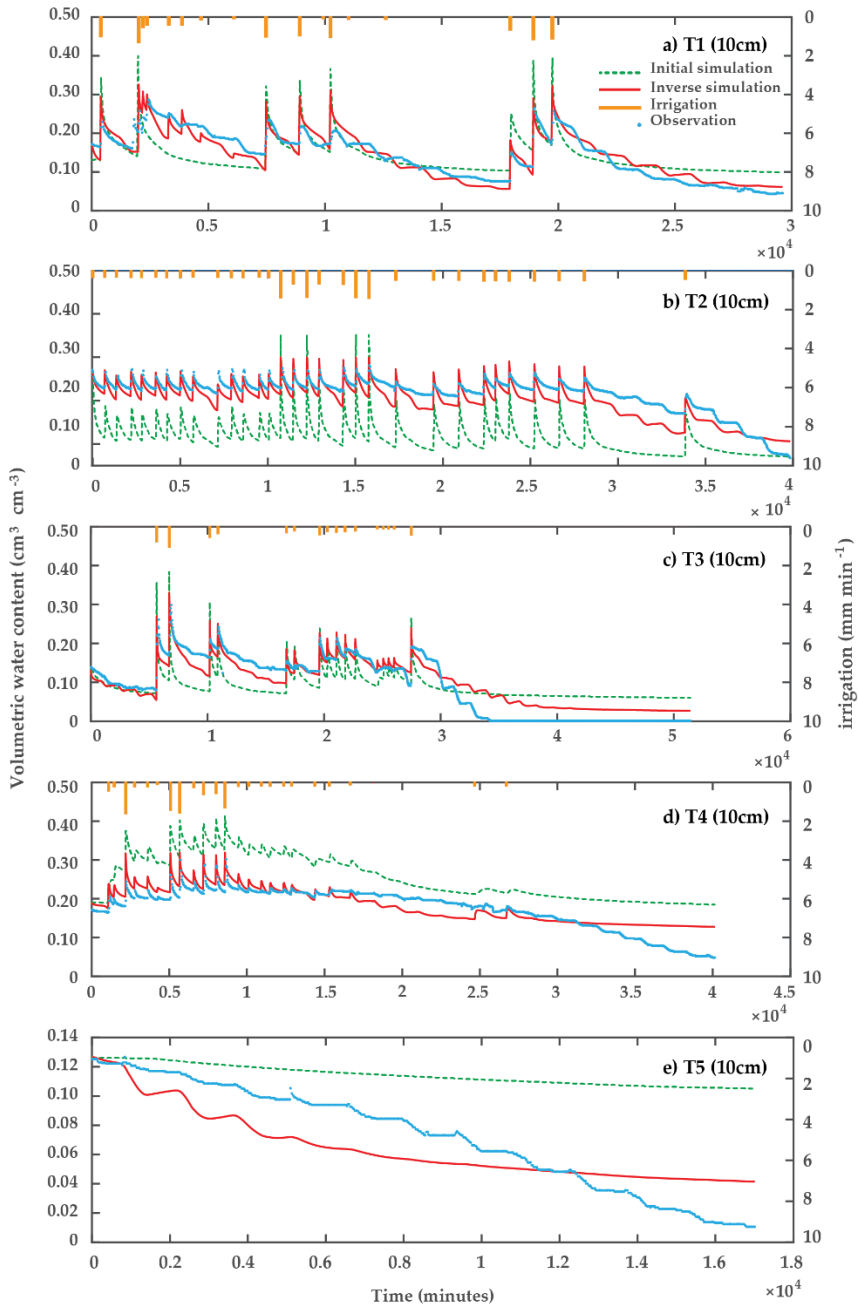
Figure 4.3-5 Observed and simulated dynamic soil moisture in 30-min timestep using inversion approach during the growing season in 2016 at different sites at 10 cm depth. (a) at site T1; (b) at site T2; (c) at site T3; (d) at site T4; (e) at site T5.
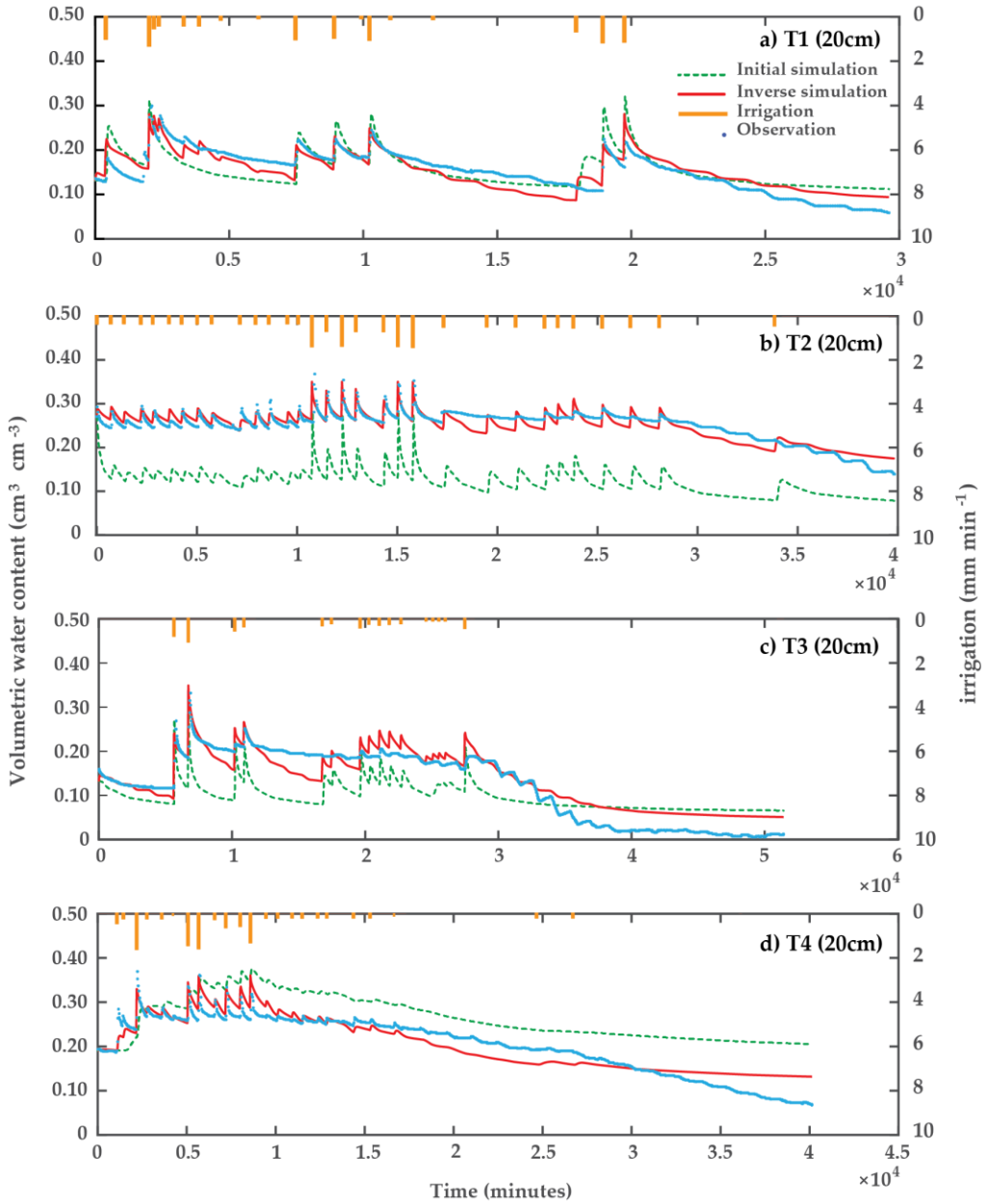
Figure 4.3-6 Observed and simulated dynamic soil moisture in 30-min timestep using inversion approach during the growing season in 2016 at different sites at 20 cm depth. (a) at site T1; (b) at site T2; (c) at site T3; (d) at site T4.

4.4 Conclusions

In this study, inversion approach using HYDRUS-1D based on only in situ measurement of soil hydraulic properties were used to estimate the van Genuchten (vG) parameters of the soil properties in experimental fields with different soil types including loamy sand, sand, and loam soil, in Chrey Bak Catchment, Cambodia. The in situ soil hydraulic measured data that were used as inverse input data included saturated hydraulic conductivity using tension infiltrometer, observed dynamic soil water content and SWRC from simultaneous measures of Decagon 10HS soil moisture and MPS-2 soil water potential sensors. To apply this approach, first we computed 5-min timestep reference evapotranspiration based on the ASCE Penman-Monteith equation and obtained reasonable results. Then we partitioned the crop evapotranspiration based on the Gallardo et al. (1996) method in the field after lettuce was planted.

Analyzing the SWRC shows that the simulated SWRC using optimum vG parameters of the inversion closely and fairly matched the field SWRC data, with RMSE ranging from 0.002 to 0.048 $cm^3 cm^{-3}$. The fair match was due to the limitation in measurement of the sensors in the wet and the driest range of moisture condition in the field. In testing water flow simulation, generally the model resulted in a good simulation performance for predicting the soil water content in the experimental period in all the studied soil textures, with the RMSE ranging from 0.02 to 0.03 $cm^3 cm^{-3}$. The results proposed that soil hydraulic properties can be estimated effectively and rapidly with inverse modelling using only the information from the field soil hydraulic measurement without the required expensive laboratory data. We found that a tension infiltrometer might be useful in determining saturated hydraulic conductivity (K_s) for inverse estimation for fine (loam) soil texture, as the generated K_s was slightly changed from the initial measured values after inversion. We confirmed that the inverse process in the model is sensitive to initial hydraulic soil parameter input, and can lead to model divergence. For further work, validation on another data set should be investigated.

It is recommended that more additional experimental data, particularly accurate field dynamic SWRC in the wet and dry encompassing new technics and methods, should be included to improve the inversion approach in further research. Additionally, the dynamic change of soil properties should be considered in the inversion model to improve the accuracy of water flow prediction.

5

Simulation of Crop Growth and Water-Saving Irrigation Scenarios for Lettuce: A Monsoon-Climate Case Study in Kampong Chhnang, Cambodia

This chapter describes the development of methodology for irrigation water saving using crop growth model. This work has been published in Water Journal.

5.1   Introduction

Humanity's environmental footprint is unsustainable within the Earth's limited natural resources and assimilative capacity (Hoekstra and Wiedmann 2014). Climate change and growth in the global population are increasing pressure on these scarce environmental resources, notably water (Bae and Dall'erba 2018; Rodríguez-Ferrero et al. 2010; Chartres 2014). Particularly, increasing relative evapotranspiration from flow regulation and irrigation over the past century raises the global human water consumption and footprint (Jaramillo and Destouni 2015). Improving food production with less water and benchmarking efficiency of resource use is therefore a great challenge of our time, and urgently needed to ensure food security (Hoekstra and Wiedmann 2014; Toumi et al. 2016; Linker and Ioslovich 2017).

Cambodia is considered to be the country most vulnerable to climate change in Southeast Asia (Touch et al. 2016). In recent decades, extreme events, such as floods and droughts, have negatively affected the livelihoods of farmers, especially in terms of the loss of crop production (Kong et al. 2012). Cambodian farmers are generally conscious of these changes and challenges (Kong et al. 2012). Guidelines for agricultural adaptation to improve crop productivity and the sustainability of the farming system and to minimise vulnerability to climate change, are therefore crucial (Touch et al. 2016; Montgomery et al. 2017). Currently, the production of vegetables, like lettuce, poses more challenges in term of managing irrigation water efficiently, due to the crop's sensitivity to water shortage (Moreira et al. 2014; Valenzuela et al. 1996; Cahn and Johnson 2017). Lettuce, the most widely consumed leaf vegetable, is also one of the most widely cultivated vegetables in the world (Domingues et al. 2012). It is also an important to local vegetable production in Cambodia (Chhean et al. 2004; De Bon et al. 2010). Improving strategies for vegetable farming productivity, including lettuce, for Cambodian farmers, is being increasingly considered (Morris et al. 2013).

Many irrigation strategies have been investigated for improving irrigation water productivity (IWP) during recent decades, with IWP defined as the ratio of agricultural output to the amount of irrigation water use (Xue et al. 2018). Full irrigation via water application with the crop evapotranspiration requirements (ETc) method is an effective irrigation practice for crop production (Adu et al. 2018; Liu and Luo 2010; Verstraeten et al. 2008; Hunsaker et al. 2015). In traditional irrigation scheduling, a technique to meet full irrigation, as well, the soil moisture in the root zone is allowed to fluctuate between an upper limit approximating "field capacity" and the lower limit of the readily accessible water (RAW), referred to as "the threshold", somewhat above where a crop begins to experience water stress (Thompson et al. 2007; Ferreira et al. 2017). These methods have been applied to improve crop water productivity in various regions of the world, including Asian regions (Li et al. 2008; Kashyap and Panda 2001; Inthavong et al. 2011; Davis and Dukes 2010; Kukal et al. 2005; Pereira et al. 2009). Nevertheless, deficit irrigation, as an adaptation strategy for regions with limited water resources or prone to drought, has been proven to be worth considering (Pereira et al. 2012; Afzal et al. 2016).

Deficit irrigation is an irrigation practice whereby a crop is irrigated with an amount of water below the full requirement for optimal plant growth, thereby saving water

and minimising the economic impact on the harvest (Adu et al. 2018). By limiting water applications to drought-sensitive growth stages such as, the vegetative stages and the late ripening period, the aims of this approach is to maximise water productivity and to stabilise, rather than maximise yields (Geerts and Raes 2009). Water deficit can be defined at five levels: severe deficit (with soil moisture (SM) less than 50% of field capacity (FC)), moderate deficit (SM < 50–60% of FC), mild deficit (SM < 60–70% of FC), no deficit or full irrigation (SM > 70% of FC), and overirrigation (application above water requirements) (Chai et al. 2016). Crops under deficit irrigation will experience some level of water stress, and often have lower yields than fully irrigated plants (Lopez et al. 2017). Deficit irrigation can allow irrigation water savings of up to 20–40% at yield reductions below 10% (Kögler and Söffker 2017), and has been widely investigated in dry regions (Kögler and Söffker 2017). Deficit irrigation can be based on applying irrigation water under crop evapotranspiration. Patanè et al. (2011) found that deficit irrigation at 50% of ETc for tomato plants resulted in no biomass (B) loss and high irrigation water-use efficiency. Experimental results obtained by Abd El-Wahed et al. (2017) suggested that deficit irrigation at 85% of ETc is favourable to save 15% of water provided, with no reduction in the bean crop. The study results of Samperio et al. (2015) offered deficit irrigation at 20% and 60% of ETc during stage II and postharvest, respectively, to "Angeleno" Japanese plum as a water-saving strategy, without negatively affecting crop yield. Results from Yang et al. (2015)confirmed that the yield loss for cotton was less than 10% under deficit irrigation of 70% of ETc and 85% of ETc. Meanwhile, crop sensitivity to water deficit can be affected by many factors, including climatic conditions, crop species and cultivars, and agronomic management practices, amongst others (Chai et al. 2016). Payero et al. (2006) suggested that deficit irrigation is not a good strategy for improving the crop water productivity of maize in a semi-arid climate. A study on deficit irrigation treatment on lettuce showed that water stress caused by deficit irrigation at 20% and 40% of ETc significantly reduced leaf number, leaf area index, and dry matter accumulation (Karam et al. 2002). Final fresh weight was reduced by 20% to 30% when compared with full irrigation. Kuslu et al. (2008) concluded that for lettuce grown in semi-arid regions, full irrigation should be used under no water shortage, and deficit irrigation by 60% of ETc could be used for 40% water saving with a 35.8% yield loss where irrigation water supplies are limited.

Elaborating irrigation strategies merely on the basis of field research is difficult and time consuming (Geerts et al. 2010; Geerts et al. 2010). Crop models are effective decision-support tools to investigate irrigation scenarios and to develop improved irrigation strategies (Linker and Ioslovich 2017; Hassanli et al. 2016; Abderrahman et al. 2001). They can provide a rapid and reasonable accurate prediction of the response of agriculture over a range of environmental conditions (Wolf et al. 1996). The model AquaCrop, developed by the Food and Agricultural Organisation of the United Nations (FAO), is a water-driven crop model that simulates daily crop growth (e.g., canopy cover and biomass production) and final crop yield, with a balance between accuracy, simplicity, and robustness in incorporating various agronomy practices (Ran et al. 2017; Steduto et al. 2009). It is considered as a valuable tool for improving irrigation water productivity in crop production planning (Toumi et al. 2016; Singh et al. 2013). AquaCrop has been calibrated and parameterised to various crops under

various environmental and irrigation conditions, including barley (Tavakoli et al. 2015), soybean (Paredes et al. 2015), sunflower (Todorovic et al. 2009), cotton (Farahani et al. 2009, Hussein et al. 2011), corn (Hsiao et al. 2009), sugar beet (Malik et al. 2017), wheat (Andarzian et al. 2011, Mkhabela and Bullock 2012), potato (Rankine et al. 2015; Casa et al. 2013), cabbage (Wellens et al. 2013), and rice (Deb et al. 2016). However, this has not yet been done in the case of lettuce. Most of these studies proved that the model is capable of accurately simulating crop growth and yield. However, some case studies still report some flaws in simulation of crop evolution and yield, especially under severe deficit irrigation and heat stress conditions. Adeboye et al. (2017) found that biomass of soybean simulated by AquaCrop was overestimated under deficit irrigation conditions. Zeleke et al. (2011) found that AquaCrop simulated the canopy cover and biomass growth of canola well, but the model was less satisfactory under severe water stress conditions in a semi-arid region. Similarly, a reduction in model reliability in biomass and canopy cover prediction for maize under the severe stress conditions of deficit irrigation in a tropical environment was indicated in a study of Greaves and Wang (2016). AquaCrop performed well in biomass simulation of potato in the experiment under deficit irrigation at 120, 100, 80, and 60% of ETc (Montoya et al. 2016). However, the potato yield simulation was overestimated due to the heat stress, with the authors suggesting the incorporation of a temperature stress coefficient into AquaCrop when a crop is affected by high temperatures. Further research is therefore required to improve the performance of AquaCrop. Furthermore, its performance simulating lettuce growth in Cambodian conditions has not yet been tested. The main objective of this study is to improve the water productivity of lettuce under limited irrigations in the Cambodian climate. More specific objectives are (i) to parameterise the crop model AquaCrop using data from farmer fields, since lettuce is not yet available in the AquaCrop catalogue; and (ii) to assess the impact of water-saving scenarios in full and deficit irrigation in silico using this calibrated model.

5.2 Materials and Methods

5.2.1 Experimental Sites

The field experiments were conducted with lettuce plants (*Lactuca sativa* var. *crispa L.*) which are widely used in the study area, during a period from August to September 2017 in two experimental sites located in the villages of Chea Rov (site T2) and Ou Roung (site T4) in the province of Kampong Chhnang, Cambodia (see Figure 3.1-1).

5.2.2 Data Collection and Measurement

5.2.2.1 Climate Data

Weather data for the experimental sites were collected from the meteorological station of first approach (chapter 4). Daily maximum and minimum temperature, relative humidity, wind speed, rainfall, and solar radiation were recorded automatically at a five minute time step. The daily reference evapotranspiration (ETo) for the growing season, used as input data in AquaCrop, was calculated using the ETo

calculator based on the FAO's Penman–Monteith method (Allen et al. 1998) (Figure 5.2-1).
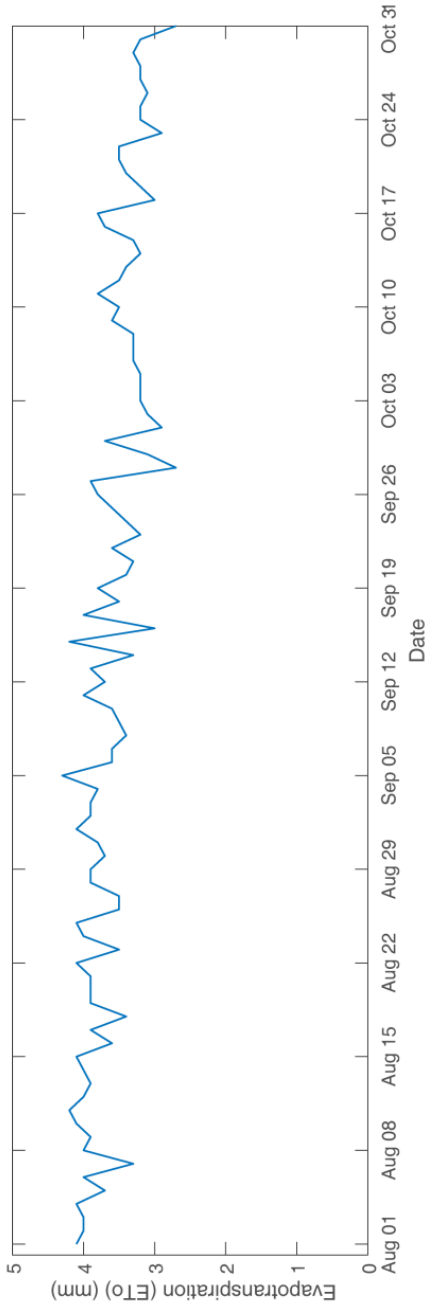
Figure 5.2-1 Daily potential evapotranspiration (ETo) during the growing season 2017.

5.2.2.2   Soil Data

The physical and chemical soil characteristics which were measured are listed in Table 5.2-1 and 5.2-2. The detail of soil data measurement methods is described in Chapter 3. Field capacity and wilting point, were derived from inverse modelling as presented in section 3.4-1. 10HS and MPS-2 sensors were used to measure soil moisture and soil potential.

Table 5.2-1. Measured soil characteristics.

Parameters	Experimental Sites	
	Chea Rov (T2)	Ou Roung (T4)
Texture	Sand	Loam
Clay (%)	4.39	7.80
Silt (%)	9.56	41.15
Sand (%)	86.03	51.04
Bulk density (g cm^{-3})	1.5	1.5
Field capacity (m^3 m^{-3}) (sand: at -10 kPa, Loam: at -33 kPa)	0.11	0.14
Wilting point (m^3 m^{-3}) (at 150 kPa)	0.05	0.06
Soil saturation (m^3 m^{-3})	0.27	0.43
Available water content (AWC) (mm m^{-1})	62.48	81.43

Table 5.2-2 Measured chemical soil characteristics.

Site	Sampling Time	pH-H$_2$O	EC	OM	N	P	K	CEC
T2	Before transplanting	6.28	108	20.31	0.098	13.29	0.77	2.80
	At harvest	6.84	97.4	20.85	0.126	17.08	0.4	4.40
T4	Before transplanting	6.7	223	19.51	0.238	24.07	2.31	7.60
	At harvest	6.8	218	19.78	0.126	15.91	1.45	5.40

Note: EC is electrical conductivity (uS cm^{-1}); OM is organic matter content (%); N is total nitrogen (%); P is available phosphorous (ppm); K is exchangeable potassium (meg 100 g^{-1}); CEC is cation exchange capacity (cmol kg^{-1}).

5.2.2.3 Crop Data

Canopy cover was measured at three-day intervals during the growing stage. Four pictures of 1 m² were taken randomly using a digital compact camera (Nikon Coolpix p600, Tokyo, Japan) at a fixed height of 1 m above ground level. The canopy cover was analysed using image processing with ImageJ® software (https://imagej.nih.gov). Aboveground dry biomass was determined by harvesting 10 heads at the surface level of each site, oven-drying plant samples at 70 °C for 48 h, and weighing them (Gallardo et al. 1996).

5.2.3 Model Parameterisation

We used the AquaCrop for estimation of crop growth and simulation of water saving scenarios. Some equations used for this approach are presented in section 2.3.2 (Chapter 2).

The process of parameterisation of AquaCrop model in this study is illustrated in Figure 5.2-2. The vegetative stage of lettuce refers to the growing period of lettuce growth after germination until harvest. A growing period during the vegetative stage of 59 days after transplanting was simulated in this study.
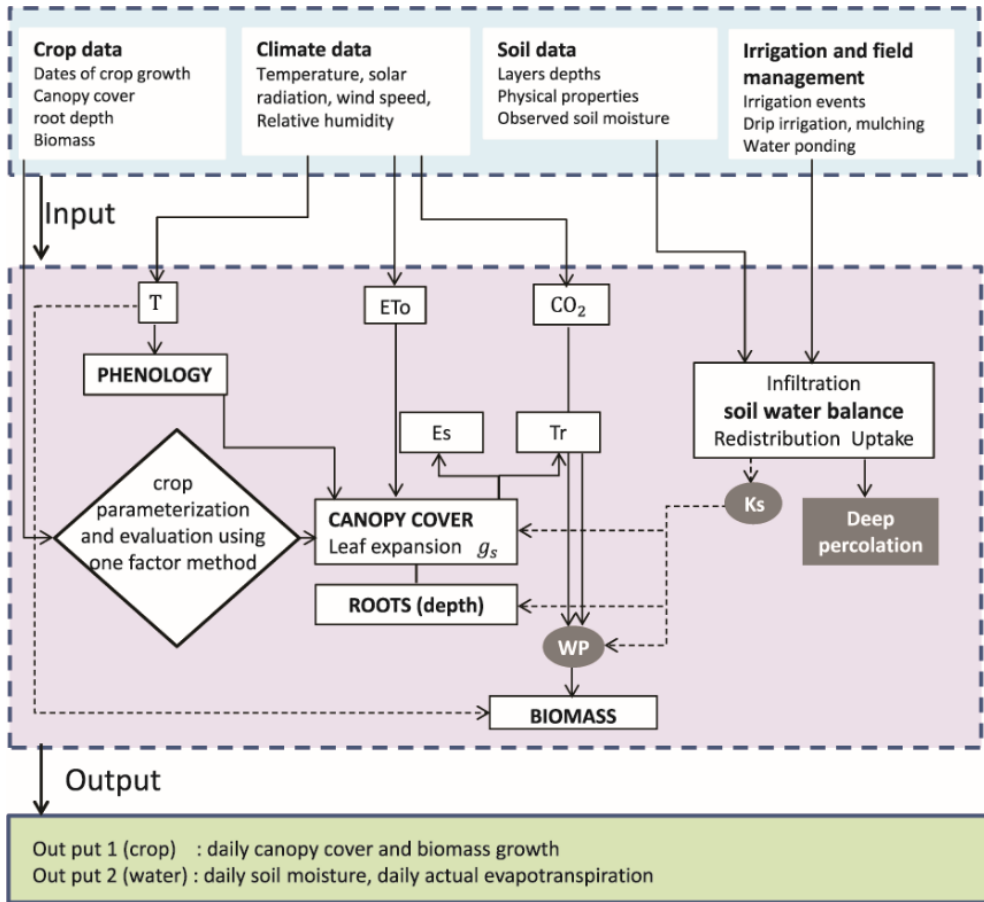
Figure 5.2-2 Flow chart of parameterisation of AquaCrop in this study (adjusted from Steduto et al. (2009b)). T is temperature, ETo is potential evapotranspiration, gs is stomatal conductance, WP is water productivity coefficient, Ks is stress coefficient, Es is soil temperature, Tr is crop transpiration.

As lettuce is a crop which is not yet parameterised in AquaCrop, calibration of the model involved adjusting the model parameters to make them match the observed data (Farahani et al. 2009; Steduto et al. 2012).

The primary variables of lettuce growth, e.g., canopy cover and aboveground biomass were parameterised. For the calibration of the curves, the measured data in two experimental fields at the Chearov site (T2) (having sand soil) and Ourong site (T4) (with loam soil) were used, during the growing season in 2017. The AquaCrop model does not allow the use of observed data to build the canopy cover and biomass curves, but allows the data to be used to calibrate the canopy cover and biomass curves (Paredes et al. 2014).

Canopy cover curves are a plot of the development of leaf expansion response to growing time per day, based on Equation (2.3-1). Biomass curves are a relationship plot of the growth of lettuce biomass response to growing time per day, based on Equation (2.3-4). The calibration of simulated canopy and biomass curves is based on one-at-a-time (OAT) methods (i.e., changing one parameter at a time while holding others constant) (Morris 1991) and adjusting the parameters by trial and error, by comparing simulated and observed field data, and minimising the function of root mean square error.

We parameterised the canopy cover curve, which is important to the model for transpiration and evaporation (Paredes et al. 2014). The main parameters of Equation (2.3-1), e.g., CCo and CGC for canopy cover curve determination, were adjusted to match the observed canopy cover data. In addition, adjusting the maximum canopy cover (CCx), time to reach maximum canopy cover, and time to recover, is crucial in order to obtain correct simulations of canopy cover growth. Subsequently, the focus was on adjusting the biomass curve of Equation (2.3-4). WP* and $Kc_{Tr,x}$ (coefficient for maximum crop transpiration) are the main parameters for regulating biomass curves in AquaCrop (Razzaghi et al. 2017). As lettuce is a C3 crop type (Stott 2002), the recommended values for WP* lie between 15 and 20 g m^{-2}. All calibrated crop parameters are shown in Table 5.2-3.

Table 5.2-3 Calibrated parameters of lettuce growth.

No	Calibration Step	Calibrated Parameters
1	Canopy cover calibration	Time to recover of transplant, Time to reach the maximum canopy cover, Initial canopy cover (CCo), Canopy growth coefficient (CGC), Maximum canopy cover growth coefficient (CCx)
2	Biomass calibration	Coefficient for maximum crop transpiration ($Kc_{Tr,x}$), Normalised biomass water productivity (WP*)

The model performance for canopy cover and biomass simulation was evaluated using statistic indicators, including root mean square error (RMSE) (Equation (3.4-7)), Nash–Sutcliffe coefficient (N) (Equation (3.4-8)), and coefficient of determination (R^2) (Equation (3.4-9)).

AquaCrop requires the selection of inputs related to the irrigation method, such as sprinkler, drip, or surface. These methods determine the fraction of the soil surface made wet by irrigation (Wellens et al. 2017) and the impact on irrigation efficiency (Zhuo and Hoekstra 2017).

Default AquaCrop settings for field management include mulching, and use an adjusted factor for the effect of mulches on soil evaporation. It varied between 0.5 for mulches derived from plant material, and 1.0 for plastic mulch (Raes et al. 2009a).

The drip irrigation method with plastic mulch was applied as the input for field management in the model during the parameterisation, as this is the actual practice of the experiment in this study.

The soil water balance calculation, including soil moisture simulation in AquaCrop, is based on the storage capacity of the soil layers, described in (Raes et al. (2017), and previously in the BUDGET model (Raes et al. 2006).

During the experimental period, water ponding at 15 cm and 20 cm below the bed soil at site T2 and T4 respectively, which was observed during the experiment, was taken into account as a boundary condition during the parameterisation of the model. This water ponding resulted in wet soil during the growing period. The values of physical soil available data in the Section 3.3.2 were adopted to simulate soil moisture in this study.

It was noted that the plantation experiment was during the rainy season when irrigation was not needed. The crop parameters obtained after parameterisation are important for the investigation of the irrigation scenarios for water saving when irrigation is necessary, especially during the dry season.

5.2.4 Irrigation Scenarios

In the current study, AquaCrop was used to simulate the full and deficit irrigation scenarios described below (and in Table 5.2-4), in order to identify the optimal water use efficiency for lettuce.

Table 5.2-4 Irrigation Scenarios.

Scenario Code		Short Description
T2 (Sand)	T4 (Loam)	
Varied readily available water (RAW) threshold irrigation scenarios		
S0RAW	L0RAW	irrigate at 0% of RAW and refill to field capacity (FC)
S50RAW	L50RAW	irrigate at 50% of RAW and refill to FC
S80RAW	L80RAW	irrigate at 80% of RAW and refill to FC
S100RAW	L100RAW	irrigate at 100% of RAW and refill to FC
S120RAW	L120RAW	irrigate at 120% of RAW and refill to FC
S130RAW	L130RAW	irrigate at 130% of RAW and refill to FC
S150RAW	L150RAW	irrigate at 150% of RAW and refill to FC
S180RAW	L180RAW	irrigate at 180% of RAW and refill to FC
S200RAW	L200RAW	irrigate at 200% of RAW and refill to FC
Varied field capacity threshold irrigation scenarios		
S100FC	L100FC	full irrigation-daily irrigation at 100% of field capacity (FC)
S70FC	L70FC	deficit irrigation at 70% of FC
S60FC	L60FC	deficit irrigation at 60% of FC
S50FC	L50FC	deficit irrigation at 50% of FC
S40FC	L40FC	deficit irrigation at 40% of FC

5.2.4.1   Varied RAW Threshold Irrigation Scenarios

Figure 5.2-3 presents the calculation process of varied RAW threshold scenarios.
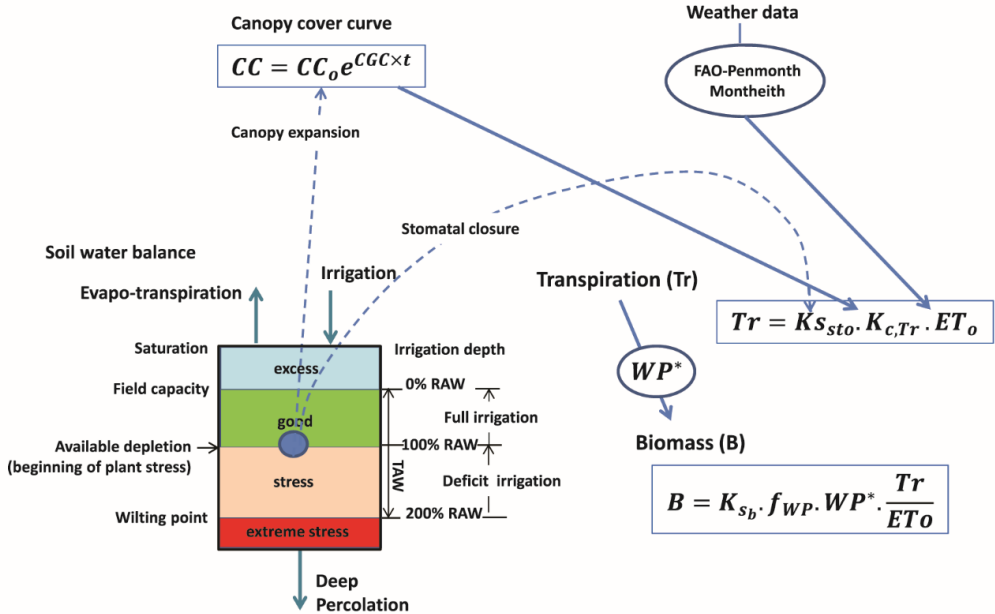
Figure 5.2-3 Schematic representation of the crop response to varied RAW threshold irrigation scenarios simulated by AquaCrop (adjusted from Steduto et al. (2012)). RAW is readily available water content, TAW is total available water content, CC is the simulated canopy cover, CC_o is initial canopy cover size, CGC is canopy growth coefficient in fraction per growing degree day (GDD), Ks_{sto} is the water stress for stomatal closure, Kc_{Tr} is the crop transpiration coefficient (determined by CC and $Kc_{Tr,x}$ at maximum canopy cover), ETo is the reference evapotranspiration, Ks_b is the stress coefficient for low-temperature effects on biomass production, f_{WP} is the adjustment factor to account for differences in chemical composition of the vegetative biomass and harvestable organs, WP* is the normalised water productivity.

These irrigation scenarios applied irrigation scheduling based on soil moisture depletion (Henrich et al. 2016) by applying readily available water depletion in the default option in AquaCrop. The time and irrigation dose were calculated with the criteria below:

1. Soil water content depleted until a fixed lower threshold (RAW) and refill to field capacity (time criteria).

2. Irrigation dose can be determined by the following Equation (5.2-4) (Raes et al. 2017a).

$$ID = AD \times RAW \qquad\qquad (5.2\text{-}1)$$

where ID is irrigation depth (mm), $RAW = p\,TAW = p\,1000(FC - PWP)Z_r$, p is soil water depletion threshold, set to 0.3 for lettuce recommended by (Allen et al. (1998), and Z_r is root depth (m). TAW is the amount of water that a crop can extract from its root zone (Allen et al. 1998a). FC is field capacity, that is, the amount of water well-drained soil should hold against gravitational forces $(m^3\,m^{-3})$ (Allen et al. 1998a). PWP is permanent wilting point, referring to soil water content when a plant fails to recover its turgidity on watering $(m^3\ m^{-3})$ (Allen et al. 1998a). RAW is readily available soil water, referring to the fraction of TAW that a crop can extract from the root zone without suffering water stress (Allen et al. 1998a). AD is allowable depletion, defined as the percentage of RAW that can be depleted before irrigation water has to be applied.

Full irrigation scenarios with varied RAW thresholds were simulated by selecting allowable depletion levels at 0, 50, 80, 100% in AquaCrop, that avoid drought stress during the growth stage (Yang et al. 2015). The irrigation schedule is generated by selecting a so-called "time" and "depth" criterion, with "back to field capacity" and "allowable depletion", respectively. In other words, the different full irrigation scenarios result in decreasing irrigation frequency.

Deficit irrigation scenarios with varied RAW thresholds were similar to the full irrigation scenario criteria, but applied allowable depletion levels at 120, 130, 150, 180, and 200%. These levels result in drought stress during the growing stage, since soil moisture can decrease to a level below RAW before an irrigation event is triggered (Yang et al. 2015).

5.2.4.2   Varied Field Capacity Threshold Irrigation Scenarios

Figure 5.2-4 illustrated concept of the varied field capacity threshold irrigation scenarios. The full irrigation scenario, based on a fixed irrigation frequency maintained the soil moisture in the root zone at field capacity on a daily basis, since the literature claims this is the optimal status to maximise lettuce yield (Sutton and Merit N 1993). The irrigation schedule was generated with a fixed time interval (daily) (time criteria) and refill to field capacity (depth criteria).

Deficit irrigation scenarios with varied field capacity threshold reduce the irrigation dose below the dose at field capacity but keeping the same irrigation frequency, as in full irrigation scenario. Daily generated irrigation doses obtained in full irrigation scenario were reduced by 70, 60, 50, and 40%.
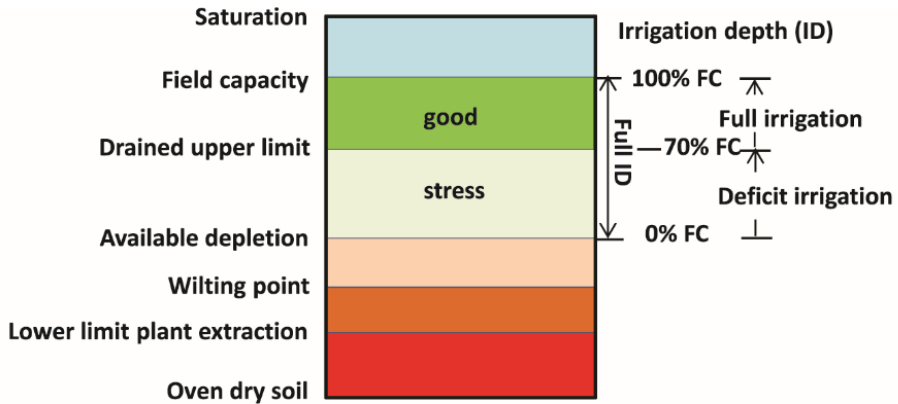
Figure 5.2-4 Schematic illustration of the soil water reservoir concepts of varied irrigation depth under field capacity irrigation scenarios (adjusted from Lamn et al. (2015)). FC is field capacity, full ID is full irrigation depth.

Irrigation water productivity (IWP) was used to evaluate the irrigation scenarios for efficient irrigation water use (Pereira et al. 2012; Tan et al. 2018). IWP is the ratio between the yield and the irrigation water use (Pereira et al. 2012).

$$IWP = \frac{Y}{I} \tag{5.2-2}$$

where IWP is irrigation water productivity (kg m^{-3}), Y is simulated yield (kg ha^{-1}) and interest yield in this study is biomass, and I is irrigation water use (mm).

The adjusted crop parameters obtained from the parameterisation process were used in the scenario simulation under the same weather conditions, using no soil surface cover in model field management, and no ground water at bottom soil profile boundary condition.

5.3 Results

5.3.1 Plant Growth and Soil Moisture Status

Figure 5.3-1 shows both the lettuce growth measurement and simulation by AquaCrop. Biomass accumulated at a very low rate during the first two weeks of the growing season, and increased sharply in the final week. This trend accords with results obtained by Gallardo et al. (1996).

The measured canopy cover and biomass yields were 34% and 0.11 ton ha^{-1}, respectively, at site T2 with sand soil, and 18.5% and 0.11 ton ha^{-1}, respectively, at site T4, which has loam soil. The measured results are comparable with Fazilah et al. (2017), who found observed canopy cover of 33% and biomass yields of 0.22 ton ha^{-1} for lettuce under similar tropical conditions. Zhang et al.(2017) (Zhang et al. 2017)found higher measured biomass for lettuce with a range of 0.33 to 0.63 ton ha^{-1} under lower temperatures of 20–25 °C. Thus, high day temperatures above 23 °C often limit lettuce production (Dufault et al. 2009). Optimum growth for lettuce occurs between 15–20 °C (Valenzuela et al. 1996). Unfavourable weather conditions, of high average temperature 33/25 °C (day/night) during the experiment, can be the reason of the low measured biomass yields for this study.
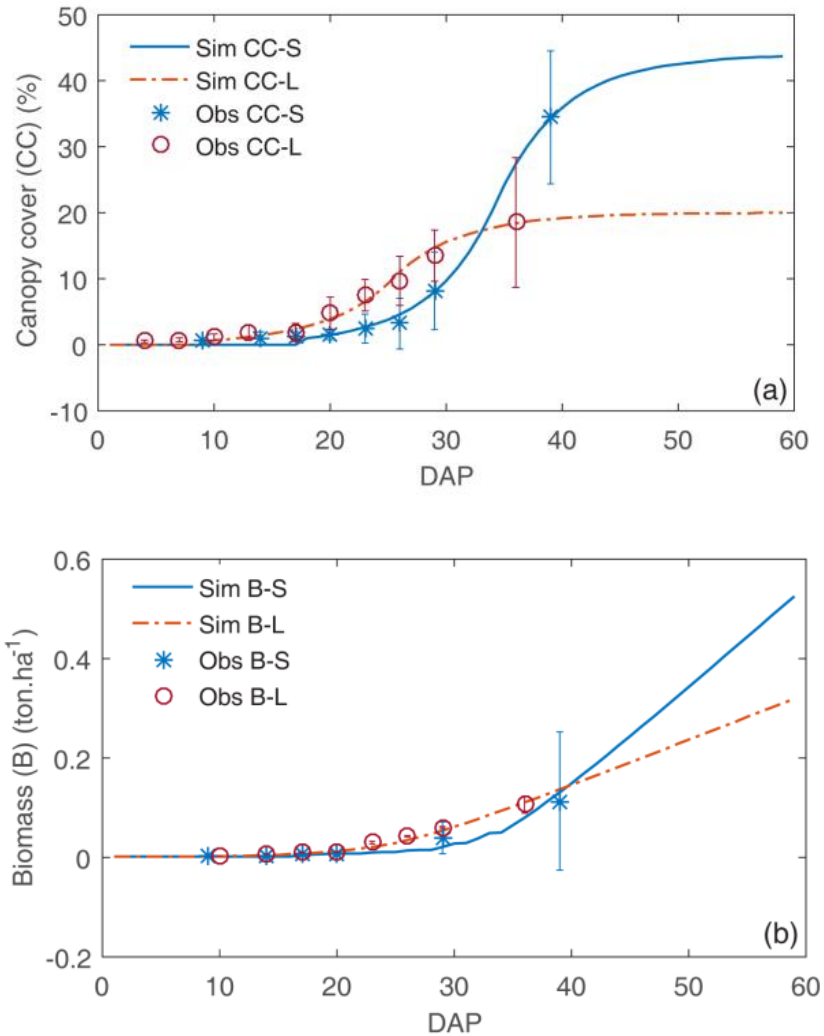
Figure 5.3-1 Observed (Obs) data and simulation (Sim) of lettuce growth of AquaCrop: (a) canopy cover at site T2 (CC-S) (sand soil) and site T4 (CC-L) (loam soil); (b) aboveground biomass at site T2 (B-S) and site T4 (B-S). The error bars were based on 10 biomass samples, except the last observed, which was based on 60 samples at harvest time. Sim CC-S is simulated canopy cover at site T2, Sim CC-L is simulated canopy cover at site T4, Obs CC-S is observed canopy cover at site T2, Obs CC-L is observed canopy cover at site T4, Sim B-S is simulated biomass at site T2, Sim B-L is simulated biomass at site T4, Obs B-S is observed biomass at site T2, Obs B-L is observed biomass at site T4.

5.3.2 Model Parameterisation and Evaluation

The primary crop variables calibrated for daily lettuce growth were canopy cover and biomass, with the daily soil moisture simulated by AquaCrop, by adapting available physical soil data.

Table 5.3-1 presents the adjusted model parameters for canopy cover and biomass curve simulation of lettuce growth. The time to recovery of transplant, the time to reach the maximum canopy cover, the initial canopy cover (CCo), the maximum canopy cover growth coefficient (CCx), the coefficient for maximum crop transpiration ($Kc_{Tr,x}$), and the normalised biomass water productivity (WP*) were mainly calibrated.

WP* was adjusted at 16 gm^{-2} for both sites, within the recommended range. $Kc_{Tr,x}$ was adjusted at 0.65 and 0.5 for site T2 and T4, respectively. These adjusted $Kc_{Tr,x}$ are lower than crop coefficient for the mid-season ($K_{cb,mid}$ = 1) proposed by FAO-56. The difference between the values proposed by FAO-56 and the adjusted $Kc_{Tr,x}$ values is due to the fact that the FAO crop coefficients were obtained for specific agroclimatic conditions, which are different from the conditions of this study (Paredes et al. 2014).

In addition, $Kc_{Tr,x}$ is a major requisite for estimating crop transpiration and biomass. The low adjusted value of this parameter resulted in low simulated biomass yields to fit to measured values.

High temperature stress observed during the experiment could be the reason for the low observed lettuce biomass production (Valenzuela et al. 1996). This observation leads to a recommendation for further development of a heat stress factor in relation to canopy cover and biomass simulations for lettuce.

The minimum root depth cannot be adjusted under 0.1 m, while the root development of lettuce was under this limit. Thus, root development in the model requires further modification (Tan et al. 2018).

The crop growth simulation of canopy cover and biomass fitted the observed data well (Figure 5.3-1). The statistical values for model evaluation in Table 5.3-2 were satisfactory, resulting in R^2 = 0.99, RMSE < 0.8%, N < 4.6 for canopy cover, and R^2 > 0.98, RMSE < 0.01 ton ha^{-1}, N < −0.07 for biomass. Thus, the model has ability to simulate well the growth of lettuce in both soil types at the two experimental sites.

Table 5.3-1. (Part I)AquaCrop variables parameterised.

Parameters	Symbol and Unit	Value				Sources
		T2		T4		
		Initial	Calibrated	Initial	Calibrated	
Crop Phenology						
Time to recovered transplant (C)	(GDD)	52	280	52	147	Default
Time to maximum canopy cover (C)	(GDD)	563	859	563	727	Default
Crop Growth						
Plant density (NC)	dp (plants m^{-2})	12	-	12	-	Measure
Initial canopy cover (NC)	CCo (%)	0.72	0.84	0.5	0.6	Default
Maximum effective rooting depth	Zr (m)	0.1	-	0.1	-	Measure
Maximum canopy cover (C)	CCx (%)	34	44	18	20	Measure

Note: C = conservative, NC = non-conservative.

Table 5.3-1. (Part I)AquaCrop variables parameterised.

Parameters	Symbol and Unit	Value				Sources
		T2		T4		
		Initial	Calibrated	Initial	Calibrated	
Crop Growth						
Canopy growth coefficient	CGC	22.7	18.5	22.7	16.8	Default
Base temperature (C)	Tbase (°C)	4	-	4	-	(Moriasi et al. 2007)
Upper temperature(C)	Tupper (°C)	28	-	28	-	(Autovino et al. 2018)
Canopy size of transplanted seeding (C)	CC (cm² plant⁻¹)	6	-	5	-	Measure
Coefficient for maximum crop transpiration (NC)	$Kc_{Tr,x}$	1.25	0.65	1.25	0.5	Default
Water productivity, (C)	WP* (g m⁻²)	15	16	15	16	Default
Canopy growth coefficient	CGC	22.7	18.5	22.7	16.8	Default

Table 5.3-2. Statistical evaluation of model simulation.

Statistical Criteria	Sites	Canopy Cover (%)	Biomass (ton ha^{-1})
RMSE	T2	0.69	0.012
	T4	0.84	0.01
R^2	T2	0.99	0.98
	T4	0.99	0.99
N	T2	1.1	−0.015
	T4	4.6	−0.07

The measured and simulated soil moisture, at both soil depths of 5 and 15 cm in both sites, also matched well (Figure 5.3-2). The soil moisture simulation resulted in good accuracy with low RMSE of 0.18 and 0.14 m^3 m^{-3} at depths of 5 and 15 cm, respectively, at site T2, and 0.05 and 0.06 m^3 m^{-3} at depths of 5 and 15 cm, respectively, at site T4.
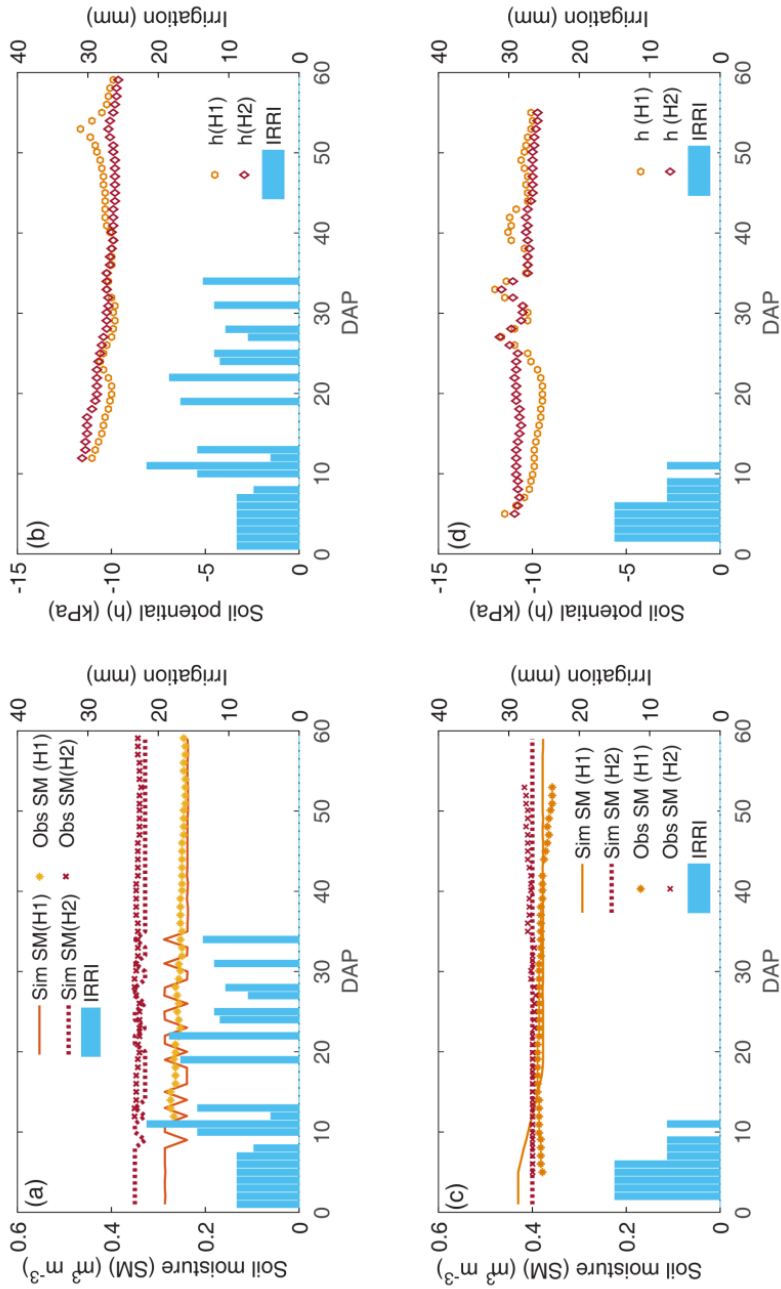
Figure 5.3-2 Simulated soil moisture and observed soil moisture data measured at depths of 5 cm (H1) and 15 cm (H2) using soil moisture sensor 10HS and soil potential MPS-2: (**a**) soil moisture at site T2; (**b**) soil potential at site T2 (**c**) soil moisture at site T4; (**d**) soil potential at site T4. DAP is day after planting, Sim SM is simulated soil moisture, Obs SM is observed soil moisture, IRRI is irrigation, h is soil potential.

5.3.3 Irrigation Scenarios

5.3.3.1   Irrigation and Soil Moisture Response

The cumulative irrigation in Figure 5.3-3, and the fluctuation of the soil moisture depletion in Figure 5.3-4, reflect the interaction between irrigation frequency and amount of water applied.

In both varied RAW and field capacity threshold irrigation scenarios, the irrigation frequency decreased together with decreasing the amount of water applied per irrigation event.

In varied RAW threshold irrigation scenarios, the simulation of irrigation resulted in irrigation depths which ranged from 57 to 104 mm in site T2 (sand soil) and 46–82 mm in site T4 (loam soil) (Figure 5.3-3 a,c). In varied field capacity threshold irrigation scenarios, irrigation depths ranged from 81–201 mm in site T2 and 83–209 mm in site T4 (Figure 5.3-3 b,d).

5.3.3.2   Crop Evapotranspiration and Biomass Growth Response

Figures 5.3-5 and 5.3-6 illustrate the cumulative crop evapotranspiration (ETc) and cumulative biomass of lettuce, respectively, under various irrigation scenarios simulated with AquaCrop calibrated for lettuce.

In varied RAW threshold irrigation scenarios, total simulated ETc ranged from 60 to 100 mm in site T2, and from 53 to 85 mm in site T4 (Figure 5.3-5 a,c). The main reason for the higher ETc yield in site T2 is the higher adjusted transpiration characteristic of lettuce in sand soil as compared to loam soil. The simulated values of ETc fall within the range reported by Abdullah et al. (2004) for lettuce, which varied from 43 mm to 285 mm in response to their different irrigation applications between 0 and 267 mm for open surface soil.

In varied field capacity threshold irrigation scenarios, simulated total crop evapotranspiration ranged from 77 to 205 mm in site T2, and from 83 to 211 mm in site T4 (Figure 5.3-5 b,d). In both irrigation scenario classes, it was noted that while reducing irrigation events, crop evapotranspiration decreased simultaneously.

Figure 5.3-6 shows the response of biomass to the different irrigation scenarios. The varied RAW threshold irrigation scenarios (Figure 5.3-6 a,c) resulted in biomass yield range from 0.88–1.77 ton ha^{-1} at site T2, and 0.44–0.91 ton ha^{-1} at site T4. By definition, biomass growth is closely related to crop evapotranspiration. Thus, the difference between biomass yields in the two experimental sites is due to the difference in the $Kc_{Tr,x}$ (coefficient for maximum crop transpiration) and CCx (maximum canopy cover) parameters between both sites.

As expected, in varied RAW threshold irrigation scenarios, the simulations maintained biomass yield at 1.77 ton ha^{-1} at site T2 and 0.90 ton ha^{-1} at site T4 in the full irrigation scenarios with allowable depletion from 0–100% of RAW (e.g., S0RAW to S100RAW for site T2 and L0RAW to L100RAW for site T4), that is due to no-water stress condition. As the water stress started below the RAW line (Payero et al. 2006), with available depletion from 120–200% of RAW thresholds, the biomass yields decreased up to 50% in the S200RAW (200% of RAW threshold) scenario at site T2 and 52% in L200RAW scenario at site T4.
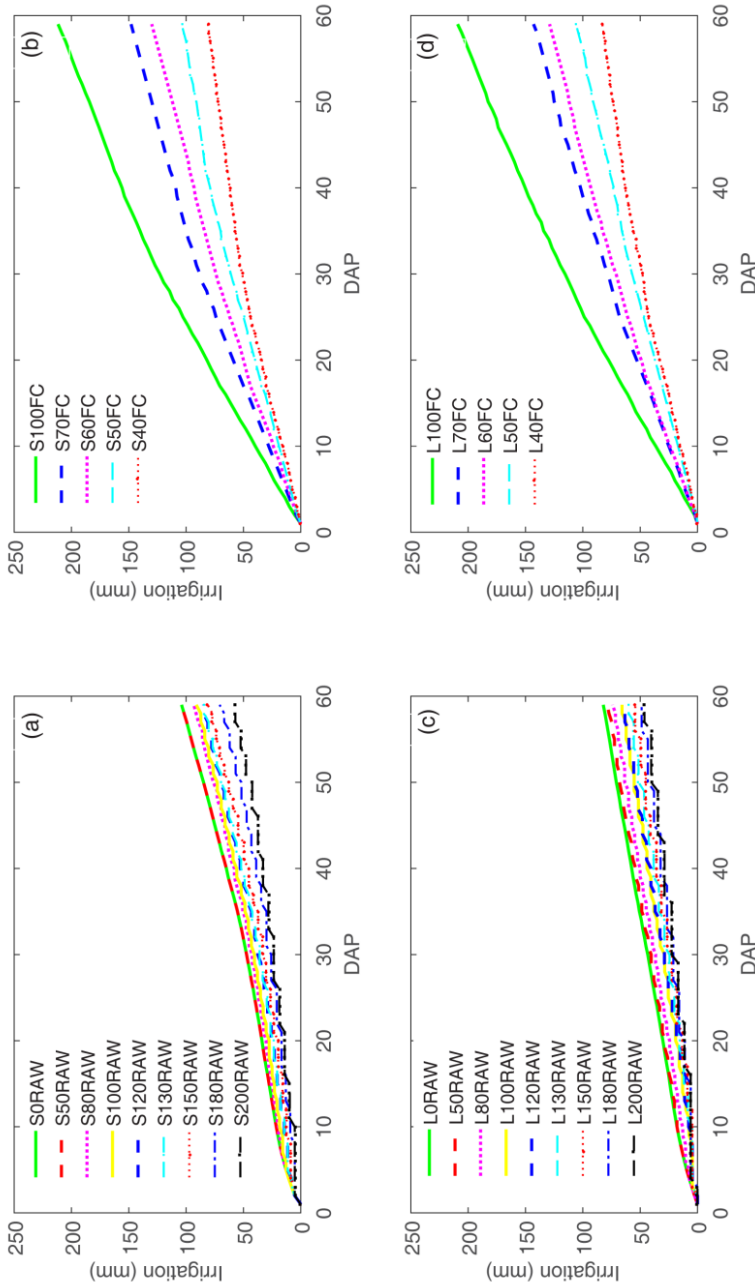
Figure 5.3-3 Irrigation accumulation response to different scenarios: (**a**) varied RAW threshold irrigation scenarios at site T2 (sand soil); (**b**) varied field capacity threshold irrigation scenarios at site T2; (**c**) varied RAW threshold irrigation scenarios at site T4 (loam soil); (**d**) varied field capacity threshold irrigation scenarios at site T4. RAW is readily available water content, S0RAW-S200RAW refers to irrigation scenarios with irrigation at 0–200% of RAW for sand soil. L0RAW-L200RAW refers to irrigation scenarios with irrigation at 0–200% of RAW for loam soil. S40FC-S100FC refers to deficit irrigation at 40-100% of field capacity for sand soil. L40FC-L100FC refers to deficit irrigation at 40-100% of field capacity for loam soil.

Figure 5.3-4 Daily soil moisture (VWC) response to different scenarios: (a) varied RAW threshold irrigation scenarios at site T2 (sand soil); (b) varied field capacity threshold irrigation scenarios at site T2; (c) varied RAW threshold irrigation scenarios at site T4 (loam soil); (d) varied field capacity threshold irrigation scenarios at site T4. RAW is readily available water content, S0RAW-S200RAW refers to irrigation scenarios with irrigation at 0–200% of RAW for sand soil. L0RAW-L200RAW refers to irrigation scenarios with irrigation at 0–200% of RAW for loam soil. S40FC-S100FC refers to deficit irrigation at 40–100% of field capacity for sand soil. L40FC-L100FC refers to deficit irrigation at 40–100% of field capacity for loam soil.

Figure 5.3-5 Crop evapotranspiration accumulation responses to different scenarios: (**a**) varied RAW threshold irrigation scenarios at site T2 (sand soil); (**b**) varied field capacity threshold irrigation scenarios at site T2; (**c**) varied RAW threshold irrigation scenarios at site T4. RAW is readily available water content, S0RAW-S200RAW refers to irrigation scenarios with irrigation at 0–200% of RAW for sand soil. L0RAW-L200RAW refers to irrigation scenarios with irrigation at 0–200% of RAW for loam soil. S40FC-S100FC refers to deficit irrigation at 40–100% of field capacity for sand soil. L40FC-L100FC refers to deficit irrigation at 40–100% of field capacity for loam soil.

Figure 5.3-6 Biomass accumulation responses to different scenarios: (**a**) varied RAW threshold irrigation scenarios at site T2 (sand soil); (**b**) varied field capacity threshold irrigation scenarios at site T2 (**c**) varied RAW threshold irrigation scenarios at site T4 (loam soil); (**d**) varied field capacity threshold irrigation scenarios at site T4. RAW is readily available water content, S0RAW-S200RAW refers to irrigation scenarios with irrigation at 0–200% of RAW for sand soil. L0RAW-L200RAW refers to irrigation scenarios with irrigation at 0–200% of RAW for loam soil. S40FC-S100FC refers to deficit irrigation at 40–100% of field capacity for sand soil. L40FC–L100FC refers to deficit irrigation at 40–100% of field capacity for loam soil.

105

In varied field capacity threshold irrigation scenarios (Figure 5.3-6 b,d), biomass yields ranged from 0.85 to 1.77 ton ha^{-1} at site T2, and 0.89 to 0.90 ton ha^{-1} at site T4. At site T2, reducing deficit irrigation at 50% of field capacity (S50FC scenario), the biomass yield started to decrease with 22% and deficit irrigation at 40% of field capacity (S40FC scenario), biomass yields decreased up to 51% compared to full irrigation scenario (S100FC). For site T4, deficit irrigation up to 40% of field capacity (L40FC) did not affect biomass yield.

5.3.3.3   Relationship between Water Productivity and Irrigation Scenarios

The responses of biomass yield and irrigation water productivity to irrigation depths in various scenarios are presented in Figure 5.3-7. Simulated water productivity of varied RAW threshold irrigation scenarios ranged from 1.5 to 2.1 kg m^{-3} for site T2 and 0.9 to 1.4 kg m^{-3} for site T4. In varied field capacity irrigation scenarios, simulated irrigation water productivity (IWP) ranged from 0.8 to 1.36 kg m^{-3} for site T2 and 0.43–1.08 kg m^{-3} for site T4. The simulated irrigation water productivity results are comparable with other studies found in the literature. For instance, Gallardo et al. (1996) found a measured IWP for lettuce dry matter of 1.86 kg m^{-3}.
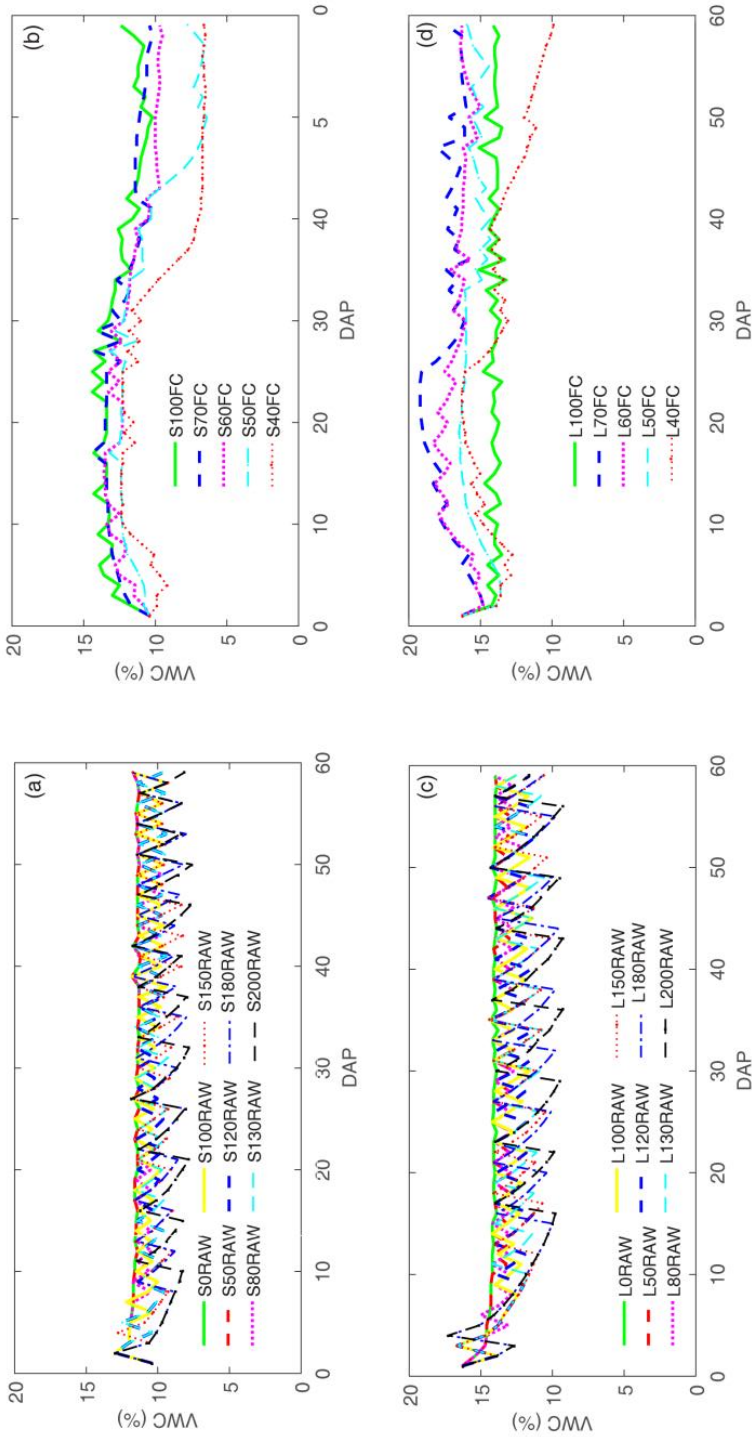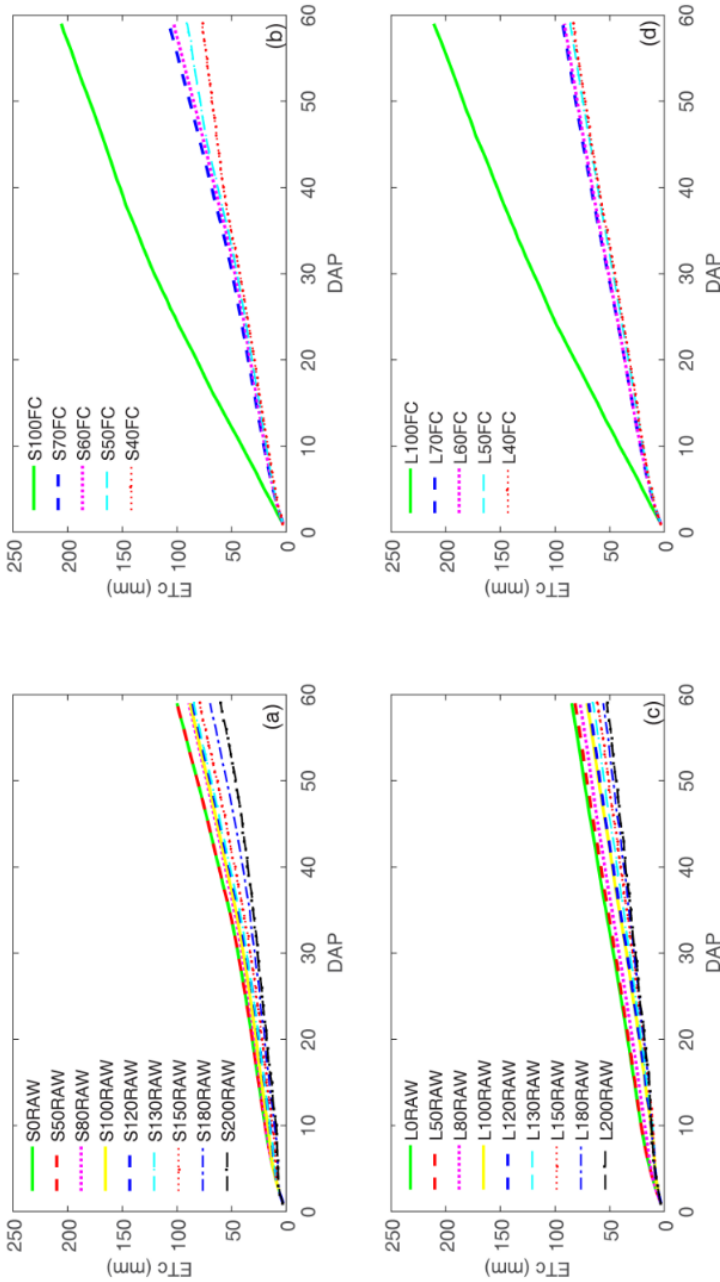
Figure 5.3-8 shows the relationship curves of biomass yield and irrigation water productivity response to irrigation scenarios. As expected, irrigation water productivity curve response to irrigation depths had parabolic relationships for both soil types in varied RAW threshold irrigation scenarios. Increasing water use efficiency can be enhanced by decreasing the irrigation to an optimum point. The optimum point, which resulted in 22% water saving for site T2, was found at the scenario with depletion of 150% of RAW (S150RAW), resulting in the irrigation water productivity = 2.07 kg m^{-3}, irrigation depth = 81 mm, and biomass yield = 1.68 ton ha^{-1}. For site T4, the optimum irrigation water productivity was at 130% of RAW scenario (L130RAW), resulting in irrigation water productivity = 1.42 kg m^{-3}, irrigation depth = 60 mm, and biomass yield = 0.85 ton ha^{-1}.

In varied field capacity threshold irrigation scenarios, for site T2, the optimum irrigation water productivity with 39% water saving was found at deficit irrigation at 60% of field capacity (S60FC) with irrigation water productivity = 1.36 kg m^{-3}, irrigation depth = 130 mm, and biomass yield = 1.77 ton ha^{-1}. For site T4, the optimum water productivity resulted in 60% water saving, which was found at deficit irrigation at 40% of field capacity (L40FC scenario) with irrigation water productivity = 1.08 kg m^{-3}, irrigation depth = 83 mm, and biomass yield = 0.89 ton ha^{-1}.

The varied RAW threshold irrigation scenarios resulted in higher simulated higher irrigation water productivity than the varied field capacity threshold scenarios in this study. Overall, deficit irrigation simulation scenarios in both irrigation scenario classes can provide a remarkable improvement in irrigation water productivity for water saving strategies.
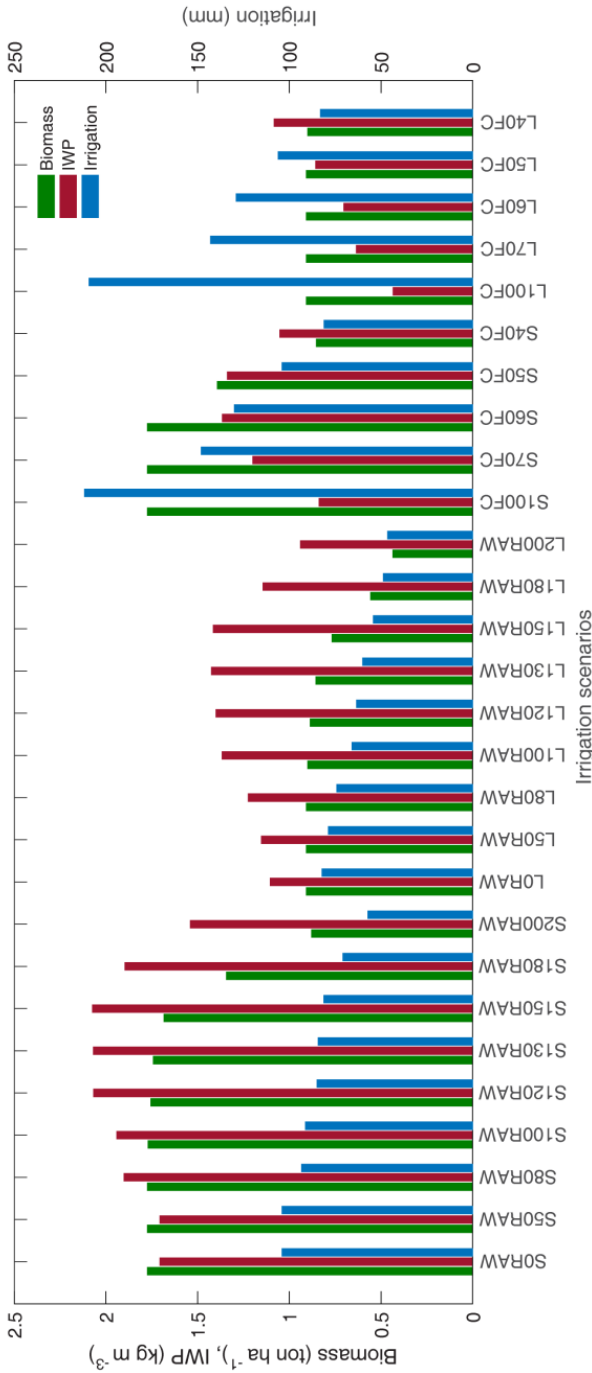
Figure 5.3-7 Comparison of biomass and water productivity response (IWP) to different irrigation scenarios. RAW is readily available water content. S0RAW-S200RAW refers to irrigation at 0–200% of RAW threshold irrigation scenarios for sand soil. L0RAW-L200RAW refers to irrigation at 0–200% of RAW threshold irrigation scenarios for loam soil. S40FC-S100FC refers to deficit irrigation at 40–100% of field capacity for sand soil. L40FC-L100FC refers to deficit irrigation at 40–100% of field capacity for loam soil.
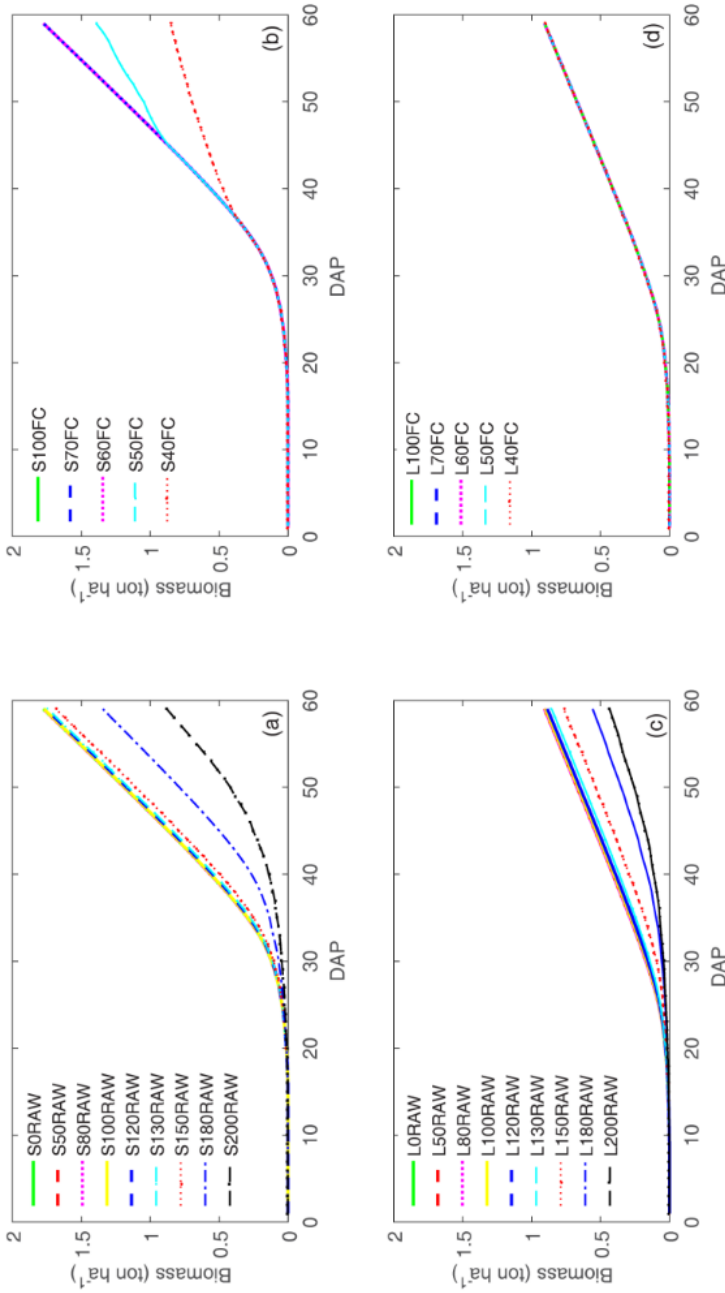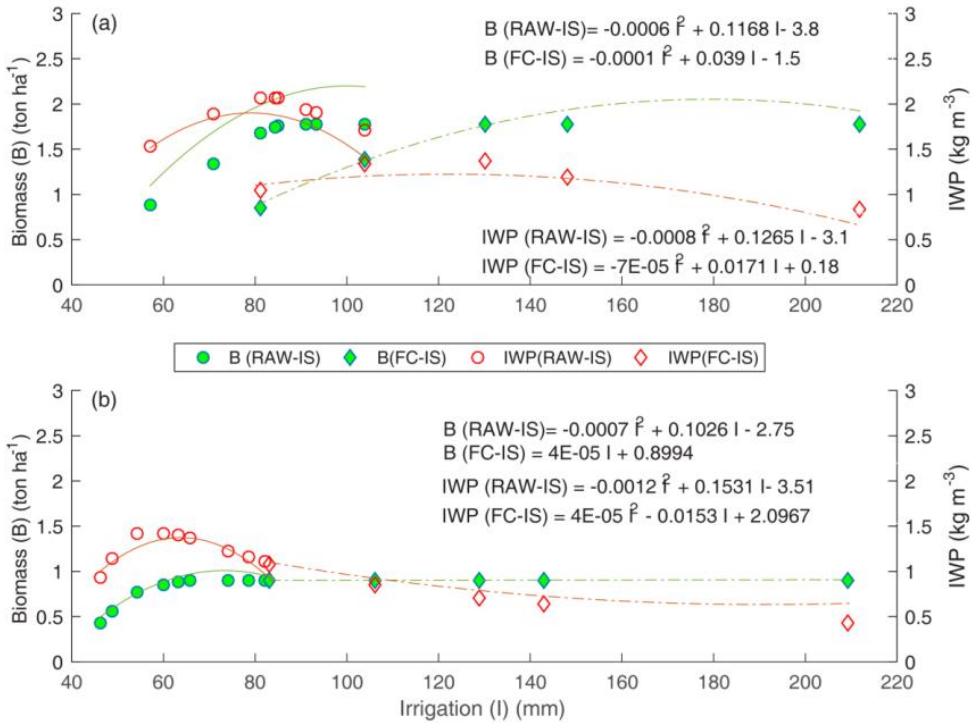
Figure 5.3-8 Relationship between biomass and irrigation water productivity responses to different scenarios: (**a**) at site T2 (sand soil) and (**b**) at site T4 (loam soil). I is irrigation, B is biomass, IWP is irrigation water productivity, RAW-IS is varied readily available water content threshold irrigation scenarios, FC-IS is varied field capacity threshold irrigation scenarios.

5.3.3.4 Limitation

Crop models, like AquaCrop, are potentially valuable tools for answering questions primarily relating to research understanding, assessing crop management, and policy decision-making (Steduto et al. 2009a; Boote et al. 1996). However, it is essential to test the models in diverse field environments, such as those with varied temperatures, elevation transects, or amidst latitudinal variations (Boote et al. 1996). Particularly, AquaCrop has some limitations in terms of predicting crop yields only at the single growth cycle, single field scale, and only factoring in vertical water balance. The results of this study, obtained using climate data and field observation data relating to lettuce from a single growth cycle experiment at farm scale, allowed important information to be obtained in terms of calibrating lettuce crop parameters for sand and loam soil, and assessing limited water irrigation scenarios in the Cambodian context. However, it remains limited and the uncertainty on parameters has to be kept in mind. This study should be repeated in a contrasting range of diverse environments. Climate

conditions and different cultural practices are the variables that differentiate the scenarios between different sites (Boote et al. 1996; Silvestro et al. 2017). It has been emphasised that uncertainty model simulation results are themselves uncertain, due to known inadequacies of the model (residual errors in measurement) and due to unknown inadequacies of the model (by inputting new cultivars or different types of management, the model may be wrong in unsuspected ways) (Wallach et al. 2008). Despite such limitations, AquaCrop has already proven its usefulness in practical applications, and should still be tested widely in broader crop management applications, in diverse field environments (Boote et al. 1996, Silvestro et al. 2017).

5.4 Conclusions

An AquaCrop model was parameterised to simulate the canopy cover and aboveground biomass growth of lettuce under drip irrigation and plastic mulching for both sand and loam soil in the tropical monsoon climate of Cambodia. The model simulated canopy cover (RMSE < 0.8%) and aboveground biomass (RMSE < 0.01 ton ha^{-1}) in a satisfactory way after adjusting several key parameters, as mentioned in Farahani et al. (2009).

Additionally, the results suggested that the incorporation of a heat stress factor affecting canopy cover and biomass growth is necessary to meet the conditions encountered in a tropical climate context.

Shortage of water in Cambodian agriculture has increased due to climate change, and this is a significant challenge facing farmers in their crop production. In this study, the AquaCrop model has helped to develop the simulation process for limited irrigation management strategies to maximise irrigation water productivity. To test the impact of different irrigation scheduling and water saving strategies, two scenario classes were explored: (i) varied readily available water (RAW) threshold irrigation and (ii) varied field capacity threshold irrigation scenarios. The irrigation scenario analysis proposed optimal irrigation strategies for lettuce.

For varied RAW threshold irrigation scenarios, the analysis proposed optimal simulated irrigation water productivity at scenarios of 150% of RAW (irrigation water productivity = 2.1 kg m^{-3}) for sand and 130% of RAW (irrigation water productivity = 1.4 kg m^{-3}) for loam soil. This can save 22% of water, and resulted in a biomass yield reduction of 5 and 2%, respectively, for sand and loam soil. For varied field capacity threshold irrigation scenarios, the optimal deficit irrigation depth was found at 60% of field capacity (irrigation water productivity of 1.4 kg m^{-3}) for sand soil, and at 40% of field capacity (irrigation water productivity of 1.0 kg m^{-3}) for loam soil. It can save water up to 39% and 60%, for sand and loam soil, respectively, maintaining biomass yields compared to full irrigation. These results suggest that deficit irrigation is worth considering as a water saving strategy for lettuce in the monsoon climate of Cambodia.

Overall, AquaCrop is a valuable tool to predict lettuce growth and to investigate different scenarios for providing irrigation scheduling strategies for water saving in Cambodia. However, further research is necessary to standardise the model

parameters for lettuce in various irrigation management, environmental, and climatic conditions.

6

General Discussion

This chapter generally discusses the findings from the study approaches and proposes recommendations for further research. This section also presents some concerns regarding the sustainable use of groundwater for irrigation.

Cambodia doesn't produce enough vegetables to meet the needs of its population. A major obstacle for Cambodian farmers is a lack of knowledge of irrigation management, especially for non-rice crops, while facing extreme weather events such as drought that are increasing in Cambodia. To overcome this issue, in this research we aim to contribute the development of vegetable production during the dry season in Cambodia.

We conducted two complementary approaches to improve water use efficiency for on-farm irrigation by optimising irrigation scheduling. These approaches were used to improve our understanding of the complex relationships between soil, water and plant responses. The first approach (Chapter 4) was conducted to address the research question "how can soil hydraulic properties be characterised for use in crop modelling?" For the second (Chapter 5), we tried to identify which are the best scenarios to maximise water use efficiency for vegetable irrigation during the dry season in Cambodia.

In the first approach, a commonly-used model for soil water flow simulation, HYDRUS-1D was used to derive the soil water retention curve (SWRC). The five experimental fields selected have different soil textures (e.g. loamy sand, sand and loam soils) and are located in the Chrey Bak catchment, Kampong Chhnang province. The experimental data recorded during the growing season of the selected vegetable, lettuce in 2016, were used to calibrate the soil van Genuchten parameters by the inverse solution method.

In the second approach, we developed a methodology to analyse irrigation scheduling that involved two steps. The first step was to calibrate crop parameters of the crop water-driven model, AquaCrop, which has been widely applied for irrigation management. The parameterisation process was solved using the field experiment for lettuce growth in 2017 on two farm fields that have sand and loam soils, and the soil parameter calibration was obtained from inverse modelling. For analysis of the crop growth simulation, we combined inputs from weather and management practices (drip irrigation, 90% plastic mulch cover). Then, we explored various full and deficit irrigation schedules. The irrigation scheduling was based on soil moisture depletion within two threshold categories. The first category involves varying the irrigation starting point, the so-called the lower limit threshold or readily available water content (RAW), between 0 to 200% of RAW. The second involves setting the stop irrigation point, the so-called the upper limit threshold or field capacity (FC), between 0 to 60% of FC deficit.

6.1 Evaluation of inverse modelling for estimating soil hydraulic properties

Our analysis of soil parameterisation confirmed that inverse modelling of a one-dimensional vadose zone model was able to successfully derive the soil parameter sets $(\theta_s, \theta_r, n, \alpha, l, K_s)$ for the SWRC. In testing water flow simulation, the model resulted in good simulation performance in predicting the soil water dynamic in all the studied soil types. This approach is not new, inverse modelling using Richard's soil water dynamic equation has been applied to estimate soil parameters in various studies in

the literature (Ritter et al. 2003a; Le Bourgeois et al. 2016; van Genuchten et al. 1997; Lazarovitch et al. 2007; Eching and Hopmans 1993; Dam 2000; Wayllace and Lu 2011). However, most of these authors only used the SWRC laboratory data for inversion input data. Field plots are more complex than applications for laboratory set-ups (Dam 2000). Furthermore, many researchers have shown the limitations of in-situ measurements of soil moisture and soil water potentials under natural boundary conditions in estimating the soil hydraulic properties (Scharnagl et al. 2011).

The soil moisture sensor, 10HS, and soil potential sensor, MPS-2, contributed to measurement of in-situ soil water retention curve variables for the inverse modelling process. This led us to better understanding of the effect of the field environment on the soil hydraulic properties. Initially, the soil parameters were derived from Rosetta and used the inverse input data for inverse modelling. Our analysis resulted in improved estimation of soil hydraulic properties (i.e., soil water retention) and water flow through the inversion method when compared to the initial condition.

The results highlight that the tension infiltrometer might be useful in determining saturated hydraulic conductivity (Ks) for inverse estimation for fine (loam) soil texture. However, there are drawbacks to inverse modelling. The imperfectness of water flow simulation has been noted. Mostly, there are uncertainties in the output of the simulation that involve the accuracy of available model inputs (e.g., soil moisture, soil water potential, irrigation, soil hydraulic conductivity in real time), model simplification, and the ill-posedness of the inverse problem (Ritter et al. 2003; Brown and Heuvelink 2005; Loos et al. 2007).

In the following we highlight the limitations and further improvements to the study.

The first input variables considered are the soil moisture and soil potential from 10HS and MPS-2, respectively. These sensors have significant limitations in capturing the accurate moisture level and soil potential in wet and very dry conditions. In the future, scientists will need to develop devices for improving measurements in these conditions. Ebel et al. (2018) recommended an improvement for near saturation conditions that involves sprinkling experiments over instrumented soil pits as used in Torres et al. (1998). For drier conditions, one suggestion is to put precipitation exclusion structures over the instrumented soil pits as in the study cases of Nepstad et al. (2007) and Cleveland et al. (2010), or to use equipment with higher capabilities for monitoring soil moisture and soil potential such as the heat dissipation sensors used in Bittelli et al. (2012). The options for soil moisture sensors with high spatial and/or temporal resolution are presented by Vereecken et al. (2014). The higher capability equipment is likely to be more costly but could be necessary to fill research gaps, whereas smallholder farmers generally prefer the low cost devices. Therefore, it is suggested that precise measurement with high price devices should be used to better understand real-world conditions, while experimental approaches using both accurate and lower accuracy instruments is suggested to understand the situation and give better recommendations to farmers.

The next example of data uncertainty in this study arises from the tension infiltrometer measurements. The tension infiltrometer used here is among the better methods for determining in-situ hydraulic conductivity K(h) (Alagna et al. 2016). However, it poorly described the soil hydraulic conductivity for coarse soil textures,

resulting in convergence issues during inverse modelling. Additionally, measurement of K(h) was conducted once in each field. Indeed, dynamic observation of in-situ hydraulic conductivity is the most challenging task soil physicists will have to face in the future. Further research should improve the ability of the device to obtain dynamic measurements and higher accuracy of K(h) measurement which would improve the simulation.

A further input source of data error is that transpiration was estimated based on a model (Gallardo et al. 1996b) that results in error prediction due to various factors such as the climate and location conditions. A better estimation or measurement of transpiration should be considered. Interestingly, Bello and Rensburg (2017) have made progress in this area, testing low-cost small lysimeters for measuring evaporation and transpiration. Their results show that the small lysimeters were able to measure evaporation and transpiration separately at high accuracy, sensitivity and precision (Loos et al. 2007).

Another issue was inaccurate irrigation data input. The data on the dynamics of irrigation amounts were estimated based on the fluctuation of soil moisture, and the flow rate as determined by the manufacturer. An accurate water balance approach using lysimeters could address this issue.

Despise the advantage of the efficiency of soil hydraulic estimation, it is confirmed in this study that inverse modelling faces problems in the non-uniqueness of the generated soil parameters and sensitivity to the initial soil input data in disconvergence of the simulation. Improvement of accuracy in the model inputs could lead to solving the inverse problems and also better outflow performance.

Aside from the data input inaccuracies, a simple assumption of the model itself has limitations in reflecting the real dynamic change of the model. The main simplification is that the model assumed the single soil hydraulic properties over the entire simulation period (Simunek 2005). Thus, the dynamic changes in soil hydraulic properties in time and space should be further developed within the model algorithm for HYDRUS-1D.

Furthermore, it is necessary to standardise the generated soil parameter sets. This can be achieved by calibration and validation from further experiments over many growing seasons.

6.2 Evaluation of lettuce growth simulation and optimal irrigation water use

In the second study approach, our analysis indicated that AquaCrop could satisfactorily predict the lettuce growth (e.g., canopy cover and above ground biomass growth) under plastic mulching in both studied sites. Crop parameters were mainly calibrated, this included time to recovery of transplant, time to reach maximum canopy cover, initial canopy cover (CCo), maximum canopy cover growth coefficient (CCx), coefficient for maximum crop transpiration ($Kc_{Tr,x}$), and normalised biomass water productivity (WP*).

Considering the importance of modelling approaches in aiding decision-making and policy changes, it is noted that to date the crop growth and irrigation simulations for leafy vegetables including lettuce are very limited and are not yet in the AquaCrop list of case studies. Therefore this study can be useful for further validation of the model's performance. The limitations of the study and parameter uncertainty during the process of calibration have been observed as follows.

Firstly, the effect of heat stress was observed in the growth of lettuce during the experiment. In AquaCrop there is only an adjustment for cold stress factors. Consequently, the calibration of the model absorbed this stress into another factor, the crop coefficient (Kc) resulting in its low value compared to FAO. This suggests that further development of the model is required to accommodate heat stress factors to adapt the model to tropical climate conditions.

The second limitation is rooting depth. AquaCrop has limited the minimum root depth data input to 10 cm, while the observed root growth is less than 10 cm. Further model development for root depth should be considered. Additionally, the obtained soil parameters from the inverse modelling have been used for the second approach. There was no observed soil water dynamic during the second approach due to water pooling. Therefore, it is recommended that further detailed studies are made on the soil parameters and water flow response of the model.

Both the limitations of the model and the uncertainties in our input data led to inaccuracy in the output of the simulation. It is noted that the transpiration and soil evaporation were estimated by the model. The model simulation would be improved by the addition of transpiration observations and field data for soil evaporation. The precise in-situ soil water balance data should be further investigated. Moreover, our lettuce growth observation was conducted only during the development stage. Therefore, observation of whole growth cycle of lettuce needs to be performed. The uncertainty of the calibrated parameters would also be reduced with a higher number of crop growth season experiments.

Despite the limitations of the model, the calibrated AquaCrop model was used to optimise irrigation scheduling for irrigation management strategies considering deficit water conditions. The analysis of irrigation scenarios suggested the highest irrigation water productivity (WP) by applying the two categories of irrigation thresholds, varied RAW and FC. For varied RAW threshold irrigation scenarios, the analysis proposed optimal simulated irrigation water productivity at scenarios of 150% of RAW (irrigation water productivity = 2.1 kg m^{-3}) for sandy soil and 130% of RAW (irrigation water productivity = 1.4 kg m^{-3}) for loamy soil. Compared to full irrigation scenarios, this can save 22% of the water used, and resulted in a biomass yield reduction of 5 and 2%, respectively, for sand and loam soils. For varied field capacity threshold irrigation scenarios, the optimal deficit irrigation depth was found to be 60% of field capacity (irrigation water productivity of 1.4 kg m^{-3}) for sandy soil, and 40% of field capacity (irrigation water productivity of 1.0 kg m^{-3}) for loam soil. Likewise, this can save up to 39% and 60% of irrigation water for sand and loam soil, respectively, maintaining biomass yields compared to full irrigation.

Consequently, with a limited amount of water deficit irrigation can increase the amount of land irrigated. For example, by comparing full irrigation at 0% and 150%

of RAW, resulting in irrigation depths of 104 and 81 mm respectively for sand, deficit irrigation can increase the land irrigated by 22%, e.g., 1 ha for 0% of RAW and 1.2 ha for 150% of RAW.

Regarding the limitations of the deficit irrigation scenarios, water stress was considered to apply to whole stages of lettuce growth. One should note that due to drought stress in particular growth stages, the length of the cropping cycle might change from that of the full irrigation condition (Geerts and Raes 2009). Thus, the use of deficit irrigation requires some specific conditions: i) crop response to drought stress should be studied carefully, and ii) irrigators should have unrestricted access to irrigation water during sensitive growth stages (Geerts and Raes 2009). In addition, many studies have shown that there are different critical crop growth stages for some crops (for example the flowering stage, fruit setting, or assimilate transfer) that are sensitive to water deficits, leading to severe yield reduction and considerable variation in WUE (Katerji et al. 2008). Further research work should repeat the deficit irrigation experiment while considering the different sensitive stages to verify the proposed irrigation scheme, calibrate and validate the deficit irrigation approaches.

Overall, this study approach has beneficially developed the methodology to optimise irrigation for on-farm irrigation management in the Cambodian context.

6.3   Improvement of field water use efficiency

In this dissertation, we focused specifically the soil hydraulic parameters and simulated irrigation scheduling in deficit irrigation conditions. The significant outcomes are the calibrated parameters of the water flow model and crop model and the optimal irrigation scheduling. We have learnt the advantages and limitations of the modelling approaches. However, our goal of improving on-farm irrigation water use efficiency was not completely reached. More work is needed, as proposed in the following points:

i) How to minimise run-off and leaching from surface drip irrigation (SDI)? We have applied the same drip irrigation rate to different experimental fields with different soil textures. It was noted that there is some run-off for fine soils like loam, and leaching in sandy soil. Further experimentation is needed to optimise efficient drip irrigation rates for the different soil textures, as presented in some papers (Provenzano 2007; Wang et al. 2006; Friedman et al. 2016; Li et al. 2018; Gamage et al. 2018; Ajdary et al. 2007). Practical/detailed guidelines are important for farmers to determine irrigation scheduling time-frames for different soil types and crops for the effective practice of WUE (Egea et al. 2016).

ii) How to minimise soil evaporation? Studies on the effects of different mulching variables are also contributing to improving WUE by minimising this factor (Wang et al. 2018; Gupta et al. 2015; Kader et al. 2017; Cosi 2017; Zhou et al. 2018; Adil et al. 2019).

iii) WUE should be evaluated for different techniques and methods, such as using sprinkler systems or surface drip irrigation for different crops in the Cambodian context (Albaji et al. 2015).

iv) The fertility of soils should be assessed globally, not just the physical properties. Soil chemistry and biology deserve as much attention as soil physics in order to guarantee the highest crop yield. Therefore, further research should focus on these factors to improve efficient water management practices in Cambodia.

6.4 How can other stakeholders apply the findings of this research?

Principally, farmers are one of the most important stakeholders as they are dominant in the system. However, there is a knowledge gap between farmers and institutions. Therefore there are some challenges in adapting the water saving findings for real-world use. This is a call for active farmer-participatory research in applying the water saving irrigation practices.

6.5 Are these study approaches suitable for other cultivated land in Cambodia?

We conducted the experiments on 5 experimental sites in the Chrey Bak catchment, with 3 distinguished soil textures, e.g., loamy sand, sand and loam soils. This study is limited compared to the scale of the catchment. Therefore, a process of scaling up this experimental research is needed to clearly characterise the different conditions and characteristics in terms of pedology, weather and different constraints that are relevant to irrigation management.

6.6 Groundwater use sustainability and transposability of the study approach

The water used during the first experiment was from groundwater. Considering the larger scale, if irrigation is to be increased during the dry season, a question will arise: is there enough groundwater to sustain this new water use? Meanwhile, the present groundwater use for irrigation in the study area is not yet significant. If increased use occurs, this could cause negative effects for the environment such as water depletion (Zhang et al. 2018). In this regard, hydrogeologists can play an active role in predicting groundwater availability and the effect of its use for irrigation in order to establish the effectiveness of policies and irrigation sustainability (Gleeson et al. 2012). There is not yet enough research to assess the long term impacts of groundwater irrigation in Cambodia (Vuthy and Ra 2011). Generally, the application of agricultural water-saving remains the best solution for sustainable groundwater use (Sun et al. 2011; Hu et al. 2010).

However, current knowledge of the water balance in the Chrey Bak catchment calls for cautiousness. The recharge of groundwater in Cambodia was estimated to be in the range of 3-15 mm/year to 100–1000 mm/year (Johnston et al. 2013). For Chrey Bak catchment (700 km²), if we select an optimal irrigation scheduling of 150% of RAW (810 m³/ha) for planting lettuce, 3 mm per year of groundwater recharge, 50% of the catchment used for irrigation, we can only irrigate 12 km² or 3.7% of the total

cultivated area. Therefore, in this case the groundwater is not enough to irrigate all the required cultivated land.

7

General Conclusion

This chapter synthesises the general conclusions from the study approaches and presents the perspectives for further research.

7.1 General conclusions

In this thesis, we tried to address the research questions of i) how to characterise soil hydraulic properties for use in crop model and ii) which are the best scenarios for irrigation water saving in Cambodia context in order to optimise irrigation water saving. To achieve the objective,we developed a method for the optimisation of agricultural irrigation water-use based on numerical model simulation. The method involves using water flow and crop-growth models as decision-making tools, and was successfully tested using field measurement data from a lowland area of the Chrey Bak catchment in Kampong Chhnang, Cambodia. The water flow model using HYDRUS-1D software was calibrated for a lettuce growing season in 2016. Additionally, AquaCrop was calibrated for the lettuce growing season in 2017 using field data from two farms that have different soil textures of sand and loam soils.

The studies yield significant twofold findings. Firstly, inverse modelling using a water flow model can effectively characterise the key soil hydraulic properties for irrigation scheduling, e.g., the soil water retention curve and soil hydraulic conductivity that are core parameters of irrigation scheduling. The results highlight the usefulness of soil water measurement using a combination of sensor 10HS and MPS-2 to collect the in-situ soil water retention curve to be used as input data for the inverse modelling, which leads to soil parameterisation. Secondly, the best irrigation scheduling scenarios were proposed for lettuce production. Our irrigation scheduling method developed from the crop growth model suggested the optimal irrigation thresholds under deficit irrigation conditions based on two irrigation threshold criteria, i.e., deficit irrigation below readily available water (RAW) and deficit irrigation below field capacity (FC). For RAW threshold irrigation scenarios, the analysis proposed optimal simulated irrigation water productivity in conditions of 150% of RAW for sand and 130 % of RAW for loam soil with a biomass yield reduction of 5 and 2%, respectively. For FC threshold irrigation scenarios, the optimal deficit irrigation depth was found to be 60% of FC for sandy soil, and 40% of FC for loam soil with no biomass yield reduction compared to full irrigation.

However, some limitations need to be kept in mind. The resulting uncertainty for both modelling approaches remains due to some limitations of instruments in collecting data, data sampling and model assumptions. Further improvement to input data collection is suggested to improve model performance. In addition, model validation through different environmental and growing seasons is needed. Nevertheless, the results indicate the reasonable and good performances of the approaches.

This approach allows us to set up irrigation strategies to find optimal irrigation scheduling and can lead to increased crop water productivity in the study area. To our knowledge, in the Cambodian context irrigation scheduling optimisation is a nascent topic. This modelling approach and methodology thus has emerged and can be considered to be a prior effective useful decision support tool and could contribute to irrigation water management. This is particularly useful in optimising irrigation scheduling to adapt to drought water events in Cambodia and may help to improve current irrigation practices.

7.2 Further work

Our study, being an early test of a water saving irrigation approach in the Cambodian context, raises a number of opportunities for future research, both in terms of methodology development and concept validation. More research will be necessary to refine our findings.

Sustainable groundwater assessment. When the purpose of this study is achieved in the study area, i.e., to raise crop on-farm production, irrigation water use using groundwater might increase accordingly. Irrigation would reach a risk point if the groundwater is put under pressure for all the desired irrigated lands. Strategic approaches that examine the sustainability of irrigation using groundwater in various scenarios are needed to provide a long-term management policy. Alternatively, as Cambodia is abundant in rainfall within annual precipitation around 2000 mm, the development of techniques for irrigation using harvest rainfall that have been successfully applied in arid areas should be conducted for increasing on-farm irrigation.

Economic-deficit irrigation scenario analyses. To complete a framework of deficit irrigation, the economic return factors should be taken into account to choose the optimal irrigation dose (Capra and Consoli 2008). Another challenge is that full or deficit irrigation scheduling techniques require specific tools. The cost might be high and they also need a high level of understanding. One question raised is how to teach this technique to farmers.

A participatory approach. Key lessons learnt from this approach include the need for a participative research and development approach which involves the different stakeholders, including policy makers (government, institution), agronomists, hydrogeologists, farmers and other relevant parties. Irrigation water saving approaches alone cannot be successful, and must be optimised to benefit the farmers. During the research experiment, some points have been noted regarding farmers' performance. The crop harvesting and equipment, including the pump and drip system, were freely provided. Therefore, farmers did not take notes or pay attention to the practice of the irrigation water saving technique. After the experiment, they did not continue to use this technique for irrigation. Some farmers that habitually cultivate rice only during the rainy season did not become familiar with vegetable production during the dry season. The farmers that do produce vegetables during the dry season using their traditional methods still like to work in their own way. They think that irrigation using the drip method takes more time than using their own irrigation technique with a small tube which is faster for their small garden farm. But, positively, they realised that drip irrigation can allow the water to inflitrate deeper.

Another challenge is the amount of lettuces harvested, these need to be sold quickly and it is difficult for the farmers to find a market, unlike rice that can be kept for a long time. However, they seemed to be receptive to the new challenge. Therefore, an approach to connect farmers with the new techniques is needed. The benefit of a good economic return is a key point to convince them. Moreover, our experiment was conducted on one farm per village among the five experimental fields. The farmers tend to follow the practices of the majority, so if there are many pilot projects to show

them, this could motivate them to adopt it as well. "What are the key arguments to convince the farmers?" is a challenging question for researchers.

Another point of view is the fact that this research has focused mainly on the specific objective of optimising irrigation scheduling. Of course, water is a key factor for crop production but there are other factors in obtaining good crop production and there are other scientific questions around the topic of crop production management. Obviously, we did not focus the other effects on crop growth such as fertiliser, different mulch, or different irrigation techniques. More detailed studies on crop growth conditions, soil fertility, etc., can lead to better understanding of the soil-plant-water relationship. Participative and multidisciplinary research would lead to rich exchanges and generate new ideas to address the in-situ challenges for the Cambodian farmers. It would also allow the farmers to demonstrate social interest in the diversification of production, and might lead to the development of encouraging policies to help farmers.

Another point of view, it is the fact that this research has focused mainly on a specific objective of optimising irrigation scheduling. Of course, water is a key factor for crop production but also there are other factors to obtain a good crop production. There are other scientific questions around the topic of crop production management. Obviously, we did not focuss the other effects on crop growth like fertiliser, different mulching, different irrigation techniques. More detailled studies on crop growth conditions, soil fertility, … can lead to better understand the soil-plant-water relationship. Participative and multidisciplinary research would led to rich exchanges and generate new ideas to address the in-situ challenges of the cambodian farmers. It would also allow the farmers to demonstrate the social interest of the diversification of the production and might lead to the development of encouraging policy to help the farmers.

APPENDIX

Results of estimating soil water retention curves using different methods

Estimated parameters

The results of the estimated van Genuchten (vG) parameters from methods M1(Rosetta method), M2 (fitted field SWRC method), M3 (fitted laboratory SWRC method), and M4 (inversion method) are presented in Table A-1. It may be noted that at site T4, the simulation of M4 with the initial input of saturated hydraulic conductivity (Ks) from the tension infiltrometer of 37 cm/day for both depths gave a simulation performance with the Nash of 0.61, RMSE of 0.004 cm^3 cm^{-3}. Trial values of Ks up to 100 cm/day at 10 cm and 45 cm/day at 20 cm depth gave better simulation performance with Nash and RMSE of 0.79 and 0.003 cm^3 cm^{-3}respectively (Table A-2). Therefore, these values of Ks were selected.

For loamy sand soil (sites T1 and T5), the estimated saturated water content (θ_s) ranged from 0.14 to 0.49 cm^3 cm^{-3}. M3 estimated the highest value (0.49 cm^3/cm^3) of θ_s at T1. M2 estimated the lowest value 0.14 cm^3 $cm^{-3}$for T5.

For sandy soil (sites T2 and T3), at T2, M3 estimated a slightly higher value of θ_s= 0.49 cm^3/cm^3 but the lowest value 0.18 cm^3 cm^{-3}at T3. This could be due to measurement errors. However, similar estimations with low range values of 0.16 cm^3/cm^3 to 0.28 cm^3 cm^{-3} were found by M2 for both sites. M4 in T3 resulted in a higher value θ_s of 0.44 cm^3/cm^3 at surface depth and a lower value of 0.38 cm^3/cm^3 at greater depth. Similar θ_s values (from 0.24 cm^3 cm^{-3} to 0.27 cm^3 cm^{-3}) were found in both depths in T2.

For loamy soil, T4, the results of θ_s were slightly different between M1, M3, and M4 with a range of 0.29 cm^3 cm^{-3} to 0.34 cm^3 cm^{-3}. However, the lowest value of 0.17 cm^3 $cm^{-3}$was proposed by M2.

Table A.1 Part (I) Soil hydraulic vG parameter sets derived from different methods: Rosetta method (M1), fitted field SWRC method (M2), fitted laboratory SWRC method (M3), and inversion method (M4).

Sites	Methods	vG parameters											
		At 10 cm depth						At 20 cm depth					
		θr	θs	α	n	Ks	L	θr	θs	α	n	Ks	L
T1	M1							0.042	0.39	0.04	2	200	0.5
	M2							0.04	0.37	0.043	1.6	200	0.5
	M3							0	0.49	0.21	1.4	200	0.5
	M4							0.049	0.34	0.033	1.6	200	0.5
T2	M1	0.046	0.38	0.037	2.3	72	0.5	0.046	0.38	0.037	2.3	72	0.5
	M2	0	0.16	0.0051	1.6	72	0.5	0.037	0.29	0.035	1.5	72	0.5
	M3	0	0.49	0.1	1.4	72	0.5	0	0.49	0.1	1.4	72	0.5
	M4	0.044	0.25	0.03	2	72	0.003	0.048	0.27	0.028	2.1	72	0.18
T3	M1	0.048	0.39	0.037	2.4	180	0.5	0.048	0.39	0.037	2.4	180	0.5
	M2	0	0.17	0.0019	2.3	180	0.5	0	0.18	0.0008	1.9	180	0.5
	M3	0	0.18	0.023	1.4	180	0.5	0	0.18	0.023	1.4	180	0.5
	M4	0.052	0.44	0.029	2.3	180	0.011	0.048	0.39	0.028	2	180	0.22

Note: θr, θs in $cm^3 cm^{-3}$, α in cm^{-1}, Ks in cm day^{-1}

Table A.1 Part (II) Soil hydraulic vG parameter sets derived from different methods: Rosetta method (M1), fitted field SWRC method (M2), fitted laboratory SWRC method (M3), and inversion method (M4).

Sites	Methods	vG parameters											
		At 10 cm depth						At 20 cm depth					
		θ_r	θ_s	α	n	Ks	L	θ_r	θ_s	α	n	Ks	L
T4	M1	0.034	0.34	0.011	1.5	100	0.5	0.034	0.34	0.011	1.5	45	0.5
	M2	0.0001	0.18	0.0024	1.3	100	0.5	0.00015	0.18	0.0013	2	45	0.5
	M3	0	0.29	0.0017	1.9	100	0.5	0	0.29	0.0017	1.9	45	0.5
	M4	0.04	0.4	0.038	1.7	100	0.078	0.043	0.43	0.029	1.6	45	0.022
T5	M1	0.039	0.39	0.043	1.7	70	0.5	0.039	0.39	0.043	1.7	70	0.5
	M2	0.0014	0.15	0.0015	3.8	70	0.5	0.00033	0.25	0.002	1.8	70	0.5
	M3	0	0.23	0.0084	1.5	70	0.5	0	0.23	0.0084	1.5	70	0.5
	M4	0.04	0.4	0.038	1.7	70	0.078	0.043	0.43	0.029	1.6	70	0.022

Note: θ_r, θ_s in cm^{3}cm^{-3}, α in cm^{-1}, Ks in cm day^{-1}

Table A-2 Statistical parameters to evaluate vG parameters in water flow simulations

		RMSE cm³ cm⁻³	Nash	R^2	RMSE cm³ cm⁻³	Nash	R^2
		At 10 cm depth			At 20 cm depth		
T1	M1				0.030	0.50	0.69
	M2				0.015	-0.57	0.71
	M3				0.016	-1.29	0.67
	M4				0.010	0.76	0.83
T2	M1	0.013	-3.19	0.95	0.011	-2.55	0.97
	M2	0.003	0.73	0.98	0.009	-1.80	0.98
	M3	0.037	-44.03	0.97	0.035	-49.00	0.81
	M4	0.004	0.89	0.95	0.002	0.91	0.96
T3	M1	0.022	0.42	0.67	0.025	0.14	0.60
	M2	0.027	-4.88	0.63	0.021	-7.41	0.62
	M3	0.011	-0.05	0.72	0.015	-2.97	0.61
	M4	0.008	0.45	0.72	0.006	0.39	0.68
T4	M1	0.025	-0.66	0.79	0.022	0.69	0.96
	M2	0.004	0.65	0.81	0.014	-3.40	0.90
	M3	0.008	-0.31	0.76	0.009	-0.74	0.95
	M4	0.003	0.79	0.95	0.002	0.92	0.97
T5	M1	0.027	0.21	0.80	0.030	0.63	0.81
	M2	0.021	-2.82	0.57	0.018	-3.82	0.66
	M3	0.009	0.30	0.85	0.017	-3.26	0.81
	M4	0.008	0.42	0.80	0.006	0.53	0.85

Water retention curves

Using the parameter sets from Table A.1 in the methods M1, M2, M3, and M4, the simulated soil moisture was plotted against the log pressure head to obtain SWRCs (Figures A.1 and A.2). Overall, it was noted that the SWRCs from all methods for coarse soil closely match for both the field and laboratory SWRC data. However, there were large differences between the estimated θ_s of SWRCs for all methods.

The Rosetta method, M1, often produced high θ_s for coarse soil (0.38 to 0.39 cm³/cm³) at T1, T2, T3, and T5 and a slightly lower value for loam soil (0.34 cm³/cm³) at T4. It was also noted that the simulated SWRCs by M1 often closely matched the field and laboratory SWRC data for for all sites, apart from laboratory data for fine soil, T4, and field data at T3 at 20 cm depth.

The fitted field SWRC method, M2, fitted the measured SWRC data excellently because it tried to fit individual field data. It was noted that there were errors of field SWRC data at near saturated points that resulted in low estimation of θ_s (from 0.14 to 0.24 cm^3/cm^3) at T2, T3, T4, and T5.

The fitted laboratory SWRC method, M3, suggested low θ_s (from 0.18 to 0.23 cm^3/cm^3) at T3 s T5, and higher values (from 0.29 to 0.49 cm^3/cm^3) at T1, T2, and T4. This can be explained by the lack of SWRC data points and their errors at lower pressures because the pressure plates were mainly applied for the higher tensions from 100 to 1500 kPa, this could cause errors for SWRCs under 100 kPa (Schindler et al. 2012). The small bulk soil core sample volume was not well representative of the real soil condition.

The inversion method, M4, had similar behaviour to M1 for simulating the SWRC. This could be influenced by the initial parameters obtained from M1. However, M4 produced slightly lower or higher values of θ_s, except for T2, M4 produced larger lower θ_s values (0.26 cm^3/cm^3) than M1.

Figure A.1 Soil water retention observed and simulated using different methods : Rosetta method (M1), fitted field SWRC method (M2), fitted laboratory SWRC method (M3), and inversion method (M4) at 10 cm depth.

Figure A.2 Soil water retention observed and simulated using different methods : Rosetta method (M1), fitted field SWRC method (M2), fitted laboratory SWRC method (M3), and inversion method (M4) at 20 cm depth.

Water flow simulation and model performance

Figures A.3 and A.4 show a comparison of different methods to simulate the water flow in a Hydrus 1D model using the optimised parameters presented in Table A.1, and their model performance evaluation is shown in Table A.2.

For T1, all methods showed a similar correlation with R^2 values from 0.67 to 0.83 in soil volumetric water content (VWC) simulation. M2 and M3 had the lowest performance described by negative Nash of -0.57 to -1.29. M1 and M4 performed similarly with RMSE of 0.01 to 0.03 cm^3/cm^3 and high Nash from 0.5 to 0.76.

In T2, all methods showed very good correlation with high R^2 ranging from 0.81 to 0.98. However, M1, M2, and M3 showed a large difference between the observed and the predicted VWC and confirmed by negative Nash values ranging from -1.88 to -49. This could be explained by large errors in estimating θ_s in these methods.

For T3, the significant underestimation found in the results from M1, M2, and M3 indicated by the high RMSE (0.01 to 0.02 cm^3/cm^3) and negative Nash (-0.05 to -7.41) for both soil depths. This showed that using the fitted method to predict the vG parameters can match well to the individual SWRC data points, but possibly result in poor simulation of water flow. M4 performed well in soil prediction with small RMSEs from 0.006 to 0.008 cm^3/cm^3. Interestingly, there was the fluctuation of VWC during the experimental period due to the lag irrigation time. It is noted that the same simulation pattern was used to predict the soil moisture. This shows simulation errors due to model assumptions that are not flexible to real phenomena e.g. the dynamic change of soil hydraulic properties during the growing season, the macropore flow, lateral flux of soil moisture. The overestimation during the dry-end events of the experiment could be due to crusts under extreme drought conditions altering the infiltration and evaporation process (Wang et al. 2016).

At T4 high correlations were found in all methods with the R^2 range from 0.78 to 0.97. M2 gave a poor model simulation for the deeper soil with the negative Nash of -0.34 but better at the surface depth with high Nash value of 0.65. In contrast, M1 performed poorly at the surface depth with Nash of -0.66 but better in the deeper soil with a Nash value of 0.69. M3 performed poorly at both soil depths with Nash of -0.31 and -0.74. M4 performed very well at both soil depths with high Nash (0.79 and 0.92) and low RMSE (0.002 and 0.003 cm^3/cm^3).

At T5, M1 and M4 performed similarly to predict soil moisture content with R^2 ranging from 0.80 to 0.85, and high Nash values from 0.2 to 0.5. M2 again gave a poor simulation performance, with high RMSE from 0.018 and 0.02 cm^3/cm^3 for both soil depths. M3 gave a better performance at the surface depth with RMSE of 0.009 cm^3/cm^3, but poorer RMSE of 0.017 cm^3/cm^3 at the greater depth, similar to M2. M4 again provided good model satisfaction with low RMSEs of 0.006 and 0.008 cm^3/cm^3. However, M4 cannot predict well for the observed dry event.

It was noted at the end dry event that for the loam soil, T4, the draining duration to reach the dry water content of 0.06 cm^3/cm^3 was 18 days longer than coarse soils, at T1, T2, T3, and T5 having the duration 6, 5, 5, and 7 days respectively. This confirms the similar draining magnitude behaviour of these coarse soils.
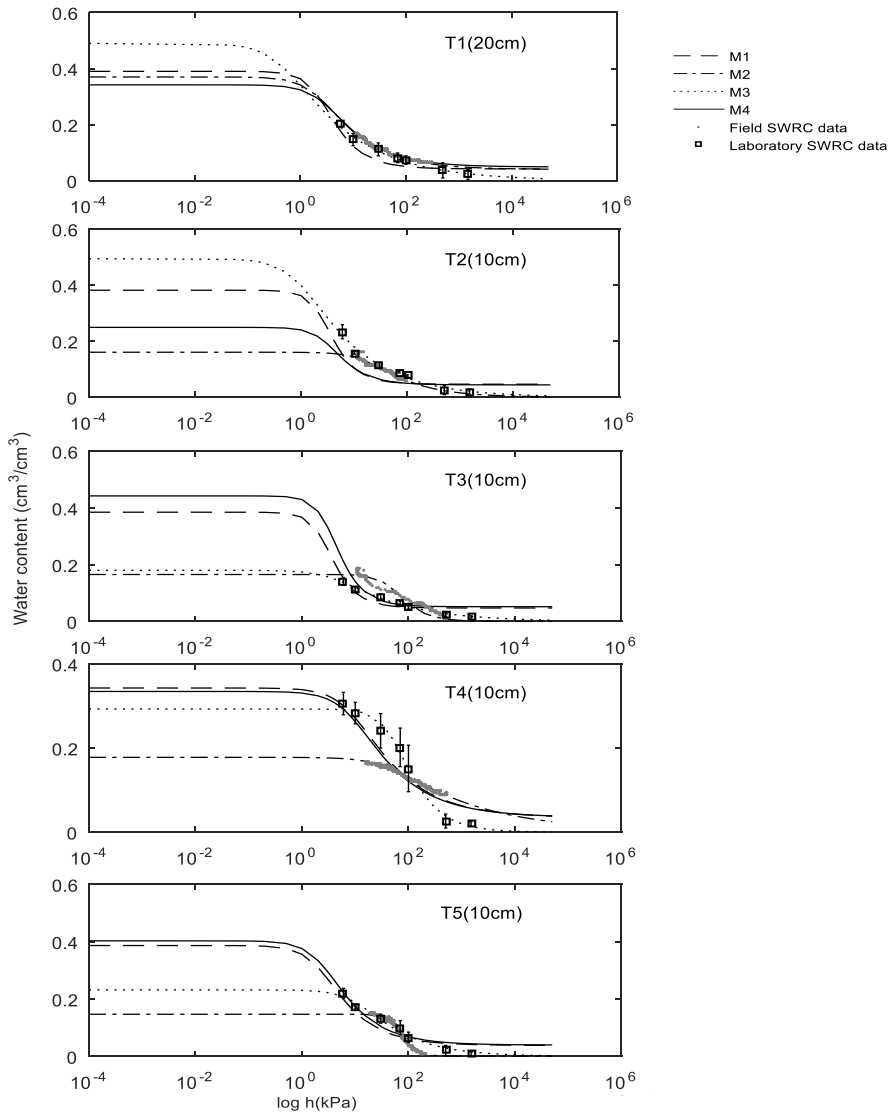
Figure A.3 Soil water flow observed and simulated using different methods : Rosetta method (M1), fitted field SWRC method (M2), fitted laboratory SWRC method (M3), and inversion method (M4) at 10 cm depth of each site, except T1 at 20 cm
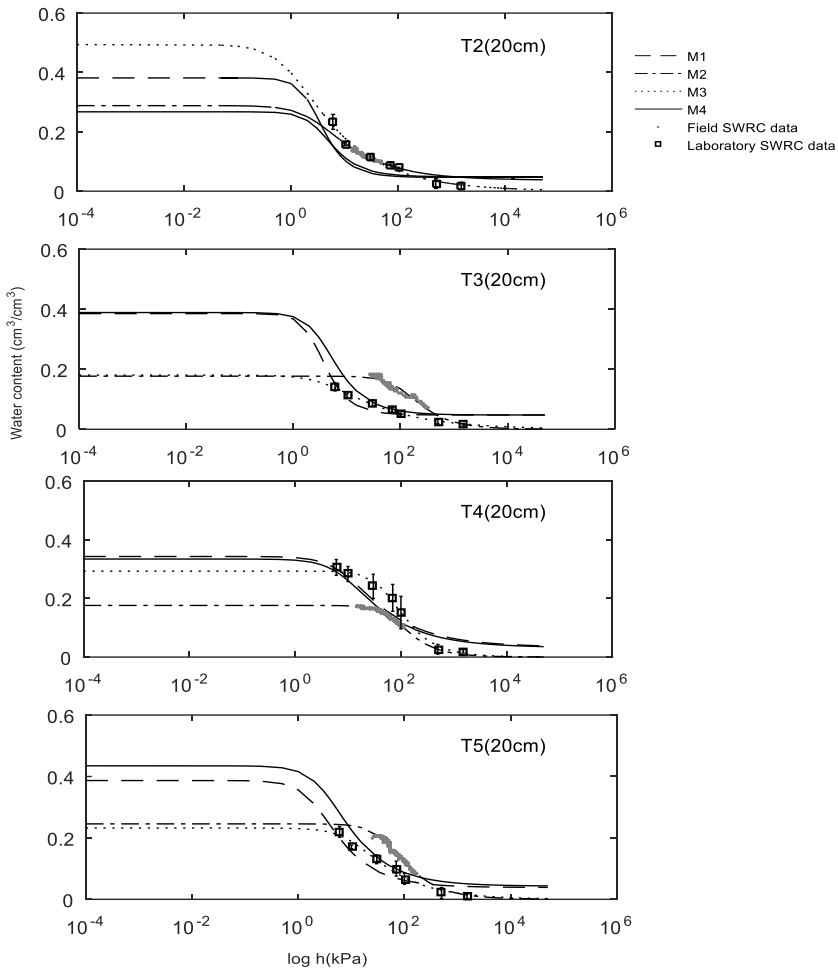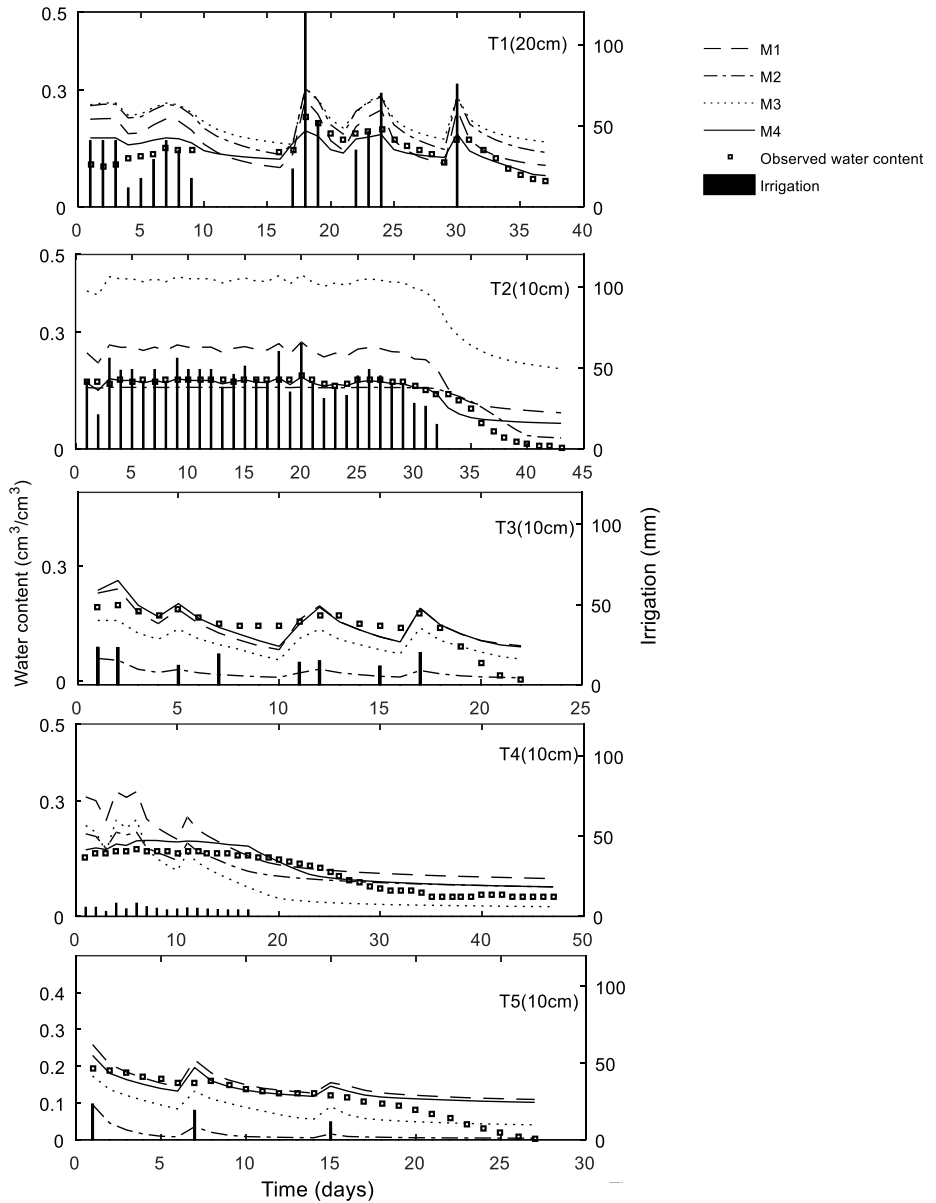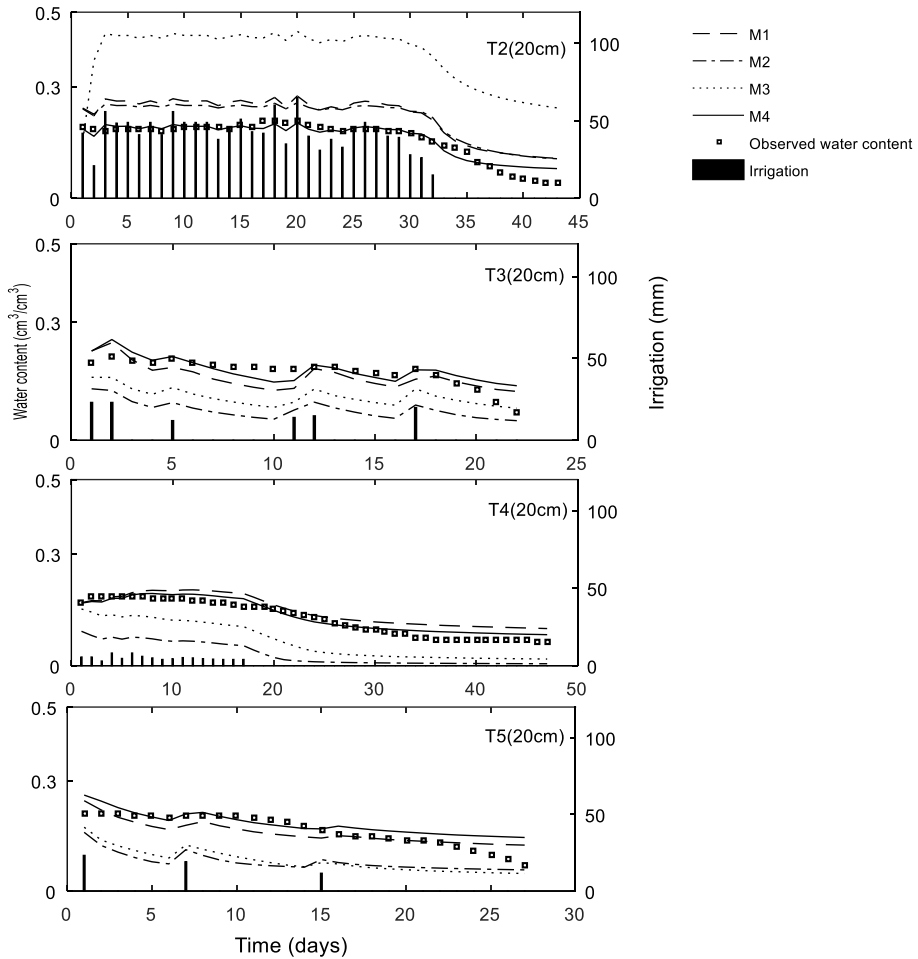
Figure A.4 Soil water flow observed and simulated using different methods : Rosetta method (M1), fitted field SWRC method (M2), fitted laboratory SWRC method (M3), and inversion method (M4) at 20 cm depth of each site.

References

Abbasi F, Simunek J, Feyen J, Shouse PJ (2003) Simulataneous inverse estimation of soil hydraulic and solute transport parameters from transient field experiments: Homogeneous soil. Am Soc Agric Eng 46:1085–1095.

Abbaspour KC, Schulin R, Genuchten MT Van (2001) Estimating unsaturated soil hydraulic parameters using ant colony optimization. Adv Water Resour 24:827–841.

Abd El-Wahed MH, Baker GA, Ali MM, Abd El-Fattah FA (2017) Effect of drip deficit irrigation and soil mulching on growth of common bean plant, water use efficiency and soil salinity. Sci Hortic (Amsterdam) 225:235–242. doi: 10.1016/j.scienta.2017.07.007

Abderrahman WA, Mohammed N, Al-Harazin IM (2001) Computerized and dynamic model for irrigation water management of large irrigation schemes in Saudi Arabia. Int J Water Resour Dev 17:261–270. doi: 10.1080/07900620120031324

Abdullah K, Ismail TG, Yusuf U, Belgin C (2004) Effects of Mulch and Irrigation Water Amounts on Lettuce's Yield, Evapotranspiration, Transpiration and Soil Evaporation in Isparta Location, Turkey. J Biol Sci 4:751–755. doi: 10.3923/jbs.2004.751.755

Adeboye OB, Schultz B, Adekalu KO, Prasad K (2017) Modelling of Response of the Growth and Yield of Soybean to Full and Deficit Irrigation by Using Aquacrop. Irrig Drain 66:192–205. doi: 10.1002/ird.2073

Adil M, Zhang X, Neumann M (2019) Can mulching of maize straw complement de fi cit irrigation to improve water use e ffi ciency and productivity of winter wheat in North China Plain ? Agric Water Manag 213:1–11. doi: 10.1016/j.agwat.2018.10.008

Adu MO, Yawson DO, Armah FA, et al (2018) Meta-analysis of crop yields of full, deficit, and partial root-zone drying irrigation. Agric Water Manag 197:79–90. doi: 10.1016/j.agwat.2017.11.019

Afzal M, Battilani A, Solimando D, Ragab R (2016) Improving water resources management using different irrigation strategies and water qualities: Field and modelling study. Agric Water Manag 176:40–54. doi: 10.1016/j.agwat.2016.05.005

Ahmad M, Bastiaanssen WGM, Feddes RA (2002) Sustainable use of groundwater for numerical analysis of the subsoil water fluxes. Irrig Drain 241:227–241.

Ajdary K, Singh DK, Singh AK, Khanna M (2007) Modelling of nitrogen leaching from experimental onion field under drip fertigation. Agric Water Manag 89:15–28. doi: 10.1016/j.agwat.2006.12.014

Al-jamal MS, Sammis TW, Mexal JG (2002) A growth-irrigation scheduling model for wastewater use in forest production. Agric Water Manag 56:57–79.

Alagna V, Bagarello V, Prima S Di, Iovino M (2016) Determining hydraulic properties of a loam soil by alternative infiltrometer techniques. Hydrol Process 275:263–275. doi: 10.1002/hyp.10607

Albaji M, Golabi M, Boroomand S (2015) Investigation of surface , sprinkler and drip irrigation methods based on the parametric evaluation approach in Jaizan Plain. J Saudi Soc Agric Sci 14:1–10. doi: 10.1016/j.jssas.2013.11.001

Ali A, Erenstein O (2017) Climate Risk Management Assessing farmer use of climate change adaptation practices and impacts on food security and poverty in Pakistan. Clim Risk Manag 16:183–194. doi: 10.1016/j.crm.2016.12.001

Allen R, Walter I, Elliott R, et al (2005) The ASCE Standardized Reference Evapotranspiration Equation.

Allen RG, Pereira LS, Raes D, et al (1998a) Crop evapotranspiration-Guidelines for computing crop water requirements. In: FAO Irrigation and Drainage Paper 56. Food and Agriculture Organization, Rome, pp 1–15

Allen RG, Pereira LS, Raes D, Smith M (1998b) Crop evapotranspiration: guidelines for computing crop water requirements. Irrig Drain 300:300. doi: 10.1016/j.eja.2010.12.001

Allen RG, Pruitt WO, Wright JL, et al (2006) A recommendation on standardized surface resistance for hourly calculation of reference ET o by the FAO56 Penman-Monteith method. Agric Water Manag 81:1–22. doi: 10.1016/j.agwat.2005.03.007

Andarzian B, Bannayan M, Steduto P, et al (2011) Validation and testing of the AquaCrop model under full and deficit irrigated wheat production in Iran. Agric Water Manag 100:1–8. doi: 10.1016/j.agwat.2011.08.023

Andersland OB, Ladanyi B, ASCE (2004) Frozen Ground Engineering, Second edi. John Wiley & Sons

Asgarzadeh H, Mosaddeghi MR, Dexter AR, et al (2014) Determination of soil available water for plants: Consistency between laboratory and field measurements. Geoderma 226–227:8–20. doi: 10.1016/j.geoderma.2014.02.020

Assouline S, Or D (2014) The concept of field capacity revisited – defining intrinsic static and dynamic criteria for soil internal drainage dynamics. Water Resour Res 50:4787–4802. doi: doi:10.1002/2014WR015475

Assouline S, Tessier D (1998) A conceptual model of the soil water retention curve. Water Resour Res 34:223–231.

Autovino D, Rallo G, Provenzano G (2018) Predicting soil and plant water status dynamic in olive orchards under different irrigation systems with Hydrus-2D: model performance and scenario analysis. Agric Water Manag 203:225–235. doi: 10.1016/j.agwat.2018.03.015

Bae J, Dall'erba S (2018) Crop Production, Export of Virtual Water and Water-saving Strategies in Arizona. Ecol Econ 146:148–156. doi: 10.1016/j.ecolecon.2017.10.018

Barbour SL (1998) Nineteenth Canadian Geotechnical Colloquium: The soil-water characteristic curve: a historical perspective. Can J Geotech 35:873–894.

Batjes NH (1996) Development of a world data set of soil water retention properties using pedotransfer rules. Geoderma 71:31–52. doi: 10.1016/0016-7061(95)00089-5

Becker R, Gebremichael M, Märker M (2018) Impact of soil surface and subsurface

properties on soil saturated hydraulic conductivity in the semi-arid Walnut Gulch Experimental Watershed, Arizona, USA. Geoderma 322:112–120. doi: 10.1016/j.geoderma.2018.02.023

Bello ZA, Rensburg LDVAN (2017) Development, calibration and testing of a low-cost small lysimeter for monitoring evaporation and transpiration. Irrig Drain 272:263–272. doi: 10.1002/ird.2095

Berg M Van Den, Klamt E, Reeuwijk LP Van (1997) Pedotransfer functions for the estimation of moisture retention characteristics of Ferralsols and related soils. Geoderma 78:161–180.

Bigelow DP, Zhang H (2018) Supplemental irrigation water rights and climate change adaptation. Ecol Econ 154:156–167. doi: 10.1016/j.ecolecon.2018.07.015

Bittelli M, Valentino R, Salvatorelli F, Rossi P (2012) Geomorphology Monitoring soil-water and displacement conditions leading to landslide occurrence in partially saturated clays. Geomorphology 174:161–173. doi: 10.1016/j.geomorph.2012.06.006

Boote KJ, Jones JW, Pickering NB (1996) Potential uses and limitations of crop models. Agron J 88:704–716. doi: 10.2134/agronj1996.00021962008800050005x

Botula YD, Van Ranst E, Cornelis WM (2014) Pedotransfer Functions to Predict Water Retention for Soils of the Humid Tropics: A Review. Rev Bras Cienc Do Solo 38:679–698. doi: 10.1590/S0100-06832014000300001

Brooks RH, Corey AT (1964) Hydraulic properties of porous media. Colorado State University, Fort Collins, Colorado

Brown JD, Heuvelink GB (2005) 79: Assessing Uncertainty Propagation Through Physically based Models of Soil Water Flow and Solute Transport. Encycl. Hydrol. Sci. 1–15.

Cahn M, Johnson L (2017) New Approaches to Irrigation Scheduling of Vegetables. Horticulturae 3:1–20. doi: 10.3390/horticulturae3020028

Cambel G., Cambel M. (2013) Irrigation scheduling using soil moisture measurement. In: Hillel D (ed) Advance in Irrigation. Elsevier, p 322

Campbell G (1974) A simple method for determining unsaturated conductivity from moisture retention data. Soil Sci 117:311–314.

Capra A, Consoli S (2008) Deficit irrigation : Theory and practice. In: Alonso D, Iglesias HJ (eds) Agricultural Irrigation Research Progress. Nova Science Publishers, Inc.,

Carrera J, Alcolea A, Medina A (2005) Inverse problem in hydrogeology. Hydrogeol J 13:206–222. doi: 10.1007/s10040-004-0404-7

Casa A De, Ovando G, Bressanini L, Martínez J (2013) Aquacrop model calibration in potato and its use to estimate yield variability under field conditions. Atmos Clim Sci 3:397–407. doi: 10.4236/acs.2013.33041

Chai Q, Gan Y, Zhao C, et al (2016) Regulated deficit irrigation for crop production under drought stress. A review. Agron Sustain Dev 36:1–21. doi: 10.1007/s13593-015-0338-6

Chan H (2015) Observed and projected changes in temperature and rainfall in

Cambodia. Weather Clim Extrem 7:61–71. doi: 10.1016/j.wace.2015.02.001

Chann S, Wales N, Frewer T (2011a) An Investigation of Land Cover and Land Use Change in Stung Chrey Bak Catchment, Cambodia. CDRI

Chartres C (2014) Is water scarcity a constraint to feeding Asia's growing population? Int J Water Resour Dev 30:28–36. doi: 10.1080/07900627.2013.846713

CHEM P, HIRSCH P, SOMETH P (2011) Hydrological Analysis in Support of Irrigation Management.

Chhean S, Diep K, Paule M (2004) Vegetable Market Flows and Chains in Phnom Penh. FSP Project 2000, Hanoi, Vietnam

Cleveland CC, Wieder WR, Reed SC, et al (2010) Experimental drought in a tropical rain forest increases soil carbon dioxide losses to the atmosphere. Ecology 91:2313–2323.

Cobos D, Chamber C (2005) Application Note Calibrating ECH 2 O Soil Moisture Sensors. 1–5.

Cortignani R, Severini S (2009) Modeling farm-level adoption of deficit irrigation using Positive Mathematical Programming. Agric Water Manag 96:1785–1791. doi: 10.1016/j.agwat.2009.07.016

Cosi M (2017) Predicting biomass and yield of sweet pepper grown with and without plastic film mulching under different water supply and weather conditions. Agric Water Manag 188:91–100.

Dam JC van (2000) Field-scale water flow and solute transport SWAP model concepts , parameter estimation and case studies. Wageningen University

Damme W Van, Leemput L Van, Por I, et al (2004) Out-of-pocket health expenditure and debt in poor households : evidence from Cambodia. Trop Med Int Heal 9:273–280.

Dane JH, Topp CG, Dane JH, Hopmans JW (2002a) 3.3.2 Laboratory. In: SSSA Book Series. Soil Science Society of America,

Dane JH, Topp CG, Gee GW, Or D (2002b) 2.4 Particle-Size Analysis. In: SSSA Book Series. Soil Science Society of America,

Datta S, Stivers J (2017) Understanding Soil Water Content and Thresholds for Irrigation Management. BAE-1537 8.

Davis SL, Dukes MD (2010) Irrigation scheduling performance by evapotranspiration-based controllers. Agric Water Manag 98:19–28. doi: 10.1016/j.agwat.2010.07.006

De Bon H, Parrot L, Moustier P (2010) Sustainable urban agriculture in developing countries . A review. Agron Sustain Dev 30:21–32. doi: 10.1051/agro

de Jong van Lier Q (2017) Field capacity, a valid upper limit of crop available water? Agric Water Manag 193:214–220. doi: 10.1016/j.agwat.2017.08.017

Deb P, Tran DA, Udmale PD (2016) Assessment of the impacts of climate change and brackish irrigation water on rice productivity and evaluation of adaptation measures in Ca Mau province, Vietnam. Theor Appl Climatol 125:641–656. doi: 10.1007/s00704-015-1525-8

Decagon Devices (2016) MPS-2 & MPS-6 Dielectric Water Potential Sensors, Operator's Manual.

Decagon Devices (2011) MPS-2 Dielectric water potential sensor: Operator's manual. Decagon Devices, Inc., Pullman

Decagon Devices (2010) 10HS Soil Moisture Sensor Operator's Manual, Version.

Degré A, van der Ploeg M, Caldwell T mailt, Gooren H (2017) Comparison of soil water potential sensors: a drying experiment. Vadose Zo J. doi: 10.2136/vzj2016.08.0067

Devendra C, Thomas D (2002) Smallholder farming systems in Asia. Agric Syst 71:17–25.

Domingues DS, Takahashi HW, Camara CAP, Nixdorf SL (2012) Automated system developed to control pH and concentration of nutrient solution evaluated in hydroponic lettuce production. Comput Electron Agric 84:53–61. doi: 10.1016/j.compag.2012.02.006

Doorenbos J, Pruitt WO (1977) Guidelines for predicting crop water requirements. Food and Agriculture Organization of the united nations, Rome, Italy

dos Santos TP, Lopes CM, Lucília Rodrigues M, et al (2007) Effects of deficit irrigation strategies on cluster microclimate for improving fruit composition of Moscatel field-grown grapevines. Sci Hortic (Amsterdam) 112:321–330. doi: 10.1016/j.scienta.2007.01.006

Dufault RJ, Ward B, Hassell RL (2009) Dynamic relationships between field temperatures and romaine lettuce yield and head quality. Sci Hortic (Amsterdam) 120:452–459. doi: 10.1016/j.scienta.2009.01.002

Durner W (1994) Hydraulic conductivity estimation for soils with heterogeneous pore structure. Water Resour Res 30:211–223. doi: 10.1029/93WR02676

Ebel BA, Godt JW, Lu N, et al (2018) Field and Laboratory Hydraulic Characterization of Landslide-Prone Soils in the Oregon Coast Range and Implications for Hydrologic Simulation. Vadose Zo J 1–15. doi: 10.236/vzj2018.04.0078

Eching SO, Hopmans JW (1993) Optimization of Hydraulic Functions from Transient Outflow and Soil Water Pressure Data. Soil Sci Soc Am J 57:1167–1175.

Ecker O, Diao X (2011) Food Security and Nutrition in Cambodia : Pattern and Pathways A Policy Discussion Paper.

Egea G, Diaz-Espejo A, Fernández JE (2016) Soil moisture dynamics in a hedgerow olive orchard under well-watered and deficit irrigation regimes: Assessment, prediction and scenario analysis. Agric Water Manag 164:197–211. doi: 10.1016/j.agwat.2015.10.034

Ehlers W, Goss MJ (2003) Water Dynamics in Plant Production. CABI

Elhakeem M, Papanicolaou ANT, Wilson CG, et al (2018) Understanding saturated hydraulic conductivity under seasonal changes in climate and land use. Geoderma 315:75–87. doi: 10.1016/j.geoderma.2017.11.011

English M (1990) Deficit Irrigation.I:Analytical Framework.. J irrig Drain Eng 116:399–412.

English M, Raja SN (1996) Perspectives on deficit irrigation. Agric Water Manag 32:1–14. doi: 10.1016/S0378-3774(96)01255-3

Erban LE, Gorelick SM (2016) Closing the irrigation deficit in Cambodia:

Implications for transboundary impacts on groundwater and Mekong River flow. J Hydrol 535:85–92. doi: 10.1016/j.jhydrol.2016.01.072

Fabiani S, Nino P, Silvia V (2016) D4.1.3 : Guidelines for on farm Water- Energy-Food audit , including training material. Farming tools for external nutrient inputs and water management (FATIMA)

FAO (2013) FAO Statistical Yearbook 2013. FAO

FAO (2006) Guidelines for soil description, Fourth edi. Food and Agriculture Organization of the united nations, Rome, Italy

Farahani HJ, Izzi G, Oweis TY (2009) Parameterization and Evaluation of the AquaCrop Model for Full and Deficit Irrigated Cotton. Agron J 101:469–476. doi: 10.2134/agronj2008.0182s

Fazilah W, Ilahi F, Ahmad D, Husain MC (2017) Effects of Root Zone Cooling on Butterhead Lettuce Grown in Tropical Conditions in a Coir-Perlite Mixture. Hortic Environ Biotechnol 58:1–4. doi: 10.1007/s13580-017-0123-3

Feddes RA, Kowalik PJ, Zaradny H (1978) Simulation of field water use and crop yield. Centre for Agricultural Publishing and Documentation, Pudoc, Wageningen, The Nethelands

Fereres E, Rabanales CU De (2007) Deficit irrigation for reducing agricultural water use. J Exp Bot 58:147–159. doi: 10.1093/jxb/erl165

Ferreira MI, Conceição N, Malheiro AC, et al (2017) Water stress indicators and stress functions to calculate soil water depletion in deficit irrigated grapevine and kiwi. Acta Hortic 1150:119–126. doi: 10.17660/ActaHortic.2017.1150.17

Filipović V, Weninger T, Filipović L, et al (2018) Inverse estimation of soil hydraulic properties and water repellency following artificially induced drought stress. J Hydrol Hydromechanics 66:170–180. doi: 10.2478/johh-2018-0002

Fisher DK, Gould PJ (2012) Is a Low-Cost Alternative for Scientific Instrumentation and Research. Mod Instrum 1:8–20. doi: 10.4236/mi.2012.12002

Friedman SP, Communar G, Gamliel A (2016) DIDAS – User-friendly software package for assisting drip irrigation design and scheduling. Comput Electron Agric 120:36–52. doi: 10.1016/j.compag.2015.11.007

Fuentes C, Haverkamp R, Parlange JY (1992) Parameter constraints on closed-form soil water relationships. J Hydrol 134:117–142.

Gallage CPK, Uchimura T (2010) Effects of dry density and grain size distribution on soil-water characteristic curves of sandy soils. Soil Found 50:161–172.

Gallardo M, Jackson LEE, Schulbach K, et al (1996a) Production and water use in lettuces under variable water supply. Irrig Sci 16:125–137. doi: 10.1007/bf02215620

Gallardo M, Snyder R, Schulbach K, Jackson L (1996b) Crop growth and water use model for lettuce. J. Irrig. Drain. Eng. 122:354–359.

Gamage DNV, Biswas A, Strachan IB (2018) Actively heated fi ber optics method to monitor three-dimensional wetting patterns under drip irrigation. Agric Water Manag 210:243–251. doi: 10.1016/j.agwat.2018.08.019

García-vila M, Fereres E (2012) Combining the simulation crop model AquaCrop with an economic model for the optimization of irrigation management at farm

level. Eur J Agron 36:21–31. doi: 10.1016/j.eja.2011.08.003

Gardner WR (1958) Some steady-state solutions of the unsaturated moisture flow equation with application to evaporation from a water table. Soil Sci 85:228–232.

Geerts S, Raes D (2009a) Deficit irrigation as an on-farm strategy to maximize crop water productivity in dry areas. Agric Water Manag 96:1275–1284. doi: 10.1016/j.agwat.2009.04.009

Geerts S, Raes D, Garcia M (2010) Using AquaCrop to derive deficit irrigation schedules. Agric Water Manag 98:213–216. doi: 10.1016/j.agwat.2010.07.003

George BA, Shende SA, Raghuwanshi NS (2000) Development and testing of an irrigation scheduling model. Agric Water Manag 46:121–136.

Ghanbarian B, Taslimitehrani V, Pachepsky YA (2017) Accuracy of sample dimension-dependent pedotransfer functions in estimation of soil saturated hydraulic conductivity. Catena 149:374–380. doi: 10.1016/j.catena.2016.10.015

Gleeson T, Alley WM, Allen DM, et al (2012) Towards Sustainable Groundwater Use : Setting Long-Term Goals , Backcasting , and Managing Adaptively. Ground Water 50:19–26. doi: 10.1111/j.1745-6584.2011.00825.x

Goutard FL, Binot A, Duboz R, et al (2015) How to reach the poor ? Surveillance in low-income countries , lessons from experiences in Cambodia and Madagascar. Prev Vet Med 120:12–26.

Greaves GE, Wang YM (2016) Assessment of fao aquacrop model for simulating maize growth and productivity under deficit irrigation in a tropical environment. Water 8:1–18. doi: 10.3390/w8120557

Grossman RB, Reinsch TG (2002) 2.1 Bulk Density and Linear Extensibility. In: SSSA Book Series. Soil Science Society of America,

Gupta B, Shah DO, Mishra B, et al (2015) Effect of top soil wettability on water evaporation and plant growth. J Colloid Interface Sci 449:506–513. doi: 10.1016/j.jcis.2015.02.018

Gupta SC, Larson WE (1979) Estimating soil water retention characteristics from particle size distribution, organic matter percent, and bulk density. Water Resour Res 15:1633–1635.

Gutmann ED, Small EE (2007) A comparison of land surface model soil hydraulic properties estimated by inverse modeling and pedotransfer functions. Water Resour Res 43:1–13. doi: 10.1029/2006WR005135

Hao DR, Liao HJ, Ning CM, Shan XP (2015) The microstructure and soil-water characteristic of unsaturated loess. In: Unsaturated Soil Mechanics - from Theory to Practice: Proceedings of the 6th Asia Pacific Conference on Unsaturated Soils (Guilin, China, 23-26 October 2015). Taylor & Francis Group, London, UK, pp 163–167

Hassanli M, Ebrahimian H, Mohammadi E, et al (2016) Simulating maize yields when irrigating with saline water, using the AquaCrop, SALTMED, and SWAP models. Agric Water Manag 176:91–99. doi: 10.1016/j.agwat.2016.05.003

Henrich L, McClure J, Crozier M (2016) A decision support system for managing irrigation in agriculture. Comput Electron Agric 36–44. doi:

10.1016/j.actamat.2015.02.029

Hewell T (2001) Enhancing water use efficiency in irrigated agriculture. Agron J 93:281–289.

Hodnett MG, Tomasella J (2002) Marked differences between van Genuchten soil water-retention parameters for temperate and tropical soils: A new water-retention pedo-transfer functions developed for tropical soils. Geoderma 108:155–180. doi: 10.1016/S0016-7061(02)00105-2

Hoekstra AY, Wiedmann TO (2014) Humanity's unsustainable environmental footprint. Science (80-) 344:1114–1117. doi: 10.1126/science.1248365

Hopmans J, Simunek J (1999) Review of inverse estimation of soil hydraulic properties. In: In: van Genuchten, M.Th., et al. (Ed.): Characterization and Measurement of the Hydraulic Properties of Unsaturated Porous Media. University of California, Riverside, California,. p 643–659.

Hopmans JANW, Romano N, Durner W (2002) 3.6.2. Inverse Methods. In: J.H. Dane, Topp GC (eds) Methods of Soil Analysis. SSSA Book Ser. 5., SSSA, Madison, WI, pp 963–1008

Hsiao TC, Heng L, Steduto P, et al (2009) AquaCrop—The FAO Crop Model to Simulate Yield Response to Water: III. Parameterization and Testing for Maize. Agron J 101:448. doi: 10.2134/agronj2008.0218s

Hu Y, Paul J, Yang Y, et al (2010) Agricultural water-saving and sustainable groundwater management in Shijiazhuang Irrigation District , North China Plain. J Hydrol 393:219–232. doi: 10.1016/j.jhydrol.2010.08.017

Huang J, Purushothaman R, McBratney A, Bramley H (2018) Soil Water Extraction Monitored Per Plot Across a Field Experiment Using Repeated Electromagnetic Induction Surveys. Soil Syst 2:11. doi: 10.3390/soilsystems2010011

Hunsaker DJ, French AN, Waller PM, et al (2015) Comparison of traditional and ET-based irrigation scheduling of surface-irrigated cotton in the arid southwestern USA. Agric Water Manag 159:209–224. doi: 10.1016/j.agwat.2015.06.016

Hussein F, Janat M, Yakoub A (2011) Simulating cotton yield response to deficit irrigation with the FAO AquaCrop model. Spanish J Agric Res 9:1319–1330. doi: 10.5424/sjar/20110904-358-10

Inthavong T, Tsubo M, Fukai S (2011) A water balance model for characterization of length of growing period and water stress development for rainfed lowland rice. F Crop Res 121:291–301. doi: 10.1016/j.fcr.2010.12.019

Irmak S, Howell TA, Allen RG, et al (2005) Standardized ASCE Penman-Monteith: Impact of sum-of-hourly vs. 24-hour timestep computations at reference weather station sites. Trans ASAE 48:1063–1077. doi: 10.13031/2013.18517

James LD, Lee RR (1971) Economics of water resources planning. McGraw-Hill, New York, USA

Jaramillo F, Destouni G (2015) Local flow regulation and irrigation raise global human water consumption and footprint. Science (80-) 350:1248–1251.

Jiang J, Feng S, Ma J, et al (2016) Field Crops Research Irrigation management for spring maize grown on saline soil based on SWAP model. F Crop Res 196:85–97. doi: 10.1016/j.fcr.2016.06.011

Johnston R, Roberts M, Thuon T, Silva S de (2013) Groundwater for Irrigation in Cambodia Groundwater for irrigation in Cambodia. Colombo, Sri Lanka

Jones HG (2004) Irrigation scheduling: Advantages and pitfalls of plant-based methods. J Exp Bot 55:2427–2436. doi: 10.1093/jxb/erh213

Jorenush MH, Sepaskhah AR (2003) Modelling capillary rise and soil salinity for shallow saline water table under irrigated and non-irrigated conditions. Agric Water Manag 61:125–141. doi: 10.1016/S0378-3774(02)00176-2

Kader MA, Senge M, Mojid MA, Ito K (2017) Recent advances in mulching materials and methods for modifying soil environment. Soil Tillage Res 168:155–166.

Kanda EK, Mabhaudhi T, Senzanje A (2018) Coupling hydrological and crop models for improved agricultural water management – A review. Bulg J Agric Sci 24:380–390.

Karam F, Mounzer O, Sarkis F, Lahoud R (2002) Yield and nitrogen recovery of lettuce under different irrigation regimes. J Appl Hortic 4:70–76.

Kargas G, Soulis K (2011) Performance Analysis and Calibration of a New Low-Cost Capacitance Soil Moisture Sensor. J Irrig Drain Eng 138:632–641. doi: 10.1061/(ASCE)IR.1943-4774.0000449

Kashyap PS, Panda RK (2001) Evaluation of evapotranspiration estimation methods and development of crop-coefficients for potato crop in a sub-humid region. Agric Water Manag 50:9–25. doi: 10.1016/S0378-3774(01)00102-0

Katerji N, Mastrorilli M, Rana G (2008) Water use efficiency of crops cultivated in the Mediterranean region : Review and analysis. Eur J Agron 28:493–507. doi: 10.1016/j.eja.2007.12.003

Kechavarzi C, Špongrová K, Dresser M, et al (2009) Laboratory and field testing of an automated tension infiltrometer. Biosyst Eng 104:266–277. doi: 10.1016/j.biosystemseng.2009.06.014

Kern JS (1995) Geographic patterns of soil water-holding capacity in the contiguous United States. Soil Sci Soc Am J 59:1126–1133. doi: 10.2136/sssaj1995.03615995005900040026x

Ket P, Garré S, Oeurng C, et al (2018) Simulation of crop growth and water-saving irrigation scenarios for Lettuce: A monsoon-climate case study in Kampong Chhnang, Cambodia. Water (Switzerland) 10:1–23. doi: 10.3390/w10050666

Kirkham MB (2014) Field Capacity, Wilting Point, Available Water, and the Nonlimiting Water Range. In: Principles of Soil and Plant Water Relations. pp 153–170

Klocke NL, Fischbach PE (1984) G84-690 Estimating soil moisture by appearance and feel. Hist. Mater. from Univ. Nebraska-Lincoln Ext. 1–9.

Kögler F, Söffker D (2017) Water (stress) models and deficit irrigation: System-theoretical description and causality mapping. Ecol Modell 361:135–156. doi: 10.1016/j.ecolmodel.2017.07.031

Köhne JM, Köhne S, Šimůnek J (2009) A review of model applications for structured soils: a) Water flow and tracer transport. J Contam Hydrol 104:4–35. doi: 10.1016/j.jconhyd.2008.10.002

Kong S, Sou S, Sam C, et al (2012) Impacst of Climate Change on Rice Production

in Cambodia. The NGO Forum on Cambodia, Environment Programme's Agricultural Monitoring Project, Phnom Penh, Cambodia

Konyai S, Sriboonlue V, Trelo-Ges V (2009) The effect of air entry values on hysteresis of water retention curve in saline soil. Am J Environ Sci 5:341–345.

Kool D, Agam N, Lazarovitch N, et al (2014) A review of approaches for evapotranspiration partitioning. Agric For Meteorol 184:56–70. doi: 10.1016/j.agrformet.2013.09.003

Kool JB, Parker JC, Van Genuchten MT (1985) Determining Soil Hydraulic Properties from One-step Outflow Experiments by Parameter Estimation: I. Theory and Numerical Studies. Soil Sci Soc Am J 49:1348–1354. doi: 10.2136/sssaj1985.03615995004900060004x

Krause P, Boyle DP (2005) Comparison of different efficiency criteria for hydrological model assessment. Adv Geosci 5:89–97. doi: 10.5194/adgeo-5-89-2005

Kucza J, Ilek A (2016) The effect of the shape parameters of a sample on the hydraulic conductivity. J Hydrol 534:230–236. doi: 10.1016/j.jhydrol.2016.01.010

Kukal SS, Hira GS, Sidhu AS (2005) Soil matric potential-based irrigation scheduling to rice (Oryza sativa). Irrig Sci 23:153–159. doi: 10.1007/s00271-005-0103-8

Kumar S, Sekhar M, Reddy D V., Mohan Kumar MS (2010) Estimation of soil hydraulic properties and their uncertainty: Comparison between laboratory and field experiment. Hydrol Process 24:3426–3435. doi: 10.1002/hyp.7775

Kuslu Y, Dursun A, Sahin U, et al (2008) Short communication. Effect of deficit irrigation on curly lettuce grown under semiarid conditions. Spanish J Agric Res 6:714–719.

Lai J, Ren L (2016) Estimation of effective hydraulic parameters in heterogeneous soils at field scale. Geoderma 264:28–41. doi: 10.1016/j.geoderma.2015.09.013

Lambot S (2002) A global multilevel coordinate search procedure for estimating the unsaturated soil hydraulic properties. Water Resour Res 38:1–15. doi: 10.1029/2001WR001224

Lamn F., Ayars J., Nakayama F. (2015) Irrigation scheduling. In: Freddie R, Lamm James E, Ayars Francis S, Nakayama F. (eds) Microirrigation for Crop Production, 1st edn. Developments in agricultural engineering 13, Elsevier Houston, Texas, USA, pp 61–128

Latorre B, Moret-Fernández D, Peña C (2013) Estimate of Soil Hydraulic Properties from Disc Infiltrometer Three-dimensional Infiltration Curve: Theoretical Analysis and Field Applicability. Procedia Environ Sci 19:580–589. doi: 10.1016/j.proenv.2013.06.066

Lazarovitch N, Ben-Gal A, Šimunek J, Shani U (2007) Uniqueness of Soil Hydraulic Parameters Determined by a Combined Wooding Inverse Approach. Soil Sci Soc Am J 71:860. doi: 10.2136/sssaj2005.0420

Le Bourgeois O, Bouvier C, Brunet P, Ayral PA (2016) Inverse modeling of soil water content to estimate the hydraulic properties of a shallow soil and the associated weathered bedrock. J Hydrol 541:116–126. doi: 10.1016/j.jhydrol.2016.01.067

Lecler NL (1998) Integrated methods and models for deficit irrigation planning. In:

Pert RM, Curry RB (eds) Agricultural systems modelling and simulation. Marcel Dekker, Inc.,

Leib BG, Elliott T V, Matthews G (2001) WISE : a web-linked and producer oriented program for irrigation scheduling. Comput Electron Agric 33:1–6.

Leij FJ, Russell WB, Lesch SM (1997) Closed-form expresion for water retention and conductivity data. Ground Water 35:848–858.

Lesk C, Rowhani P, Ramankutty N (2016) Letter: Influtence of extreme weather disasterson global crop production. Nature 529:84–87. doi: 10.1038/nature16467

Levenberg K (1944) a method for the solution of certain problems in leaset squares. Q Appl Math 2:164–168.

Levidow L, Zaccaria D, Maia R, et al (2014) Improving water-efficient irrigation : Prospects and difficulties of innovative practices. Agric Water Manag 146:84–94. doi: 10.1016/j.agwat.2014.07.012

Li S, Kang S, Li F, Zhang L (2008) Evapotranspiration and crop coefficient of spring maize with plastic mulch using eddy covariance in northwest China. Agric Water Manag 95:1214–1222. doi: 10.1016/j.agwat.2008.04.014

Li X, Jin M, Zhou N, et al (2018a) Inter-dripper variation of soil water and salt in a mulched drip irrigated cotton fi eld : Advantages of 3-D modelling. Soil Tillage Res 184:186–194. doi: 10.1016/j.still.2018.07.016

Li Y-B, Liu Y, Nie W-B, Ma X-Y (2018b) Inverse Modeling of Soil Hydraulic Parameters Based on a Hybrid of Vector-Evaluated Genetic Algorithm and Particle Swarm Optimization. Water 10:1–23. doi: 10.3390/w10010084

Liang X, Liakos V, Wendroth O, Vellidis G (2016) Scheduling irrigation using an approach based on the van Genuchten model. Agric Water Manag 176:170–179. doi: 10.1016/j.agwat.2016.05.030

Liénard A, Colinet G (2018) Transfert en cadmium et zinc vers l 'orge de printemps en sols contaminés et non contaminés de Belgique : évaluation et prédiction. Cah Agric 27:1–10.

Linker R, Ioslovich I (2017) Assimilation of canopy cover and biomass measurements in the crop model AquaCrop. Biosyst Eng 162:57–66. doi: 10.1016/j.biosystemseng.2017.08.003

Liu Y, Luo Y (2010) A consolidated evaluation of the FAO-56 dual crop coefficient approach using the lysimeter data in the North China Plain. Agric Water Manag 97:31–40. doi: 10.1016/j.agwat.2009.07.003

Liu Y, Pereira LS, Fernando RM (2006) Fluxes through the bottom boundary of the root zone in silty soils : Parametric approaches to estimate groundwater contribution and percolation. Agric Water Manag 84:27–40. doi: 10.1016/j.agwat.2006.01.018

Loos C, Gayler S, Priesack E (2007) Assessment of water balance simulations for large-scale weighing lysimeters. J Hydrol 335:259–270. doi: 10.1016/j.jhydrol.2006.11.017

Lopez JR, Winter JM, Elliott J, et al (2017) Integrating growth stage deficit irrigation into a process based crop model. Agric For Meteorol 243:84–92. doi:

10.1016/j.agrformet.2017.05.001

Lorite IJ, Mateos L, Orgaz F, Fereres E (2007) Assessing deficit irrigation strategies at the level of an irrigation district. Agric Water Manag 91:51–60. doi: 10.1016/j.agwat.2007.04.005

Lu N (2014) Validating the effective stress principle in unsaturated soil using non-failure tests. In: Khalili N, Russell A, Khoshghalb A (eds) Unsaturated Soils: Research & Applications. CRC Press, London, UK, pp 31–41

Lu N, Godt JW (2013) Hillslope Hydrology and Stability. Cambridge University Press

Lu N, Wayllace A, Oh S (2013) Infiltration-induced seasonally reactivated instability of a highway embankment near the Eisenhower Tunnel, Colorado, USA. Eng Geol 162:22–32. doi: 10.1016/j.enggeo.2013.05.002

Luo P, Zhou M, Deng H, et al (2018) Science of the Total Environment Impact of forest maintenance on water shortages : Hydrologic modeling and effects of climate change. Sci Total Environ 615:1355–1363. doi: 10.1016/j.scitotenv.2017.09.044

MAFF (2018) Annua report for agricultural forestry and fisheries 2017-2018 and direction 2018-2019. Phnom Penh, Cambodia

Mainuddin M, Kirby M (2009) Spatial and temporal trends of water productivity in the lower Mekong River Basin. Agric Water Manag 96:1567–1578. doi: 10.1016/j.agwat.2009.06.013

Malik A, Shakir AS, Ajmal M, et al (2017) Assessment of AquaCrop Model in Simulating Sugar Beet Canopy Cover, Biomass and Root Yield under Different Irrigation and Field Management Practices in Semi-Arid Regions of Pakistan. Water Resour Manag 31:4275–4292. doi: 10.1007/s11269-017-1745-z

March P (2000) Comparison of Tension Infiltrometer, Pressure Infiltrometer, and Soil Core Estimates of Saturated Hydraulic Conductivity. Soil Sci Soc Am J 64:478–484.

Margesin R, Schinner F (2005) Manual for Soil Analysis - Monitoring and Assessing Soil Bioremediation. Springer Science & Business Media, Berlin, Germany

Martin RJ (2017) Weed research issues , challenges , and opportunities in Cambodia. Crop Prot 2014:1–9. doi: 10.1016/j.cropro.2017.06.019

May P, Genuchten V (2008) Modeling Nonequilibrium Flow and Transport Processes Using HYDRUS. Vadose Zo J 7:782–797. doi: 10.2136/vzj2007.0074

Mazzacavallo MG, Kulmatiski A (2015) Modelling Water Uptake Provides a New Perspective on Grass and Tree Coexistence. PLoS One 1–16. doi: 10.1371/journal.pone.0144300

Meyer PD, Gee GW (1999) Flux-Based Estimation of Field Capacity. J Geotech Geoenvironmental Eng 125:595–599. doi: 10.1061/(ASCE)1090-0241(1999)125:7(595)

Minasny B, McBratney A, Bristow K (1999) Comparison of different approaches to the development of pedotransfer functions for water-retention curves. Geoderma 93:225–253.

Mittelbach H, Lehner I, Seneviratne SI (2012) Comparison of four soil moisture sensor types under field conditions in Switzerland. J Hydrol 430–431:39–49.

doi: 10.1016/j.jhydrol.2012.01.041

Miyazawa Y, Tateishi M, Komatsu H, et al (2014) Tropical tree water use under seasonal waterlogging and drought in central Cambodia. J Hydrol 515:81–89. doi: 10.1016/j.jhydrol.2014.04.049

Mkhabela MS, Bullock PR (2012) Performance of the FAO AquaCrop model for wheat grain yield and soil moisture simulation in Western Canada. Agric Water Manag 110:16–24. doi: 10.1016/j.agwat.2012.03.009

Molle F (2007) Irrigation and water policies: trends and challenges. In: Democratizing water governance in the Mekong. pp 9–36

Montgomery S, Guppy C, Martin R, et al (2017a) Productivity and profitability of upland crop rotations in Northwest Cambodia. F Crop Res 203:150–162. doi: 10.1016/j.fcr.2016.12.010

Montgomery SC, Martin RJ, Guppy C, et al (2017) Farmer knowledge and perception of production constraints in Northwest Cambodia. J Rural Stud 56:12–20. doi: 10.1016/j.jrurstud.2017.09.003

Montoya F, Camargo D, Ortega JF, et al (2016) Evaluation of Aquacrop model for a potato crop under different irrigation conditions. Agric Water Manag 164:267–280. doi: 10.1016/j.agwat.2015.10.019

Moreira MA, Santos CAP Dos, Lucas AAT, et al (2014) Lettuce production according to different sources of organic matter and soil cover. Agric Sci 05:99–105. doi: 10.4236/as.2014.52013

Moret-Fernández D, Latorre B (2017) Estimate of the soil water retention curve from the sorptivity and β parameter calculated from an upward infiltration experiment. J Hydrol 544:352–362. doi: 10.1016/j.jhydrol.2016.11.035

Moriasi DN, Arnold JG, Liew MW Van, et al (2007) Model evaluation quidelines for systematic quantification of accuracy in watershed simulations. Engineersngineers 50:885–900.

Morris MD (1991) Factorial plans for preliminary computational experiments. Technometrics 33:161–174.

Morris S., Davies W., Baines RN (2013) Challenges and opportunities for increasing competitiveness of vegetable production in Cambodia. Acta Hortic 1006:253–260. doi: 10.17660/ActaHortic.2013.1006.31

Morton JF (2007) The impact of climate change on smallholder and subsistence agriculture. PNAS 104:19680–19685.

Mualem Y (1976) A new model for predicting the hydraulic conductivity of unsaturated porous media. Water Resour Res 12:513–522.

Mun W, Teixeira T, Balci MC, et al (2016) Rate effects on the undrained shear strength of compacted clay. Soil Found 56:719–731. doi: 10.1016/j.sandf.2016.07.012

MWRM (2003) Irrigated Agriculture. Ministry of Water Resources and Meteorology, Phnom Penh, Cambodia

Nascimento CS, Filho ABC, Mendoza-Cortez JW, et al (2018) Effect of population density of lettuce intercropped with rocket on productivity and land-use efficiency. PLoS One 13:1–14. doi: 10.1371/journal.pone.0194756

Nemes A, Pachepsky YA, Timlin DJ (2011) Toward Improving Global Estimates of Field Soil Water Capacity. Soil Sci Soc Am J 75:807. doi: 10.2136/sssaj2010.0251

Nepstad DC, Tohver IM, Ray D, Moutinho P (2007) Mortality of Large Trees and Lianas following Experimental Drought in an Amazon Forest. Ecology 88:2259–2269.

Ngoc K, Jha MK, Reyes MR, et al (2018) Evaluating carbon sequestration for conservation agriculture and tillage systems in Cambodia using the EPIC model. Agric Ecosyst Environ 251:37–47. doi: 10.1016/j.agee.2017.09.009

NIS (2015) Census of Agriculture of the Kingdom of Cambodia 2013. National Institute of Statistics, Phnom Penh, Cambodia

Nobuhiro T, Shimizu A, Kabeya N, et al (2010) Advanced Bash-Scripting Guide An in-depth exploration of the art of shell scripting Table of Contents. Hydrol Process 22:2267–2274. doi: 10.1002/hyp

Novák V, Havrila J (2006) Method to estimate the critical soil water content of limited availability for plants. Biol. doi: 10.2478/s11756-006-0175-9

Novák V, Hlaváčiková H (2018) Applied Soil Hydrology. Springer

Oki T, Kanae S (2006) Global Hydrological Cycles and world water resources. Science (80-) 313:1068–1073.

Ortega JF, Juan JA De, Tarjuelo JM (2005) Improving water management : The irrigation advisory service of Castilla-La Mancha (Spain). Agric Water Manag 77:37–58. doi: 10.1016/j.agwat.2004.09.028

Osorio-Murillo CA, Over MW, Savoy H, et al (2015) Software framework for inverse modeling and uncertainty characterization. 98–109.

Ottoni Filho TB, Ottoni MV, Oliveira MB de, et al (2014) Revisiting Field Capacity (FC): variation of definition of FC and its estimation from pedotransfer functions. Bras Ci Solo 38:1750–1764. doi: 10.1590/S0100-06832014000600010

Panigrahi B, Panda SN (2003) Field test of a soil water balance simulation model. Agric Water Manag 58:223–240.

Pansu M, Gautheyrou J (2007) Handbook of Soil Analysis: Mineralogical, Organic and Inorganic Methods. Springer Science & Business Media, Berlin, Germany

Papajorgji P, Shatar TM (2004) Using the Unified Modeling Language to develop soil water- balance and irrigation-scheduling models. Environ Model Softw 19:451–459. doi: 10.1016/S1364-8152(03)00160-9

Paredes P, de Melo-Abreu JP, Alves I, Pereira LS (2014a) Assessing the performance of the FAO AquaCrop model to estimate maize yields and water use under full and deficit irrigation with focus on model parameterization. Agric Water Manag 144:81–97. doi: 10.1016/j.agwat.2014.06.002

Paredes P, Rodrigues GC, Alves I, Pereira LS (2014b) Partitioning evapotranspiration, yield prediction and economic returns of maize under various irrigation management strategies. Agric Water Manag 135:27–39. doi: 10.1016/j.agwat.2013.12.010

Paredes P, Wei Z, Liu Y, et al (2015) Performance assessment of the FAO AquaCrop

model for soil water, soil evaporation, biomass and yield of soybeans in North China Plain. Agric Water Manag 152:57–71. doi: 10.1016/j.agwat.2014.12.007

Parker RO (2009) Plant & Soil Science: Fundamentals and Applications, 1st edn. Clifton Park, New York, NY, USA

Passioura J (2006) Increasing crop productivity when water is scarce — from breeding to field management. Agric Water Manag 80:176–196. doi: 10.1016/j.agwat.2005.07.012

Patanè C, Tringali S, Sortino O (2011) Effects of deficit irrigation on biomass, yield, water productivity and fruit quality of processing tomato under semi-arid Mediterranean climate conditions. Sci Hortic (Amsterdam) 129:590–596. doi: 10.1016/j.scienta.2011.04.030

Patil NG, Tiwary P, Pal DK, et al (2013) Soil Water Retention Characteristics of Black Soils of India and Pedotransfer Functions Using Different Approaches. J Irrig Drain Engeniering 139:313–325. doi: 10.1061/(ASCE)IR.1943-4774.0000527.

Payero JO, Melvin SR, Irmak S, Tarkalson D (2006) Yield response of corn to deficit irrigation in a semiarid climate. Agric Water Manag 84:101–112. doi: 10.1016/j.agwat.2006.01.009

Peake AS, Carberry PS, Raine SR, et al (2016) An alternative approach to whole-farm deficit irrigation analysis: Evaluating the risk-efficiency of wheat irrigation strategies in sub-tropical Australia. Agric Water Manag 169:61–76. doi: 10.1016/j.agwat.2016.02.013

Pereira LS, Cordery I, Iacovides I (2012) Improved indicators of water use performance and productivity for sustainable water conservation and saving. Agric Water Manag 108:39–51. doi: 10.1016/j.agwat.2011.08.022

Pereira LS, Paredes P, Sholpankulov ED, et al (2009) Irrigation scheduling strategies for cotton to cope with water scarcity in the Fergana Valley, Central Asia. Agric Water Manag 96:723–735. doi: 10.1016/j.agwat.2008.10.013

Pereira LS, Teodoro PR, Rodrigues PN, Teixeira JL (2003) Irrigation scheduling simulation: the model isareg. In: G. Rossi, A. Cancelliere, L.S. Pereira, T. Oweis MS and AZ (ed) Tools for Drought Mitigation in Mediterranean Regions. Kluwer Academic Publishers, Dordrecht, the Netherlands, pp 161–180

Peters A, Durner W (2008) Simplified evaporation method for determining soil hydraulic properties. J Hydrol 356:147–162. doi: 10.1016/j.jhydrol.2008.04.016

Phalla C, Hirsch P, Paradis S (2011) Hydrological Analysis in support of irrigation management. A case study of Stung Chrey Bak catchment, Cambodia. CDRI

Poláková J, Farmer A, Berman S, et al (2013) Sustainable management of natural resources with a focus on water and agriculture. Brussels

Popova Z, Kercheva M (2004) Intergrated strategies for maize irrigation and fertilization under water scarcity and environmental pressure in Bulgaria. Irrig Drain 113:105–113.

Popova Z, Pereira LS (2011) Modelling for maize irrigation scheduling using long term experimental data from Plovdiv region , Bulgaria. Agric Water Manag 98:675–683. doi: 10.1016/j.agwat.2010.11.009

Poulton PL, Dalgliesh NP, Vang S, Roth CH (2016) Resilience of Cambodian lowland

rice farming systems to future climate uncertainty. F Crop Res 198:160–170. doi: 10.1016/j.fcr.2016.09.008

Provenzano G (2007) Using HYDRUS-2D Simulation Model to Evaluate Wetted Soil Volume in Subsurface Drip Irrigation Systems. J Irrig Drain Eng 133:342–349.

Radcliffe DE, Simunek J (2010) Soil Physics with Hydrus Modeling and Applications. CRC Press, Taylor and Francis Group, LLC, Boca Raton

Raes D, Geerts S, Kipkorir E, et al (2006) Simulation of yield decline as a result of water stress with a robust soil water balance model. Agric Water Manag 81:335–357. doi: 10.1016/j.agwat.2005.04.006

Raes D, Steduto P, Hsiao TC, Fereres E (2017a) FAO crop-water productivity model to simulate yield response to water. In: AquaCrop version 6.0-Reference manual. The Food and Agriculture Organization of the United Nations (FAO), Rome, Italy,

Raes D, Steduto P, Hsiao TC, Fereres E (2009a) Aquacrop-The FAO crop model to simulate yield response to water: II. main algorithms and software description. Agron J 101:438–447. doi: 10.2134/agronj2008.0140s

Raes D, Steduto P, Hsiao TC, Fereres E (2017b) Calculation procedures. In: AquaCrop-Reference manual. The Food and Agriculture Organization (FAO), Rome, Italy,

Raes D, Steduto P, Hsiao TC, Fereres E (2009b) AquaCrop — The FAO Crop Model to Simulate Yield Response to Water: II. Main Algorithms and Software Description. Agron J 101:438–447. doi: 10.2134/agronj2008.0140s

Ramos TB, Gonçalves MC, Martins JC, et al (2006) Estimation of Soil Hydraulic Properties from Numerical Inversion of Tension Disk Infiltrometer Data. Vadose Zo J 5:684. doi: 10.2136/vzj2005.0076

Ran H, Kang S, Li F, et al (2017) Performance of AquaCrop and SIMDualKc models in evapotranspiration partitioning on full and deficit irrigated maize for seed production under plastic film-mulch in an arid region of China. Agric Syst 151:20–32. doi: 10.1016/j.agsy.2016.11.001

Ranatunga K, Nation ER, Barratt DG (2008) Review of soil water models and their applications in Australia. Environ Model Softw 23:1182–1206. doi: 10.1016/j.envsoft.2008.02.003

Rankine DR, Cohen JE, Taylor MA, et al (2015) Parameterizing the FAO AquaCrop Model for Rainfed and Irrigated Field-Grown Sweet Potato. Agron J 107:375. doi: 10.2134/agronj14.0287

Rashid NSA, Askari M, Tanaka T, et al (2015) Inverse estimation of soil hydraulic properties under oil palm trees. Geoderma 241–242:306–312. doi: 10.1016/j.geoderma.2014.12.003

Rawls WJ, Brakensiek DL, Saxton KE (1982) Estimation of Soil Water Properties. Trans ASAE 25:1316–1320 & 1328. doi: 10.13031/2013.33720

Razzaghi F, Zho Z, Andersen M, Plauborg F (2017) Simulation of potato yield in temperate condition by the AquaCrop model. Agric water Manag 191:113–123.

Reynolds CA, Jackson TJ, Rawls WJ (2000) Estimating soil water-holding capacities by linking the Food and Agriculture Organization soil map of the world with

global pedon databases and continuous pedotransfer functions. Water Resour Res 36:3653–3662. doi: 10.1029/2000WR900130

Rezaei M, Seuntjens P, Shahidi R, et al (2016) The relevance of in-situ and laboratory characterization of sandy soil hydraulic properties for soil water simulations. J Hydrol 534:251–265. doi: 10.1016/j.jhydrol.2015.12.062

Richards L a (1931) Capillary conduction of liquids throuhg porous media. Physics (College Park Md) 1:318–333.

Ringler C, Rosegrant MW, Ringler C, Zhu T (2009) Water for Agriculture : Maintaining Food Security Under Growing Water for Agriculture : Maintaining Food Security under Growing Scarcity. Annu. Rev. Environ. Resour.

Ritter A, Hupet F, Mun R, et al (2003) Using inverse methods for estimating soil hydraulic properties from field data as an alternative to direct methods. Agric Water Manag 59:77–96.

Rodríguez-Ferrero N, Salas-Velasco M, Sanchez-Martínez MT (2010) Assessment of productive efficiency in irrigated areas of Andalusia. Int J Water Resour Dev 26:365–379. doi: 10.1080/07900627.2010.489288

Romano N (2014) Soil moisture at local scale : Measurements and simulations. J Hydrol 516:6–20. doi: 10.1016/j.jhydrol.2014.01.026

Roulier Â, Angulo-jaramillo R, Vandervaere J, et al (2000) Field measurement of soil surface hydraulic properties by disc and ring infiltrometers: A review and recent developments. Soil Tillage Res 55:1–29.

Saccon P (2018) Water for agriculture , irrigation management. Appl Soil Ecol 123:793–796. doi: 10.1016/j.apsoil.2017.10.037

Sammis T, Sharma P, Shukla MK, et al (2012) A water-balance drip-irrigation scheduling model. Agric Water Manag 113:30–37.

Samperio A, Moñino MJ, Vivas A, et al (2015) Effect of deficit irrigation during stage II and post-harvest on tree water status, vegetative growth, yield and economic assessment in "Angeleno" Japanese plum. Agric Water Manag 158:69–81. doi: 10.1016/j.agwat.2015.04.008

Santamarta JC, Neris J, Rodríguez-Martín J, et al (2014) Climate Change and Water Planning : New Challenges on Islands Environments. Procedia IERI 9:59–63. doi: 10.1016/j.ieri.2014.09.041

Schaap MG, Leij FJ, Th. VGM (2001) Rosetta: A computer program for estimating soil hydraulic parameters with hierarchical pedotransfer functions. J Hydrol 251:163–176.

Scharnagl B, Vrugt JA, Vereecken H, et al (2011) Inverse modelling of in situ soil water dynamics : investigating the effect of different prior distributions of the soil hydraulic parameters. Hydrol Earth Syst Sci 15:3043–3059. doi: 10.5194/hess-15-3043-2011

Schelle H, Durner W, Iden SC, Fank J (2013) Simultaneous Estimation of Soil Hydraulic and Root Distribution Parameters from Lysimeter Data by Inverse Modeling. Procedia Environ Sci 19:564–573. doi: 10.1016/j.proenv.2013.06.064

Schindler U, Mueller L, da Veiga M, et al (2012) Comparison of water-retention

functions obtained from the extended evaporation method and the standard methods sand/kaolin boxes and pressure plate extractor. J Plant Nutr Soil Sci 175:527–534. doi: 10.1002/jpln.201100325

Schwartz RC, Evett SR (2003) Conjunctive Use of Tension Infiltrometry and Time-Domain Reflectometry for Inverse Estimation of Soil Hydraulic Properties. Vadose Zo J 2:530–538. doi: 10.2136/vzj2003.0530

Schwartz RC, Evett SR (2002) Estimating Hydraulic Properties of a Fine-textured Soil Using a Disc Infiltrometer. Soil Sci Soc Am J 66:1409–1423. doi: 10.2136/sssaj2002.1409

Schwen A, Bodner G, Loiskandl W (2011) Time-variable soil hydraulic properties in near-surface soil water simulations for different tillage methods. Agric Water Manag 99:42–50. doi: 10.1016/j.agwat.2011.07.020

Seki K, Ackerer P, Lehmann F (2015) Geoderma Sequential estimation of hydraulic parameters in layered soil using limited data. Geoderma 247–248:117–128. doi: 10.1016/j.geoderma.2015.02.013

Seng V, Bell RW, White PF, et al (2005) Sandy soils of Cambodia. In: FAO.

Shi L, Song X, Tong J, et al (2015) Impacts of different types of measurements on estimating unsaturated flow parameters. J Hydrol 524:549–561. doi: 10.1016/j.jhydrol.2015.01.078

Shwetha P, Varija K (2015) Soil Water Retention Curve from Saturated Hydraulic Conductivity for Sandy Loam and Loamy Sand Textured Soils. Aquat Procedia 4:1142–1149. doi: 10.1016/j.aqpro.2015.02.145

Silva S De, Johnston R, Sellamuttu SS (2013) Agriculture, irrigation and poverty reduction in Cambodia: policy narratives and ground realities compared. International Water Management Institute (IWMI)

Silvestro PC, Pignatti S, Yang H, et al (2017) Sensitivity analysis of the Aquacrop and SAFYE crop models for the assessment of water limited winter wheat yield in regional scale applications. PLoS One 1–30.

Simunek J (2005) 78 : Models of Water Flow and Solute Transport. Encycl. Hydrol. Sci. 1–10.

Šimůnek J, Jarvis NJ, van Genuchten MT, Gärdenäs (2003) Review and comparison of models for describing non-equilibrium and preferential flow and transport in the vadose zone. J Hydrol 272:14–35.

Šimůnek J, Šejna M, Saito H, et al (2005) The HYDRUS-1D Software Package for Simulating the One-Dimensional Movement of Water Heat, and Multiple Solutes in Variably-Saturated Media. Department of Environmental Sciences, University of California Riverside, Riverside, California, USA

Simůnek J, van Genuchten MT (1997) Estimating Unsaturated Soil Hydraulic Properties From Multiple Tension Disc Infiltrometer Data. Soil Sci 162:383–398. doi: 10.1097/00010694-199706000-00001

Šimůnek J, van Genuchten MT, Wendroth O (1998) Parameter Estimation Analysis of the Evaporation Method for Determining Soil Hydraulic Properties. Soil Sci Soc Am J 62:894–905. doi: 10.2136/sssaj1998.03615995006200040007x

Singh A, Saha S, Mondal S (2013) Modelling Irrigated Wheat Production Using the

Fao Aquacrop Model in West Bengal, India, for Sustainable Agriculture. Irrig Drain 62:50–56. doi: 10.1002/ird.1722

Sithirith M (2017) Water Governance in Cambodia: From Centralized Water Governance to Farmer Water User Community. Resources 6:44. doi: 10.3390/resources6030044

Smagin A V. (2012) Column-centrifugation method for determining water retention curves of soils and disperse sediments. Eurasian Soil Sci 45:416–422. doi: 10.1134/S1064229312040126

Soltani A, Azimi M, Deng A, Taheri A (2017) A simplified method for determination of the soil – water characteristic curve variables. Int J Geotech Eng 1–10. doi: 10.1080/19386362.2017.1344450

Song-hao S, Xiao-min MAO (2011) A Physicoempirical Model for Soil Water Simulation in Crop Root Zone. Pedosph An Int J 21:512–521. doi: 10.1016/S1002-0160(11)60153-7

Sparks DL, Page AL, Helmke PA, et al (1996a) Lime Requirement. In: SSSA Book Series. Soil Science Society of America, American Society of Agronomy,

Sparks DL, Page AL, Helmke PA, et al (1996b) Cation Exchange Capacity and Exchange Coefficients. In: SSSA Book Series. Soil Science Society of America, American Society of Agronomy,

Sparks DL, Page AL, Helmke PA, et al (1996c) Phosphorus. In: SSSA Book Series. Soil Science Society of America, American Society of Agronomy,

Steduto P, Hsiao TC, Fereres E, Raes D (2012) Crop yield response to water. The Food and Agriculture Organization (FAO), Rome, Italy

Steduto P, Hsiao TC, Raes D, Fereres E (2009a) AquaCrop—The FAO Crop Model to Simulate Yield Response to Water: I. Concepts and Underlying Principles. Agron J 101:426–437. doi: 10.2134/agronj2008.0139s

Steduto P, Raes D, Hsiao T, Fereres E (2009b) AquaCrop: a new model for crop prediction under water deficit conditions. Options Méditerranéennes 33:285–292.

Stott LD (2002) The influence of diet on the δ13C of shell carbon in the pulmonate snail Helix aspersa. Earth Planet Sci Lett 195:249–259. doi: 10.1016/S0012-821X(01)00585-4

Sun Q, Kröbel R, Müller T, et al (2011) Optimization of yield and water-use of different cropping systems for sustainable groundwater use in North China Plain. Agric Water Manag 98:808–814. doi: 10.1016/j.agwat.2010.12.007

Sutton B., Merit N (1993) Maintenance of lettuce root zone at field capacity gives best yields with drip irrigation. Sci Hortic (Amsterdam) 56:1–11. doi: https://doi.org/10.1016/0304-4238(93)90096-9

Tan S, Wang Q, Zhang J, et al (2018) Performance of AquaCrop model for cotton growth simulation under film-mulched drip irrigation in southern Xinjiang, China. Agric Water Manag 196:99–113. doi: 10.1016/j.agwat.2017.11.001

Tavakoli AR, Mahdavi Moghadam M, Sepaskhah AR (2015) Evaluation of the AquaCrop model for barley production under deficit irrigation and rainfed condition in Iran. Agric Water Manag 161:136–146. doi:

10.1016/j.agwat.2015.07.020

Theiveyanathan S, Benyon RG, Marcar NE, Myers BJ (2004) An irrigation-scheduling model for application of saline water to tree plantations. For Ecol Manage 193:97–112. doi: 10.1016/j.foreco.2004.01.025

Thompson RB, Gallardo M, Valdez LC, Fernández MD (2007) Determination of lower limits for irrigation management using in situ assessments of apparent crop water uptake made with volumetric soil water content sensors. Agric Water Manag 92:13–28. doi: 10.1016/j.agwat.2007.04.009

Tian Z, Kool D, Ren T, et al (2018) Determining in-situ unsaturated soil hydraulic conductivity at a fine depth scale with heat pulse and water potential sensors. J Hydrol 564:802–810. doi: 10.1016/j.jhydrol.2018.07.052

Tickner V (1996) Food Security In Cambodia. United Nations Research Institute For Social Development, Phnom Penh, Cambodia

Todorovic M, Albrizio R, Zivotic L, et al (2009) Assessment of AquaCrop, CropSyst, and WOFOST Models in the Simulation of Sunflower Growth under Different Water Regimes. Agron J 101:509. doi: 10.2134/agronj2008.0166s

Tolk JA (1998) Soils, Permanent Wilting Points. Encycl. Water Sci. 61:122.

Tolk JA, Evett SR, Schwartz RC (2015) Field-Measured, Hourly Soil Water Evaporation Stages in Relation to Reference Evapotranspiration Rate and Soil to Air Temperature Ratio. Vadose Zo J 14:1–14. doi: 10.2136/vzj2014.07.0079

Tong K, Hem S, Santos P (2011) What Limits Agricultural Intensification in Cambodia? The Role of Emigration, Agricultural Extension Services and Credit Constraints. Phnom Penh, Cambodia

Toorman AF, Wierenga PJ, Hills RG (1992) Parameter estimation of hydraulic properties from one- step outflow data. Water Resour Res 28:3021–3028. doi: 10.1029/92WR01272

Torres R, Dietrich WE, Montgomery DR, et al (1998) Unsaturated zone processes and the hydrologic response of a steep , unchanneled catchment. Water Resour Res 34:1865–1879.

Touch V, Martin RJ, Scott JF, et al (2016) Climate change adaptation options in rainfed upland cropping systems in the wet tropics: A case study of smallholder farms in North-West Cambodia. J Environ Manage 182:238–246. doi: 10.1016/j.jenvman.2016.07.039

Toumi J, Er-Raki S, Ezzahar J, et al (2016) Performance assessment of AquaCrop model for estimating evapotranspiration, soil water content and grain yield of winter wheat in Tensift Al Haouz (Morocco): Application to irrigation management. Agric Water Manag 163:219–235. doi: 10.1016/j.agwat.2015.09.007

Tripathi AD, Mishra R, Maurya KK, et al (2019) Chapter 1. Estimates for World Population and Global Food Availability for Global Health. Elsevier Inc.

Valenzuela HR, Bernard K, John C (1996) Lettuce production guidelines for Hawaii. Res. Ext. Ser. 164 1–24.

van Dam JC, Stricker JNM, Droogers P (1992) Inverse Method for Determining Soil Hydraulic Functions from One-Step Outflow Experiments. Soil Sci Soc Am J

56:1042–1050. doi: 10.2136/sssaj1992.03615995005600040007x

Van Den Berg M, Klamt E, Van Reeuwijk LP, Sombroek WG (1997) Pedotransfer functions for the estimation of moisture retention characteristics of Ferralsols and related soils. Geoderma 78:161–180. doi: 10.1016/S0016-7061(97)00045-1

van Genuchten MT (1980) A Closed-form Equation for Predicting the Hydraulic Conductivity of Unsaturated Soils. Soil Sci Soc Am J 44:892–898. doi: 10.2136/sssaj1980.03615995004400050002x

van Genuchten MT, Leij FJ, Wu L (1997) Characterization and measurement of the hydraulic properties of unsaturated porous media (parts 1 and 2). In: Proceedings of the International Workshop, Riverside, Calif., 22–24 Oct. p 20

van Genuchten MT, Pachepsky YA (2017) Hydraulic Properties of Unsaturated Soils. Encycl. Agrophysics 44:368–376.

Vanclooster M, Viaene P, Diels J, Christiansen K (1994) WAVE, a deterministic model for simulating water and agrochemicals in the soil and vadose environment. K.U. Leuven

Ventrella D, Losavio N, Vonella A V., Leij FJ (2005) Estimating hydraulic conductivity of a fine-textured soil using tension infiltrometry. Geoderma 124:267–277. doi: 10.1016/j.geoderma.2004.05.005

Verbist K, Cornelis WM, Gabriels D, et al (2009) Using an inverse modelling approach to evaluate the water retention in a simple water harvesting technique. Hydrol Earth Syst Sci 13:1979–1992.

Vereecken H, Huisman JA, Pachepsky Y, et al (2014) On the spatio-temporal dynamics of soil moisture at the field scale. J Hydrol 516:76–96. doi: 10.1016/j.jhrol.2013.11.061

Vereecken H, Schnepf A, Hopmans JW, et al (2016) Modeling Soil Processes: Review, Key Challenges, and New Perspectives. Vadose Zo J 15:1–57. doi: 10.2136/vzj2015.09.0131

Vereecken H, Weynants M, Javaux M, et al (2010) Using Pedotransfer Functions to Estimate the van Genuchten–Mualem Soil Hydraulic Properties: A Review. Vadose Zo J 9:795. doi: 10.2136/vzj2010.0045

Verstraeten WW, Veroustraete F, Feyen J (2008) Assessment of Evapotranspiration and Soil Moisture Content Across Different Scales of Observation. Sensors 8:70–117. doi: 10.3390/s8010070

Visconti F, de Paz JM, Martínez D, Molina MJ (2014) Laboratory and field assessment of the capacitance sensors Decagon 10HS and 5TE for estimating the water content of irrigated soils. Agric Water Manag 132:111–119. doi: 10.1016/j.agwat.2013.10.005

Vrugt JA, Stau PH, Wöhling T, et al (2008) Inverse Modeling of Subsurface Flow and Transport Properties: A Review with New Developments. Vadose Zo J 7:843–864. doi: 10.2136/vzj2007.0078

Vrugt JA, Wijk MT Van, Hopmans JW (2001) One-, two-, and three-dimensional root water uptake functions for transient modeling. Water Resour Res 37:2457–2470.

Vuthy T, Ra K (2011) Review of Agricultural Policy and Policy Research A Policy Discussion Paper.

Wallach D, Keussayan N, Brun F, et al (2008) Assessing the uncertainty when using a modle to compare irrigation strategies. Agron J 104:1274–1283. doi: 10.2134/agronj2012.0038

Wang C, Gu F, Chen J, et al (2015) Assessing the response of yield and comprehensive fruit quality of tomato grown in greenhouse to deficit irrigation and nitrogen application strategies. Agric Water Manag 161:9–19. doi: 10.1016/j.agwat.2015.07.010

Wang F, Kang Y, Liu S (2006) Effects of drip irrigation frequency on soil wetting pattern and potato growth in North China Plain. Agric Water Manag 79:248–264. doi: 10.1016/j.agwat.2005.02.016

Wang J, Zhang Y, Gong S, et al (2018) Evapotranspiration , crop coe ffi cient and yield for drip-irrigated winter wheat with straw mulching in North China Plain. F Crop Res 217:218–228. doi: 10.1016/j.fcr.2017.05.010

Wang JE, Xiang W (2014) Transient water release and imbibition properties of remolded sliding zone soil of Huangtupo landslide in Three Gorges Reservoir Area, China. In: Global view of engineering geology and the environment, proceedings of the international symposium and 9th Asian regional conference of IAEG, BEIJING, CHINA, 23-25 September 2013. CRC Press, p 228

Wang T, Franz TE, Yue W, et al (2016) Feasibility analysis of using inverse modeling for estimating natural groundwater recharge from a large-scale soil moisture monitoring network. J Hydrol 533:250–265. doi: 10.1016/j.jhydrol.2015.12.019

Wang Z, Wu L, Wu QJ (2000) Water-entry value as an alternative indicator of soil water-repellency and wettability. J Hydrol 231–232:76–83.

Wayllace A, Lu N (2011) A Transient Water Release and Imbibitions Method for Rapidly Measuring Wetting and Drying Soil Water Retention and Hydraulic Conductivity Functions. Geotech Test J 35:1–15.

WBG (2011) Vulnerability, risk reduction, and adaptation to climate change. 12.

Wellens J, Raes D, Traore F, et al (2013) Performance assessment of the FAO AquaCrop model for irrigated cabbage on farmer plots in a semi-arid environment. Agric Water Manag 127:40–47. doi: 10.1016/j.agwat.2013.05.012

Wellens J, Raes D, Tychon B (2017) On the Use of Decision-Support Tools for Improved Irrigation Management : AquaCrop-Based Applications. In: Current Perspective on Irrigation and Drainage. INTECH, London, UK, pp 53–67

Wen Y, Shang S, Yang J (2017) Optimization of irrigation scheduling for spring wheat with mulching and limited irrigation water in an arid climate. Agric Water Manag 192:33–44. doi: 10.1016/j.agwat.2017.06.023

Werisch S, Grundmann J, Al-Dhuhli H, et al (2014) Multiobjective parameter estimation of hydraulic properties for a sandy soil in Oman. Environ Earth Sci 72:4935–4956. doi: 10.1007/s12665-014-3537-6

Wheeler TR, Hadley P, Morison JI., Ellis RH (1993) Effects of temperature on the growth of lettuce (Lactuca sativa L.) and the implications for assessing the impacts of potential climate change. Eur J Agron 2:305–311. doi: 10.1016/S1161-0301(14)80178-0

Wohling T, Vrugt JA, Barkle GF (2008) Comparison of Three Multiobjective

Optimization Algorithms for Inverse Modeling of Vadose Zone Hydraulic Properties. Soil Sci Soc Am J 72:305–319. doi: 10.2136/sssaj2007.0176

Wolf J, Evans LG, Semenov MA, et al (1996) Comparison of wheat simulation models under climate change. I. Model calibration and sensitivity analyses. Clim Res 7:253–270. doi: 10.3354/cr007253

Wooding RA (1968) Steady Infiltration from a Shallow Circular Pond. Water Resour Res 4:1259–1273. doi: 10.1029/WR004i006p01259

Wösten JHM, Pachepsky YA, Rawls WJ (2001) Pedotransfer functions: bridging the gap between available basic soil data and missing soil hydraulic characteristics. J Hydrol 251:123–150. doi: 10.1016/S0022-1694(01)00464-4

Xinchun C, Mengyang W, Xiangping G, et al (2017) Science of the Total Environment Assessing water scarcity in agricultural production system based on the generalized water resources and water footprint framework. Sci Total Environ 609:587–597. doi: 10.1016/j.scitotenv.2017.07.191

Xu C, Xu X, Liu M, et al (2017) Enhancing pedotransfer functions (PTFs) using soil spectral reflectance data for estimating saturated hydraulic conductivity in southwestern China. Catena 158:350–356. doi: 10.1016/j.catena.2017.07.014

Xue J, Huo Z, Wang F, et al (2018) Untangling the effects of shallow groundwater and deficit irrigation on irrigation water productivity in arid region: New conceptual model. Sci Total Environ 619–620:1170–1182. doi: 10.1016/j.scitotenv.2017.11.145

Yang C, Luo Y, Sun L, Wu N (2015) Effect of Deficit Irrigation on the Growth, Water Use Characteristics and Yield of Cotton in Arid Northwest China. Pedosphere 25:910–924. doi: 10.1016/S1002-0160(15)30071-0

Yang H, Du T, Qiu R, et al (2017) Improved water use efficiency and fruit quality of greenhouse crops under regulated deficit irrigation in northwest China. Agric Water Manag 179:193–204. doi: 10.1016/j.agwat.2016.05.029

Yates M V. (2000) Measurement of Virus and Indicator Survival and Transport in the Subsurface. American Water Works Association

Yoon Y, Kim J, Hyun S (2007) Estimating soil water retention in a selected range of soil pores using tension disc infiltrometer data. Soil Tillage Res 97:107–116. doi: 10.1016/j.still.2007.09.003

Zeleke KT, Luckett D, Cowley R (2011) Calibration and testing of the FAO AquaCrop model for canola. Agron J 103:1610–1618. doi: 10.2134/agronj2011.0150

Zeng C, Wang Q, Zhang F, Zhang J (2013) Temporal changes in soil hydraulic conductivity with different soil types and irrigation methods. Geoderma 193–194:290–299. doi: 10.1016/j.geoderma.2012.10.013

Zhai Q, Rahardjo H (2013) Quanti fi cation of uncertainties in soil – water characteristic curve associated with fi tting parameters. Eng Geol 163:144–152. doi: 10.1016/j.enggeo.2013.05.014

Zhang G, Johkan M, Hohjo M, et al (2017) Plant Growth and Photosynthesis Response to Low Potassium Conditions in Three Lettuce (Lactuca sativa) Types. Hortic J 86:229–237. doi: 10.2503/hortj.OKD-008

Zhang H, Oweis T (1999) Water - yield relations and optimal irrigation scheduling of wheat in the Mediterranean region.

Zhang J, Campana PE, Yao T, et al (2018) The water-food-energy nexus optimization approach to combat agricultural drought: a case study in the United States. Appl Energy 227:449–464. doi: 10.1016/j.apenergy.2017.07.036

Zhang Y, Kendy E, Qiang Y (2004) Effect of soil water deficit on evapotranspiration , crop yield , and water use efficiency in the North China Plain. Agric Water Manag 64:107–122. doi: 10.1016/S0378-3774(03)00201-4

Zhou L, He J, Qi Z, et al (2018) Effects of lateral spacing for drip irrigation and mulching on the distributions of soil water and nitrate , maize yield , and water use efficiency. Agric Water Manag 199:190–200.

Zhuo L, Hoekstra A. (2017) The effect of different agricultural management practices on irrigation efficiency, water use efficiency and green and blue water footprint. Front Agric Sci Eng 4:185–194. doi: 10.15302/J-FASE-2017149

Zijlstra J, Dane JH (1996) Identification of hydraulic parameters in layered soils based on a quasi-Newzon method. J Hydrol 181:233–250.

List of publications

Ket P, Garré S, Oeurng C, Hok, L., Degré, A. (2018) Simulation of crop growth and water-saving irrigation scenarios for Lettuce: A monsoon-climate case study in Kampong Chhnang, Cambodia. Water (Switzerland). doi: 10.3390/w10050666

Ket P, Oeurng C, Degré A (2018) Estimating Soil Water Retention Curve by Inverse Modelling from Combination of In Situ Dynamic Soil Water Content and Soil Potential Data. Soil Syst 2:14–19. doi: 10.3390/soilsystems2040055